

IDCOR

Program Report

DRAFT

Technical Report 23.1

GRAND GULF NUCLEAR STATION

INTEGRATED CONTAINMENT ANALYSIS

8408230119 840807
PDR ADOCK 05000327
P PDR

DRAFT

GRAND GULF NUCLEAR STATION
IDCOR Task 23.1
Integrated Containment Analysis

TABLE OF CONTENTS

	<u>Page</u>
LIST OF FIGURES	v
LIST OF TABLES	ix
1.0 INTRODUCTION	1-1
1.1 Statement of the Problem	1-1
1.2 Relationship to Other Tasks	i-1
2.0 STRATEGY AND METHODOLOGY	2-1
2.1 References	2-2
3.0 DESCRIPTION OF MODELS AND MAJOR ASSUMPTIONS	3-1
3.1 Plant Specific Information	3-1
3.1.1 Nuclear System	3-1
3.1.2 Containment	3-2
3.2 Modular Accident Analysis Program (MAAP)	3-4
3.2.1 MAAP Nodalization	3-4
3.2.2 Grand Gulf Systems Modeled in MAAP	3-6
3.2.3 Fission Product Release from Fuel	3-9
3.2.4 Description of the Natural Circulation Model	3-11
3.2.5 Aerosol Deposition	3-13
3.2.6 Fission Product and Aerosol Release from Core-Concrete Attack	3-14
3.3 References	3-15
4.0 PLANT RESPONSE TO SEVERE ACCIDENTS	4-1
4.1 Plant Response to the T ₁ QUV Accident	4-3
4.1.1 Sequence Description	4-3
4.1.2 Primary System and Containment Response	4-3

TABLE OF CONTENTS (Continued)

	<u>Page</u>
4.1.3 Manual Depressurization Sensitivity Analysis	4-15
4.2 Plant Response to the AE Accident	4-17
4.2.1 Sequence Description	4-17
4.2.2 Primary System and Containment Response	4-17
4.3 Plant Response to the T ₂₃ QW Accident	4-27
4.3.1 Sequence Description	4-27
4.3.2 Primary System and Containment Response	4-27
4.4 Plant Response to the T ₂₃ C Accident	4-35
4.4.1 Sequence Description	4-35
4.4.2 Primary System and Containment Response	4-39
5.0 PLANT RESPONSE WITH RECOVERY ACTION	5-1
5.1 Plant Response to the T ₁ QUV Accident with Operator Action	5-5
5.2 Plant Response to the AE Accident with Operator Action	5-8
5.3 Plant Response to the T ₂₃ QW Accident with Operator Action	5-10
5.4 Plant Response to the T ₂₃ C Accident with Operator Action	5-11
6.0 FISSION PRODUCT RELEASE, TRANSPORT AND DEPOSITION	6-1
6.1 Introduction	6-1
6.2 Modeling Approach	6-1
6.3 Sequences Evaluated	6-3
6.3.1 T ₁ QUV Sequence	6-3
6.3.2 AE Sequence	6-9
6.3.3 T ₂₃ QW Sequence	6-10
6.3.4 AE Sequence	6-10
6.4 References	6-11

TABLE OF CONTENTS (Continued)

	<u>Page</u>
7.0 SUMMARY OF RESULTS	7-1
7.1 Base Case Analyses	7-1
7.2 Operator Action Analyses	7-5
8.0 CONCLUSIONS	8-1
APPENDIX A - Grand Gulf Parameter File	A-1
APPENDIX B - Supplemental Plots for the Base Accident Sequences . .	B-1
Supplemental Plots for Sequence T ₁ QUV	B-3
Supplemental Plots for Sequence AE	B-9
Supplemental Plots for Sequence T ₂₃ QW	B-15
Supplemental Plots for Sequence T ₂₃ C	B-29

DRAFT

LIST OF FIGURES

<u>Figure No.</u>		<u>Page</u>
3.1	BWR primary system	3-5
3.2	Schematic representation of Grand Gulf Mark III containment and MAAP nodalization	3-7
3.3	Schematic representation of Grand Gulf safety and other systems	3-8
3.4	BWR natural circulation model	3-12
4.1	Pressure in the drywell	4-7
4.2	Temperature of gas in the drywell	4-8
4.3	Pressure in Compartment B	4-9
4.4	Temperature of gas in Compartment B	4-10
4.5	Average corium temperature in the pedestal	4-11
4.6	Concrete ablation depth in the pedestal	4-12
4.7	Temperature of the suppression pool	4-14
4.8	Average corium temperature in the pedestal	4-20
4.9	Concrete ablation depth in the pedestal	4-21
4.10	Temperature of gas in the drywell	4-23
4.11	Temperature of the suppression pool	4-24
4.12	Temperature of gas in Compartment B	4-25
4.13	Pressure in Compartment B	4-26
4.14	Temperature of the suppression pool	4-30
4.15	Temperature of gas in Compartment B	4-31
4.16	Pressure in Compartment B	4-32
4.17	Temperature of gas in the drywell	4-34
4.18	Average corium temperature in the pedestal	4-36
4.19	Concrete ablation depth in the pedestal	4-37

DRAFT

LIST OF FIGURES (C tinned)

<u>Figure No.</u>		<u>Page</u>
4.20	Average core power	4-40
4.21	Reactor vessel water level	4-41
4.22	Pressure in the drywell	4-43
4.23	Temperature of gas in the drywell	4-44
4.24	Pressure in Compartment B	4-45
4.25	Temperature of gas in Compartment B	4-46
4.26	Average corium temperature in the pedestal	4-49
4.27	Concrete ablation depth in the pedestal	4-50
B.1	Total H ₂ generated	B-4
B.2	Total H ₂ generated	B-5
B.3	Reactor vessel water level	B-6
B.4	Temperature of structure, °F	B-7
B.5	Fission product decay power on structure, Btu/hr	B-8
B.6	Total CO generated	B-9
B.7	Mass of water in the pedestal	B-10
B.8	Mole fraction of H ₂ in Compartment B	B-11
B.9	Mole fraction of O ₂ in Compartment B	B-12
B.10	Mole fraction of CO ₂ in Compartment B	B-13
B.11	Mole fraction of steam in Compartment B	B-14
B.12	Volumetric flow out of containment	B-15
B.13	Mass of UO ₂ in core region	B-16
B.14	Total H ₂ generated	B-18
B.15	Total H ₂ generated	B-19
B.16	Reactor vessel water level	B-20

LIST OF FIGURES (Continued)

<u>Figure No.</u>		<u>Page</u>
B.17	Temperature of structure, °F	B-21
B.18	Fission product decay heat on structure, Btu/hr	B-22
B.19	Total CO generated	B-23
B.20	Mass of water in the pedestal	B-24
B.21	Mole fraction of H ₂ in Compartment B	B-25
B.22	Mole fraction of O ₂ in Compartment B	B-26
B.23	Mole fraction of CO ₂ in Compartment B	B-27
B.24	Mole fraction of steam in Compartment B	B-28
B.25	Volumetric flow out of containment	B-29
B.26	Mass of UO ₂ in core region	B-30
B.27	Total H ₂ generated	B-32
B.28	Total H ₂ generated	B-33
B.29	Reactor vessel water level	B-34
B.30	Temperature of structure, °F	B-35
B.31	Fission product decay heat on structure, Btu/hr	B-36
B.32	Total CO generated	B-37
B.33	Mass of water in the pedestal	B-38
B.34	Mole fraction of H ₂ in Compartment B	B-39
B.35	Mole fraction of O ₂ in Compartment B	B-40
B.36	Mole fraction of CO ₂ in Compartment B	B-41
B.37	Mole fraction of steam in Compartment B	B-42
B.38	Mass of UO ₂ in core region	B-43
B.39	Total H ₂ generated	B-46
B.40	Total H ₂ generated	B-47

LIST OF FIGURES (Continued)

<u>Figure No.</u>		<u>Page</u>
B.41	Reactor vessel water level	B-48
B.42	Temperature of structure, °F	B-49
B.43	Fission product decay heat on structure, Btu/hr	B-50
B.44	Total CO generated	B-51
B.45	Mass of water in the pedestal	B-52
B.46	Mole fraction of H ₂ in Compartment B	B-53
B.47	Mole fraction of O ₂ in Compartment B	B-54
B.48	Mole fraction of CO ₂ in Compartment B	B-55
B.49	Mole fraction of steam in Compartment B	B-56
B.50	Volumetric flow out of containment	B-57
B.51	Mass of UO ₂ in core region	B-58

LIST OF TABLES

<u>Table No.</u>		<u>Page</u>
3.1	Initial Inventories of Fission Products and Structural Materials Released from the Fuel	3-10
4.1	Grand Gulf Nuclear Station, T ₁ QUV - Base Case, Accident Chronology	4-4
4.2	Effects of Depressurization in the T ₁ QUV Accident	4-16
4.3	Grand Gulf Nuclear Station, AE Base Case, Accident Chronology	4-18
4.4	Grand Gulf Nuclear Station, T ₂₃ QW - Base Case, Accident Chronology	4-28
4.5	Grand Gulf Nuclear Station, T ₂₃ C Base Case, Accident Chronology	4-38
5.1	Systems Available for Core and Core Debris Cooling	5-2
5.2	Systems Available for Containment Cooling and Pressure Control	5-3
5.3	Operator Response Selection	5-4
5.4	Grand Gulf Nuclear Station, T ₁ QUV - Operator Action Case, Accident Chronology	5-6
5.5	Grand Gulf Nuclear Station, AE - Operator Action Case, Accident Chronology	5-9
5.6	Grand Gulf Nuclear Station, T ₂₃ QW - With Operation Action, Accident Chronology	5-12
5.7	Grand Gulf Nuclear Station, T ₂₃ C - Operator Action Case, Accident Chronology	5-14
6.1	Distribution of CsI in Plant and Environment (Fraction of Core Inventory)	6-4
6.2	T ₁ QUV Fission Product Release	6-5
6.3	AE Fission Product Release	6-6
6.4	T ₂₃ QW Fission Product Release	6-7
6.5	T ₂₃ C Fission Product Release	6-8

DRAFT

- x -

LIST OF TABLES (Continued)

<u>Table No.</u>		<u>Page</u>
7.1	Summary of Fractional Radionuclide Releases to the Environment	7-2

1.0 INTRODUCTION

1.1 Statement of the Problem

The objective of this investigation was to calculate the response of the Grand Gulf Nuclear Station (GGNS) primary system and containment to postulated severe accident sequences which have been identified as potentially leading to core degradation and melting. These analyses include evaluations of the thermal-hydraulic response, the release of fission products from degraded fuel, and the transport of the released fission products within the containment. These calculations were performed on a best estimate basis phenomenologically and include assessments of the major uncertainties associated with state-of-the-art modeling. This study includes assessments of the results of a limited set of operator interventions in these sequences and an assessment of the influence of a specific mitigating feature associated with the Grand Gulf Nuclear Station design.

1.2 Relationship to Other Tasks

The primary system and containment response analyses of IDCOR Subtask 23.1 are dependent upon the primary system and containment thermal-hydraulic models developed in Subtasks 16.2 and 16.3 (Executive Analysis Program) and the fission product release and retention models developed in IDCOR Task 11 (Fission Product Transport). The accident sequences used for the analyses along with the operator interventions were developed by considering the dominant accident sequences identified in Subtask 3.2 (Assess Dominant Sequences) and the physical processes occurring during these accidents.

It should be noted that the analyses developed as part of IDCOR Subtasks 16.2 and 16.3 involve the detailed consideration of many different phenomena which are themselves considered in separate IDCOR subtasks. These include: hydrogen generation; distribution and combustion (Subtasks 12.1, 12.2 and 12.3); steam generation (Subtask 14.1); core heatup (Subtask 15.1); debris behavior (Subtask 15.2) and core-concrete interactions (Subtask 15.3).

DRAFT

Operator intervention sequences were developed as part of Subtask 23.1 and applied to the specific accident sequences in the Grand Gulf Nuclear Station design to determine those potential actions which could terminate the accident sequence and result in a safe stable state. These results were used in IDCOR Subtask 22.1 (Safe Stable States) which discusses both the inherent and intervention means of terminating the various core damage sequences considered for the Grand Gulf Nuclear Station design. The mitigative design feature sequence for GGNS was developed via a review of a list of mitigative and preventative design features identified in IDCOR Task 21 (Risk Reduction Potential).

The ultimate structural capability of the containments associated with the reference plants and other typical designs were assessed in IDCOR Subtask 10.1. These analyses define the containment failure pressure and failure mode in this analysis.

Calculations of the rate and amount of fission products released from the containment, for those sequences which result in containment failure, were supplied to IDCOR Subtask 18.1 (Atmospheric and Liquid Pathway Dose) to formulate assessments of the health consequences associated with these postulated accident scenarios. These health consequence analyses were then supplied to IDCOR Subtask 21.1 to evaluate the risk reduction potential for possible mitigating operator actions and containment mitigative design features.

Detailed considerations for each of the related subtasks can be found in the final reports submitted for the specific task. Individual issues are addressed in this report only as required to understand the specific behaviors obtained for the accident sequences considered.

2.0 STRATEGY AND METHODOLOGY

The basic strategy of this subtask was to analyze accident sequences which have been previously identified as potential contributors to core melt frequency. These analyses consisted of plant thermal hydraulic response and fission product transport calculations for accident sequences which led to core degradation and melting. These analyses model performance of the ECCS systems and the containment engineered safety systems, such as the suppression pool, decay heat removal system, etc.

The MAAP code [2.1] was used to perform the primary system and containment thermal-hydraulic response analyses. This code considers the major physical processes associated with an accident progression, including hydrogen generation, steam formation, debris coolability, debris dispersal, core-concrete interactions, and hydrogen combustion. The FPRAT module for MAAP was adopted from [2.2] to evaluate the fission product release from the fuel. Natural and forced circulation within the primary system is modeled both before and after vessel failure and is integrated with the fission product release model to determine the transport of vapors and aerosols throughout the primary system and containment. Fission product deposition processes modeled include vapor condensation, steam condensation and sedimentation.

For each of the four GGNS accident scenarios selected for analysis, thermal-hydraulic calculations were performed both with and without selected operator actions during the accident. The "base case" analyses, which assume only minimal operator response during the accident, establish a reference system response during each of the accident scenarios. The "operator action" analyses are branch calculations of the base cases. These operator intervention cases demonstrate the effect of selected operator actions on the progression of an accident, based on the time windows available to the operator to take such action. Additional uncertainty and sensitivity analyses have been performed on several key parameters associated with the accident response. These are reported in Ref. [2.4].

2.1 References

- 2.1 "MAAP, Modular Accident Analysis Program User's Manual," Technical Report on IDCOR Tasks 16.2 and 16.3, May 1983.
- 2.2 "Analysis of In-Vessel Core Melt Progression," Technical Report on IDCOR Subtask 15.1B, September 1983.
- 2.3 Richard K. McCardell, "Severe Fuel Damage Test 1-1 Quick Look Report," EG&G Idaho, October 1983.
- 2.4 IDCOR Technical Report on Task 23.4, "Uncertainty and Sensitivity Analyses for the IDCOR Reference Plants," to be published.

3.0 DESCRIPTION OF MODELS AND MAJOR ASSUMPTIONS

The Modular Accident Analysis Program (MAAP), Ref. [3.1] is used to model the Grand Gulf Nuclear Station (GGNS) response to postulated severe accidents. This code includes containment response, fission product release, and fission product transport. In addition, both the thermal hydraulic response and the fission product behavior are modeled for the reactor building which surrounds the primary containment.

3.1 Plant Specific Information

The Grand Gulf Nuclear Station (GGNS) is a two unit boiling water reactor located in Claiborne County, Mississippi, on the east side of the Mississippi River approximately 25 miles south of Vicksburg and 37 miles north-northeast of Natchez, Mississippi. The two units are nearly identical; both will be operated by Mississippi Power & Light Company (MP&L). Unit 1 is scheduled to go into commercial operation in early 1985; Unit 2 is scheduled to do so several years later. Each unit is designed with a core thermal output of 3833 MWth, a gross electrical power output of 1306 MWe, and a net electrical output of 1250 MWe. Each unit is powered by a BWR-6 water reactor, designed and supplied by General Electric Company. Each reactor is housed in a steel-lined reinforced concrete Mark III containment building.

3.1.1 Nuclear System

The primary system consists of the equipment and instrumentation necessary to produce, contain, and control the steam power required by the turbine-generator. Principal components of the system are the reactor pressure vessel (RPV) and internals, reactor water recirculation system, and the main steam system. Other important systems include the condensate and main feedwater systems which close the primary system flow loop by condensing the steam and water exhausted by the turbines and pumping this condensate back into the RPV. The reactor vessel houses the reactor core, contains the heat, produces steam within its boundaries, and serves as one of the fission product barriers during normal operation and in the event of fuel failure.

The core is composed of 800 fuel assemblies, each containing 62 fuel rods and two hollow water rods. These fuel rods are sealed Zircaloy-2 tubes, which are loaded with UO_2 fuel pellets, with the Zircaloy-2 cladding providing both structural support and a fission product barrier between the fuel and the primary system water. The remaining reactor pressure vessel internal components support and align the fuel and provide the water circulation flow paths to distribute coolant to the fuel. Upper vessel internals also furnish moisture removal for the steam generated within the core, to minimize the moisture content of the exiting steam. The major internal components consist of the core, the shroud top grid, core plate, steam generator and dryer, jet pumps, control rods, and control rod drives.

The reactor water recirculation system provides a forced continuous internal circulation of coolant water through the core. Four main steam lines direct steam to the balance of the plant. During an abnormal event occurring during power operation, main steam isolation valves (MSIVs) on each of these lines provide isolation of the reactor vessel from the balance of the plant. If their closure is required, a set of 20 safety/relief valves (SRVs) provide reactor vessel overpressure protection, with their discharge being directed to the suppression pool.

The majority of the primary system data used in this analysis came from the Grand Gulf FSAR [3.2]. This information includes initial conditions, pressures, temperatures, flow rates, enthalpies, masses, system pressure setpoints, control logic, and other parameters. A plant parameter file for MAAP was prepared based on these data; it appears in Appendix A.1.

3.1.2 Containment

The reactor vessel is housed in the containment building. This structure is designed to condense the steam (pressure suppression) and contain the fission products which may be released as a result of a Loss of Coolant Accident (LOCA). The Mark III containment is a steel-lined reinforced concrete structure, with a cylindrical shape, topped with a hemispherical dome. The containment foundation is a thick, circular reinforced concrete slab. Major elements of this pressure-suppression design are an inner volume and an

outer volume, separated by a large heat capacity suppression pool. The inner region, the drywell, is a cylindrical volume containing the reactor pressure vessel, which is supported by a hollow concrete cylinder called the pedestal. The drywell and outer containment volumes communicate via horizontal vent openings located below the suppression pool surface. A water seal between the inner and outer volumes is accomplished by the drywell weir wall. The pool which provides in steam suppression during postulated LOCA events. The outer containment volume consists of the annular space above the suppression pool and the dome. The upper containment pool, located in the outer containment volume, provides a post-LOCA source of makeup water to the suppression pool. Containment sprays, also located in the outer compartment, provide an additional means of rapidly removing possible post-accident steam and/or fission products from the outer containment atmosphere. In addition to these features, hydrogen igniters are located in both drywell and outer containment volumes to control hydrogen accumulations following postulated severe accidents.

The GGNS BWR-6/Mark III design, like that of other nuclear plants, is based on a defense-in-depth principle. Thus, if an abnormal event were to occur, backups to the normal systems are designed to maintain the integrity of the fuel cladding, the reactor pressure vessel, and the containment barriers. These backup systems perform two general functions: core cooling and containment pressure control. Those systems which perform the first function include the reactor core isolation cooling (RCIC) system, the high pressure and low pressure emergency core cooling systems (ECCS), the automatic depressurization system (ADS), and the standby liquid control (SLC) system. The containment pressure control function is accomplished via the suppression pool makeup system, the drywell purge system, the post-LOCA vacuum breakers, the suppression pool cooling and containment spray modes of the residual heat removal (RHR) system, and the hydrogen ignition system.

MAAP input data, including initial conditions, heat transfer coefficients, exposed surface areas, and flow areas between volumes are based on information from the Grand Gulf FSAR [3.2], and architect/engineer drawings. These data appear in the MAAP parameter file listed in Appendix A.1.

3.2 Modular Accident Analysis Program (MAAP)

Within the IDCOR Program, the phenomenological models developed in Tasks 11, 12, 14 and 15 have been incorporated into an integrated analysis package in Subtask 16.3, while Subtask 16.2 provides a computer code (MAAP) to analyze the major degraded core accident scenarios for both Pressurized Water Reactors (PWRs) and Boiling Water Reactors (BWRs). The MAAP code is designed to provide realistic assessments for severe core damage accident sequences using first principle models for the major phenomena that govern the accident progression, the release of fission products from the fuel matrix, the transport of these fission products and their deposition within the primary system and containment. The following sections describe the primary system and containment nodalization and include a description of the safety systems modeled in MAAP.

3.2.1 MAAP Nodalization

The BWR primary system nodes are illustrated in Figure 3.1 and include the lower plenum, downcomer, core, and upper plenum. Also indicated are the flow entry locations for CRD flow, feedwater, HPCS, RCIC, LPCI and LPCS as well as the standby liquid control system (SLCS). The SLCS is only modeled as an additional water source since MAAP does not have a neutronics model. Individual mass and energy equations are written for each of these nodes using the water addition locations and the appropriate connecting flow paths. The primary system model also represents the main steam isolation valves and the main steam safety and relief valves. The latter exhaust into the suppression pool.

Modeling of the primary system is used to determine if a given sequence (1) leads to core uncover, (2) results in core damage, (3) yields Zircaloy clad oxidation and hydrogen formation, (4) leads to core melt and vessel failure, or (5) can be recovered before vessel failure. The code predicts the times of these occurrences. The transient response to the spectrum of accident scenarios considered requires the specification of pump curves, valve set points, system logic, etc. With the specification of the accident sequence, the primary system model determines the vessel water

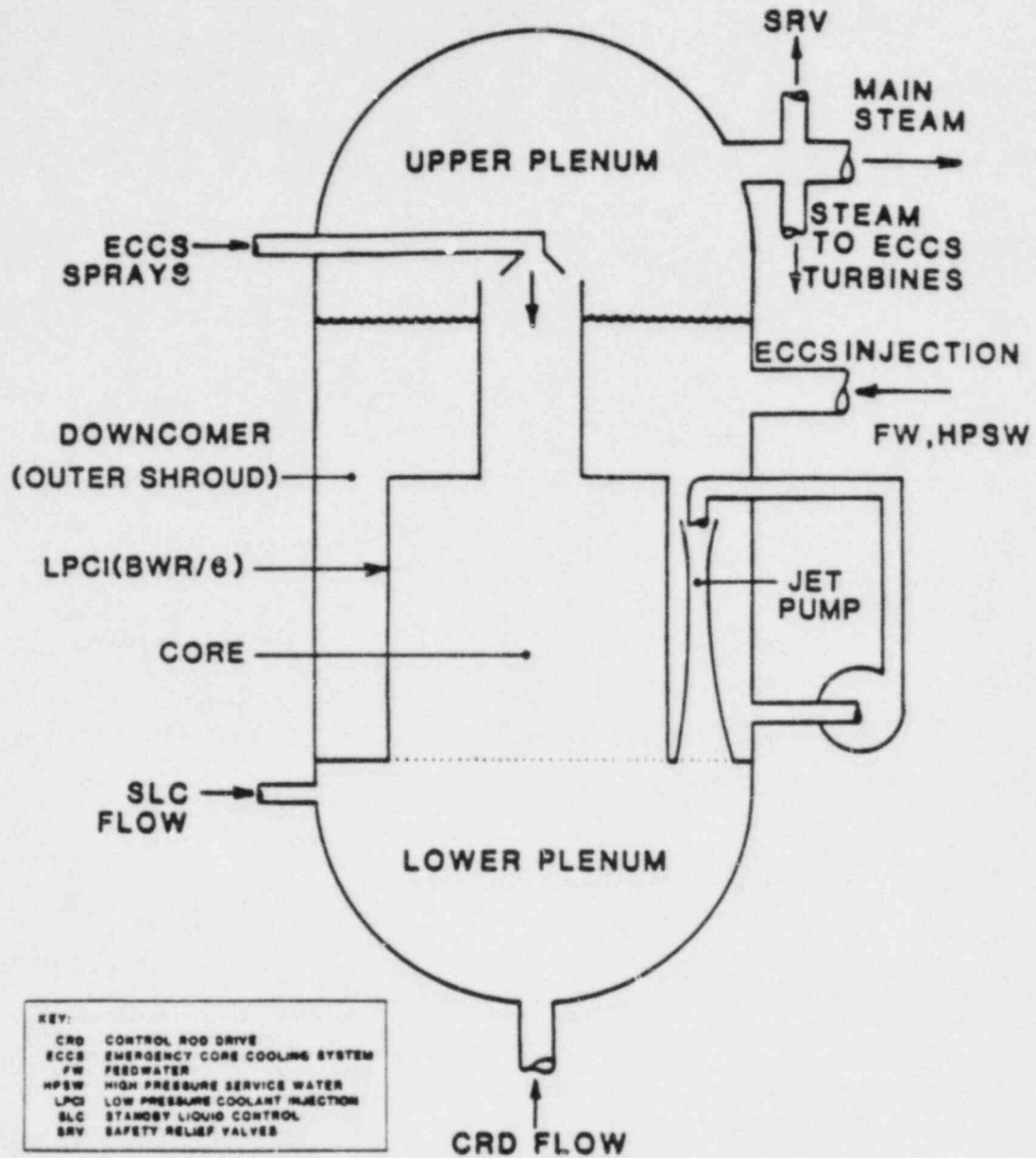


Fig. 3.1 BWR primary system.

inventory, including the boiled-up level in the core, to evaluate the potential for core uncover. If the collapsed water level decreases below the top of the core, the HEATUP subroutine calculates the temperature increases for the fuel and cladding. Steam cooling and the oxidation of the Zircaloy clad and channels are determined by the appropriate rate laws and oxygen starvation. The model accounts for the cooling effect of CRD flow. If available, this flow can limit core damage for long-term heat removal failure events.

The Mark III (Grand Gulf) containment nodalization scheme, as shown in Fig. 3.2, separates the containment into five compartments: the pedestal, the drywell, wetwell, Compartment A (annulus above the wetwell), and Compartment B (above the operating deck) regions. MAAP evaluates the behavior of the various compartments during the entire progression of the accident sequence by calculating the mass and energy flow rates between these compartments.

Individual compartment (region) pressures and gas temperatures are derived from the mass and energy balances. MAAP models the transport of all material throughout the containment due to drainage, vaporization, condensation and mass addition to assess the potential for cooling core debris. Separate water and corium temperatures are calculated for each containment compartment.

3.2.2 Grand Gulf Systems Modeled in MAAP

In general, MAAP characterizes the response of the primary system, the containment, and many of the balance of plant systems to user specified event sequences. Figure 3.3 illustrates the plant systems modeled in the code including the various water sources available and the valve line-ups which would allow this water to be injected into either the primary system and/or containment during a postulated sequence. Particular systems of importance include, the control rod drive (CRD) flow from the condensate storage tank, main steam lines, MSIVs, turbine bypass, feedwater, reactor core isolation cooling (RCIC), high pressure core spray (HPCS), low pressure coolant injection (LPCI) and other RHR system modes, low pressure core spray (LPCS), standby liquid control system (SLCS), and high pressure service water (HPSW). In addition to these plant systems, MAAP nodalizes both the primary system and

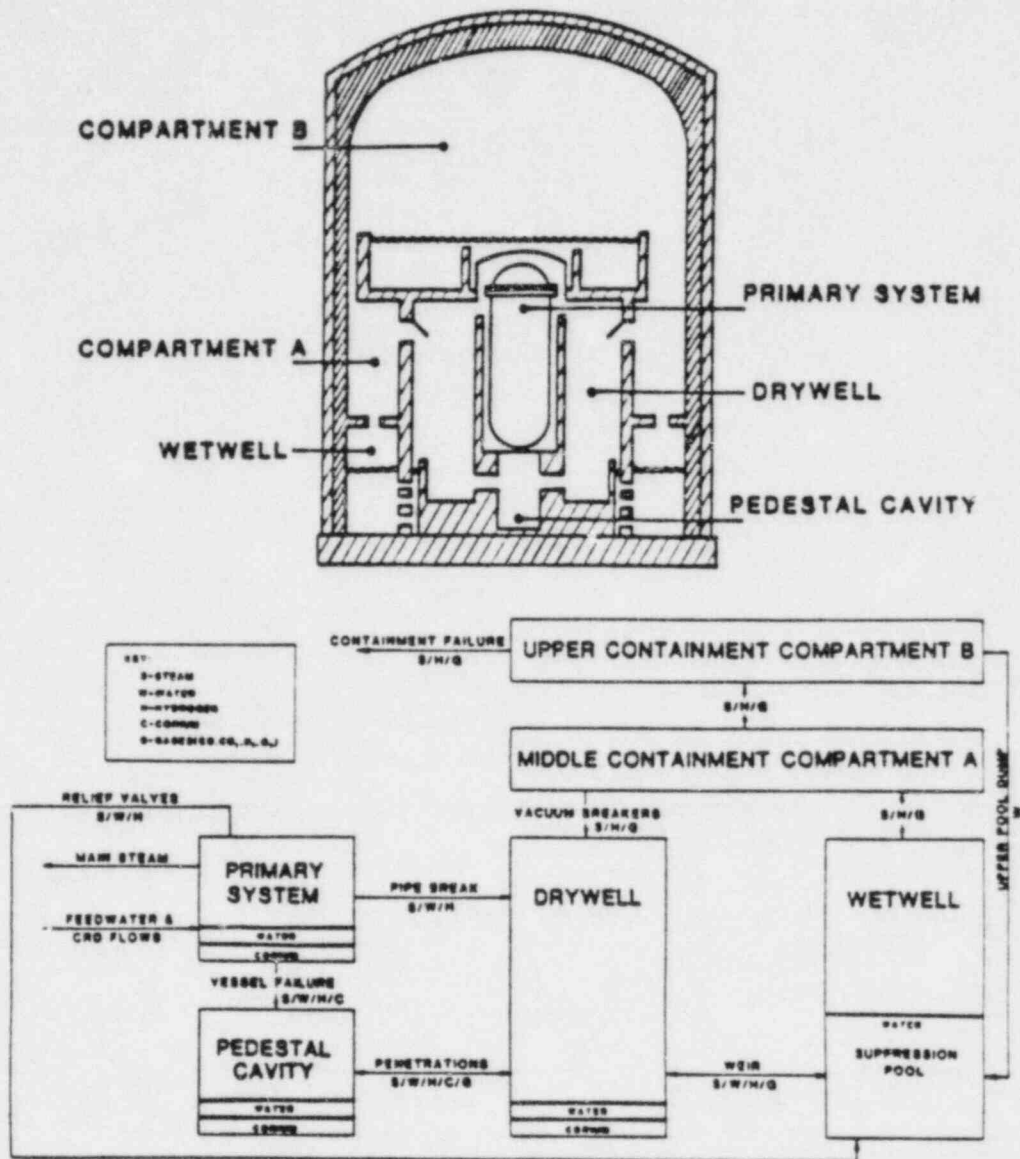


Fig. 3.2 Schematic representation of Grand Gulf Mark III containment and MAAP nodalization.

DRAFT

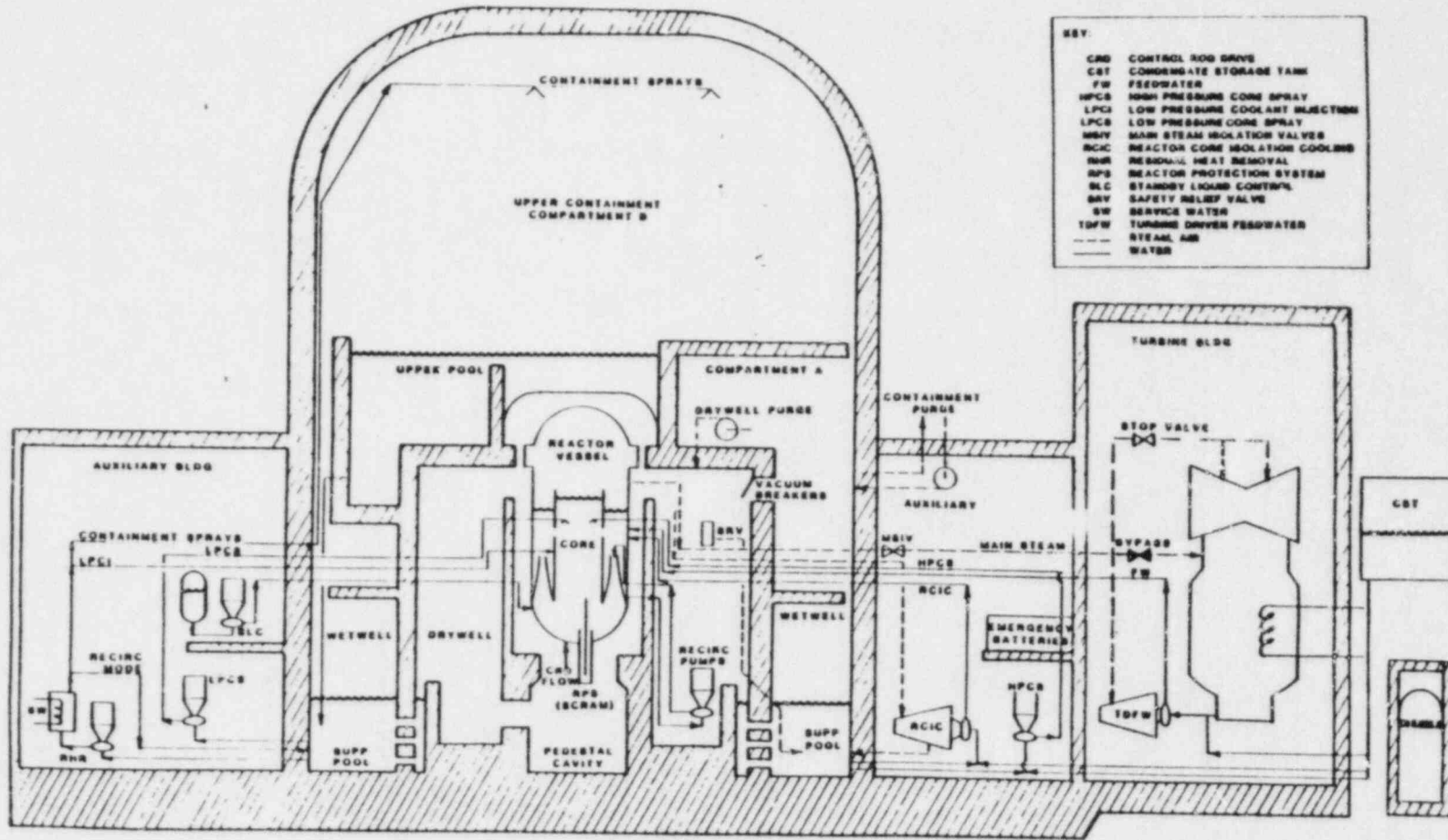


Fig. 3.3 Schematic representation of Grand Gulf safety and other systems.

containment to model their response to postulated core damage and recovery scenarios.

3.2.3 Fission Product Release from Fuel

The FPRAT module in MAAP, as adapted from Ref. [3.3] was used to calculate the release rates of fission products from the fuel matrix. These rates are dependent upon the fuel temperature history during heatup and upon characteristics of the atmosphere within the vessel which effect saturation of the chemical species as discussed in IDCOR Task 11.1 [3.4]. Fuel temperature histories for the thirty regions in the core are tracked to determine the release characteristics for the fission products and inert materials. The initial inventories of the various fission products were obtained from Ref. [3.5] and are given in Table 3.1.

The gas flow through each node is assumed to be saturated with the vapor of each constituent. If the flow cools as it is transported to higher nodes, the gas cools and creates aerosols of each species to remain saturated. This flow provides the aerosol and vapor source for the upper plenum. For the regions in which blockage has occurred, it is assumed that sufficient flow exists to remove the volatile fission products as saturated vapor. Once this flow is determined, the removal of the remaining less volatile species is evaluated based upon saturation of this calculated flow. The required FPRAT input for MAAP is given in the parameter file in Appendix A.1.

The calculations consider evaporation and condensation characteristics of chemical species. Several key assumptions consistent with the recommendations of IDCOR Subtask 11.1 were made regarding the physical and chemical forms of released fission products. These are:

1. Cesium and iodine combine to form CsI upon entry to the fission product release pathway. The excess cesium forms CsOH. Both chemical species exhibit similar physical behavior, hence the source rate for the Cs,I fission product group is assumed to be the sum of the Cs and I release rates. As stated above, it is assumed to be liberated in vapor form.

Table 3.1
INITIAL INVENTORIES OF FISSION PRODUCTS AND
STRUCTURAL MATERIALS RELEASED FROM THE FUEL

Fission Products	Initial Inventory (kg)
Kr	27.3
Xe	412
Cs	220
I	17.7
Te	37.1
Sr	66.7
Ru	183
Mo	252
Sn	1190
Mn	268

2. Tellurium is assumed to be released as vaporized TeO_2 .
3. Inert aerosol generation rate is the combined release rates for volatile structure material (Mn and Sn).
4. Strontium and ruthenium represent their respective nonvolatile fission product groups as defined in WASH-1400. They are also calculated to be released as vapor which quickly forms aerosols when they exit the core.
5. Release of the volatile fission products (Cs, I, Te) and the noble gases (Xe and Kr) is allowed to continue until complete, even if the vessel has failed first.

3.2.4 Description of the Natural Circulation Model

Substantial quantities of fission products are released during core degradation, but before vessel failure. Gas flow through the primary system determines the aerosol transport and deposition throughout the reactor vessel. Following vessel failure, most fission products remain within the primary system and subsequently heat the adjacent structures. As the structure and gas temperatures increase, density differences within the primary system would result in natural circulation flows that could distribute both heat and mass throughout the primary system.

The natural circulation model determines flows within the primary system, and includes descriptions for fission product heat generation, material vaporization, condensation and deposition. Also, the nodalization allows for a representation of the structural heatup in each node as well as the heat losses from these nodes to the containment environment. The circulation for the BWR system after vessel failure is graphically represented in Fig. 3.4. As illustrated, the throat area for the jet pumps controls the circulation rate and the containment pressurization/depressurization influences the flow from the primary system.

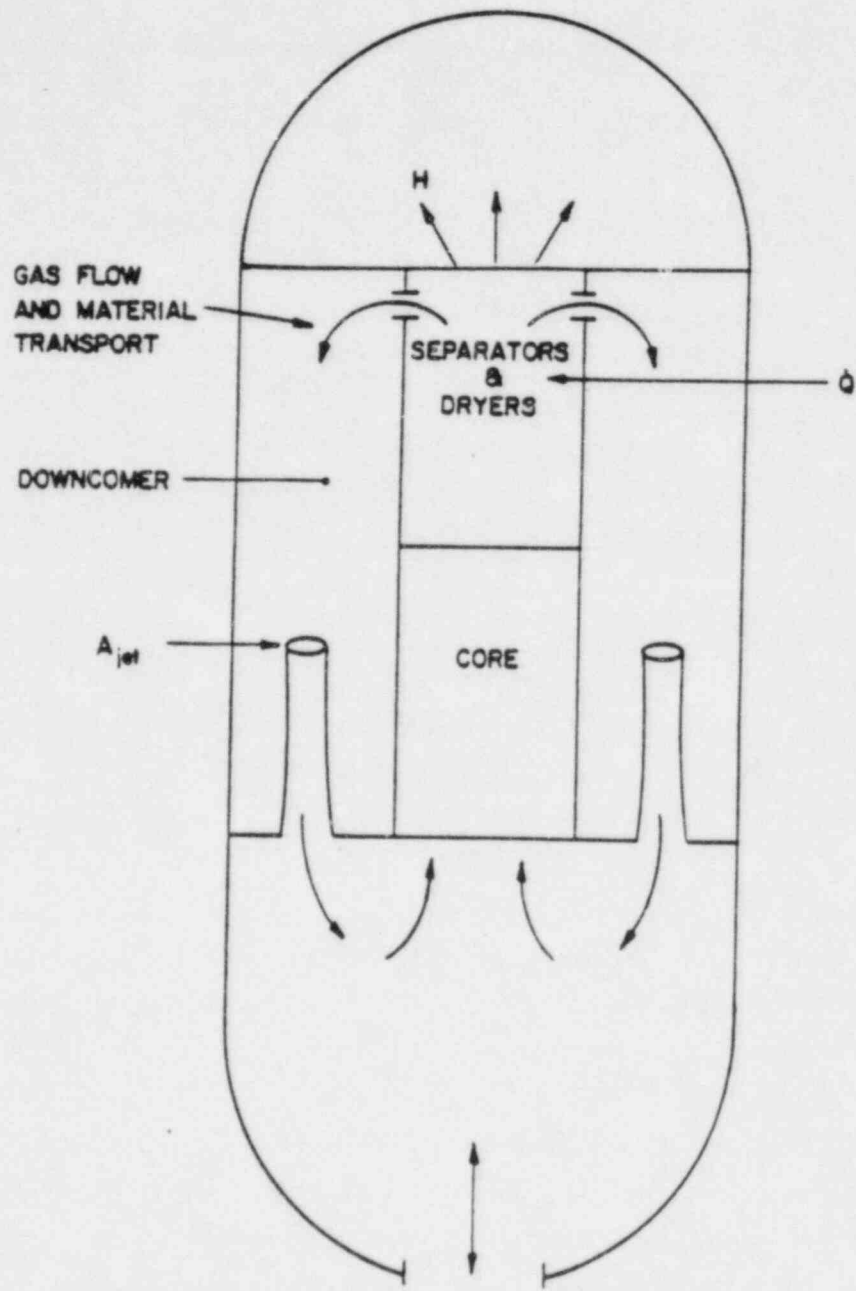


Fig. 3.4 BWR natural circulation model.

Since natural circulation flows are driven by the gas density differences between various regions, and since the volatile fission products are dense vapors, calculation of the gaseous flows within the primary system must account for the gas mixture properties in the various nodes. In addition, with the reflective insulation used on the Grand Gulf reactor vessel, the heat losses from the vessel must also include the magnitude of heat losses as a function of the primary system temperature and the potential for oxidation of the stainless steel layers in the reflective insulation.

These analyses have been coupled with models for aerosol deposition and heatup to evaluate the primary system flows after reactor vessel failure. Such assessments provide the rate and amount of material lost from the primary system as a result of the subsequent heatup of primary system structures. In this analysis, the difference between the primary system and containment pressurization determines the flows between these two systems which govern the release of fission products to the containment environment.

3.2.5 Aerosol Deposition

IDCOR Task 11.3, Ref. [3.6], applied state-of-the-art fission product behavior models to produce the RETAIN code, which describes the aerosol agglomeration and removal processes based upon an assumed log-normal distribution [3.6]. Both vapor and aerosol forms of fission products are considered. MAAP represents the aerosol removal rate due to settling as a function of the aerosol cloud density [3.5]. This is consistent with the general behavior predicted by detailed descriptions, such as RETAIN, and more importantly, is in good agreement with the results of large scale experiments. MAAP models physical mechanisms for vapor condensation on structures and aerosol retention due to steam condensation in addition to gravitational settling. These removal processes substantially reduce the magnitude of the release to the environment.

The primary system and containment nodalization for fission product transport are the same as those used for the thermal hydraulic calculations. The specific transport paths were earlier illustrated in Fig. 3.2 for the primary system and containment.

The key assumptions in the aerosol modeling are:

1. Cesium and iodine are assumed to be released as CsI with excess cesium as CsOH.
2. The decontamination factor associated with the wetwell suppression pool is estimated to be 1000 for releases through the spargers and 600 for releases through the horizontal vents [3.8].
3. Prior to vessel failure any fission products that may enter the drywell (such as from a LOCA pathway from the primary system) are available to enter Compartment A via the slight design-basis drywell leakage. These pathways are assumed to be closed off following vessel failure due to plugging by aerosols [3.9].
4. Fission products reaching the SRV discharge lines were treated as having reached the suppression pool.
5. Hygroscopic aerosols, such as cesium hydroxide, are assumed to accumulate an equilibrium concentration of water as determined by the steam partial pressure and temperature.
6. Release of volatile fission products (Cs, I, Te) and the noble gases (Xe and Kr) is allowed to continue until complete, even if the vessel has already failed.

3.2.6 Fission Product and Aerosol Release from Core-Concrete Attack

The release of aerosols due to core-concrete attack was determined using a model based on the concrete ablation rates from MAAP. The mass of low volatility fission products and inert aerosols released from core debris is based upon a vapor stripping model assuming the melt constituents follow Raoult's law. This calculation is dependent upon the amount of gas sparging through the core debris, the molar concentration of fission products in the

core debris, the vapor pressure of the chemical species of interest, and the temperature of the core debris.

The key assumptions are:

1. The masses of CO_2 and water vapor released per cubic meter ablated for the limestone concrete used at Grand Gulf are 572 kg and 130 kg respectively.
2. Stripping only occurs when the corium is calculated to be molten.
3. The gases released by the downward attack pass through the molten pool and cause stripping. Gases generated by sidewall attack are assumed to bypass the pool.
4. The predominant form of Sr is SrO , of Ru is elemental Ru, and of La is La_2O_3 .
5. Inert aerosols of CaO may be generated during core-concrete attack. This chemical form is used as a surrogate for the various concrete melt constituents that could be added to the corium pool.
6. Deposition of fission products in the SRV discharge lines was neglected.
7. Concrete aerosol generation was not incorporated into the overall fission product removal calculations but was used to make an assessment of the extent of plugging of the drywell to compartment A pathway.

3.3 References

- 3.1 "MAAP, Modular Accident Analysis Program," Technical Report on IDCOR Subtasks 16.2 and 16.3, 1983.

DRAFT

3-16

- 3.2 Final Safety Analysis Report, Grand Gulf Nuclear Station, Mississippi Power and Light Company, 1979.
- 3.3 "Analysis of In-Vessel Core Melt Progression," Technical Report on IDCOR Subtask 15.1B, September 1983.
- 3.4 "Estimation of Fission Product and Core-Material Source Characteristics," Technical Report on IDCOR Subtasks 11.1, 11.4, and 11.5, 1983.
- 3.5 Radionuclide Release Under Specific LWR Accident Conditions -- Volume III BWR, Mark III Design, Battelle Columbus Laboratories, 1984.
- 3.6 "Fission Product Transport in Degraded Core Accidents," Technical Report on IDCOR Subtask 11.3, December 1983.
- 3.7 "Aerosol Deposition Model," FAI report to be published.
- 3.8 Personal Communication, K. Holtzclaw (GE) to R. Henry (FAI), March 1984.
- 3.9 H. A. Morewitz, "Leakage of Aerosols from Containment Buildings," Health Physics, Vol. 42, No. 2, pp. 195-207, 1982.

4.0 PLANT RESPONSE TO SEVERE ACCIDENTS

This section provides the results of plant thermal-hydraulic analyses of four base case accident sequences, using the MAAP code. The accident scenarios are specific cutsets of each accident sequence and, as such, are not necessarily representative of all cutsets of these sequences. The accident scenarios are defined below, followed by descriptions of the reactor coolant system response and the containment response. The time dependence of the most significant MAAP-generated thermal-hydraulic parameters associated with each scenario are presented in Appendix B. The plant parameters utilized to characterize Grand Gulf in these analyses are listed in Appendix A.

The base sequences are:

1. T_1QUV - Transient with failure of injection.
2. AE - A large LOCA with failure of injection.
3. $T_{23}QW$ - Transient followed by loss of containment heat removal.
4. $T_{23}C$ - Transient followed by failure of the reactor to scram and standby liquid control (without operator action to reduce power level).

The T_1QUV was analyzed both with and without manual activation of the ADS in order to determine if this action would play a significant role in the overall containment response and fission product release.

The sequences analyzed in this section are low probability core damage events. The sequences exclude all, or nearly all, operator actions that could prevent or significantly delay core melt or that could mitigate its consequences. Operator actions which would prevent the accident are considered in the determination of the sequence probabilities. Those which would mitigate the consequences are not considered. This approach was taken to produce results which bound or are at the high end of the range of possible consequences for the four selected sequences. Generally, only minimal

operator actions to control selected plant systems are assumed for these events. For example, it is assumed that the operators regulate low pressure injection to maintain water level at the high level trip.

As a result of the minimal operator response models employed in this analysis, the results presented here do not represent what would be realistically expected to occur for the specified equipment failures and are extremely improbable. The more probable expected plant response to the specified equipment failures is evaluated in Section 5. This later section includes in the sequence definition some examples of actions which the operator would be expected to take in accordance with the Emergency Procedure Guidelines. As a result of these actions the operator is able to terminate the event prior to core melt or significantly mitigate its consequences. Section 5 considers only some examples of the many actions available to the operator to prevent or mitigate the accident.

A major objective of excluding mitigating operator actions in this analysis and allowing the events to progress unchecked was to provide the added perspective of defining the time windows available for operator intervention. The results clearly demonstrate that the operator has an extensive time period to implement primary or alternative actions that will successfully terminate or mitigate postulated severe accidents.

The following subsections discuss plant response for each severe accident sequence analyzed. In these analyses the containment ultimate pressure capacity is based on the evaluation contained in the IDCOR Task 10.1 report [4.1], Containment Structure Capability of Light Water Nuclear Power Plants. The ultimate pressure capability was calculated to be 71.3 psia with the defined failure condition (twice the elastic strain) occurring at the "transition" between the cylindrical and spherical parts of the containment. (It should be noted that a detailed assessment of penetration behavior under high strain conditions was not part of the analysis.)

A containment break size of 0.1 ft^2 (1.5 ft^2 for TC) is assumed because it permits depressurization of containment enabling airborne fission products to be transported out the break. This assumption is consistent with

the concept of yield leading to rupture resulting in diminishing yield as the containment depressurizes.

4.1 Plant Response to the T₁QUV Accident

4.1.1 Sequence Description

The T₁QUV accident is assumed to occur during full-power operation. It is initiated by a loss of off-site power event (T₁). During the accident, all systems not automatically transferred to the emergency busses are assumed to be unavailable. Thus, both the main feedwater and main condenser systems are assumed to be unavailable (Event Q) for the entire accident. The accident also specifies that neither the high-pressure nor the low-pressure emergency core cooling systems (ECCS) are available at any time during the accident (Events U and V, respectively). The faults in these makeup systems are taken to be such that the systems are unavailable in any of their modes of operation. In addition, the control rod drive (CRD) flow to the reactor pressure vessel (RPV) is modeled as being lost due to the accident initiator. Thus, for this event, no water makeup to the RPV occurs; and, neither primary system nor containment heat removal is assumed available. All other plant systems, including emergency diesels, are modeled to be available. No credit is taken for any operator action other than to energize the containment igniter system at the accident initiation and to manually depressurize the vessel when the water level drops to the RPV Level 2 LOCA setpoint. The T₁QUV base case accident chronology is provided on Table 4.1.

4.1.2 Primary System and Containment Response

The loss of off-site power, the loss of feedwater, the turbine stop valve (TSV) closures, and the turbine bypass valve (TBV) closures are modeled to occur simultaneously. Loss of off-site power and the TSV closures actuate a reactor scram which is modeled to bring the reactor subcritical by 7.8 sec. The core power remains at decay heat levels for the remainder of the event. The TSV and TSB closures cause a RPV pressure excursion which is relieved by the safety/relief valves (SRV). Steam released from the RPV through the SRVs is routed to the suppression pool (SP), where it is quenched. By 95 sec,

Table 4.1
GRAND GULF NUCLEAR STATION
T₁QUV - BASE CASE
ACCIDENT CHRONOLOGY

Time	Event
0.0 sec	Initiating Event: Loss of off-site power; Loss of main feedwater; TSV/TBV closures
7.8 sec	Reactor scram completed
95 sec	RPV Level 2 LOCA setpoint reached
26.0 min	RPV Level 1 LOCA setpoint reached; Vessel depressurization manually initiated
26.5 min	DW purge system actuates
28.0 min	Core begins to uncover
57.0 min	SPMU actuates
2.0 hr	Fuel melting begins
2.35 hr	High DW pressure LOCA setpoint reached
2.35 hr	Core plate failure followed by vessel failure
47.0 hr	Containment failure

sufficient RPV water inventory has been lost through the cycling SRVs to lower the RPV water level to the RPV Level 2 LOCA setpoint. At the Level 2 setpoint, signals are automatically generated to trip off the recirculation pumps and to actuate the high pressure core spray (HPCS) and reactor core isolation cooling (RCIC) systems. Since both HPCS and RCIC are unavailable, the RPV water level continues to drop, reaching the RPV Level 1 LOCA setpoint at 26 min. At this point, it is assumed that manual depressurization of the vessel is initiated. In addition, permissive signals are automatically generated for the drywell (DW) purge, the suppression pool makeup (SPMU), the low pressure core spray (LPCS), and low pressure coolant injection (LPCI) systems. The DW purge system is modeled to actuate after a programmed 30 sec delay. Then, the DW purge compressors pressurize the DW atmosphere to the 1.89 psig High DW Pressure LOCA setpoint by 2.35 hours into the event. The SPMU system actuates the upper containment pool dump following a programmed 30 min delay. Since neither LPCS nor the LPCI are available, the RPV level continues to fall, and the core begins to uncover at 28 min.

Temperatures in the uncovered fuel regions begin to rise, and begin to reach 2000°F in about .5 hour after core uncover. The cladding oxidation rate increases rapidly above the 2000°F fuel temperature point. Oxidation of the Zircaloy cladding increases the fuel heatup rate and thus tends to promote further cladding oxidation. Cladding oxidation within a channel is limited, however, by refreezing of molten cladding in lower, cooler portions of the channel. The steam trying to enter the channel is diverted around the blockage, thus preventing further oxidation and hydrogen formation within the channel (see Ref. [4.2]). Hydrogen generated by the Zircaloy-steam reaction in the core is released to the wetwell via the cycling SRVs. The amount released in the vessel is insufficient to cause burning. The maximum release rate being approximately 0.05 lb/sec.

Fuel melting is predicted to begin at 2.0 hr. Molten fuel is modeled to relocate to the core plate. By 2.35 hr, sufficient molten core material is accumulated on the core plate (20% of total) to cause it to fail. The core debris then flows to the bottom of the RPV, initiates thermal attack of the vessel wall and fails the vessel at a welded penetration. Following vessel failure, the molten core debris is discharged onto the pedestal floor.

DRAFT

Due to the depressurized state at the time of vessel failure, no core debris is dispersed from the pedestal onto the drywell floor. The discharge of molten core debris from the vessel is followed by the lower plenum water. Some of this water spills from the pedestal to the drywell. After vessel failure, about 50,000 lb of water remains in the lower downcomer region of the vessel.

Following vessel failure, the pedestal and drywell volumes are filled with steam; and, the air in these compartments is exhausted through the SP vents into the outer containment compartments. The pressures and temperatures in the drywell and in the outer containment are shown on Figs. 4.1 through 4.4. Drywell leakage flow paths bypassing the suppression pool are modeled to plug with aerosols. These aerosols are released from the vessel when it fails and from the core-concrete interaction in the pedestal. All flow exiting the drywell to the outer containment is afterward forced to pass through the suppression pool. Within ten minutes after vessel failure, the core debris bed in the pedestal is cooled to below concrete ablation temperatures by the lower plenum water; an ablation depth of 0.3 ft is predicted to this point in the accident sequence. The core debris temperature and concrete penetration depth in the pedestal are provided on Figs. 4.5 and 4.6. The debris remains quenched until its blanket of water is boiled away, which occurs at 4.0 hr into the event. Corium within the pedestal re-heats, renewing its attack on the pedestal concrete floor and walls at about five hours.

The thermal decomposition of the pedestal concrete floor and walls causes significant ablation (see Fig. 4.6), and produces large volumes of carbon dioxide and steam. As these two gases pass through the partially molten corium debris bed in the pedestal, they oxidize the zirconium in the bed to produce hydrogen gas and elemental carbon. The hydrogen production resulting from the core-concrete interaction in the pedestal raises the hydrogen concentration to ignitable levels; and within minutes after vessel failure, the igniters start the hydrogen burning. The igniters, which are powered by the emergency bus, provide for an almost continuous controlled burn-off of all combustible gases being evolved during the accident. The burnoff prevents the accumulation of high concentrations of combustible gases. By about 13 hr, 100% of the zirconium has been oxidized. About 1800 lb of

T10UV - GRAND GULF

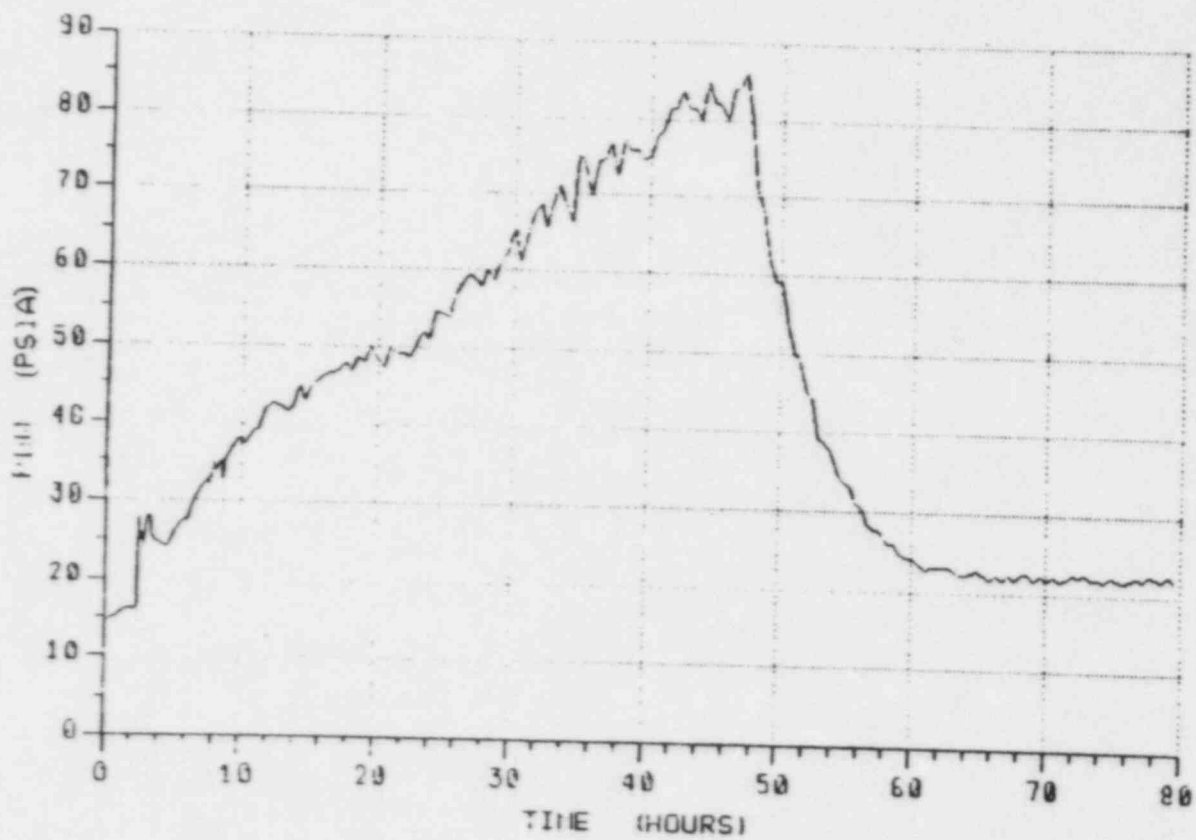


Fig. 4.1 Pressure in the drywell.

T10UV - GRAND GULF

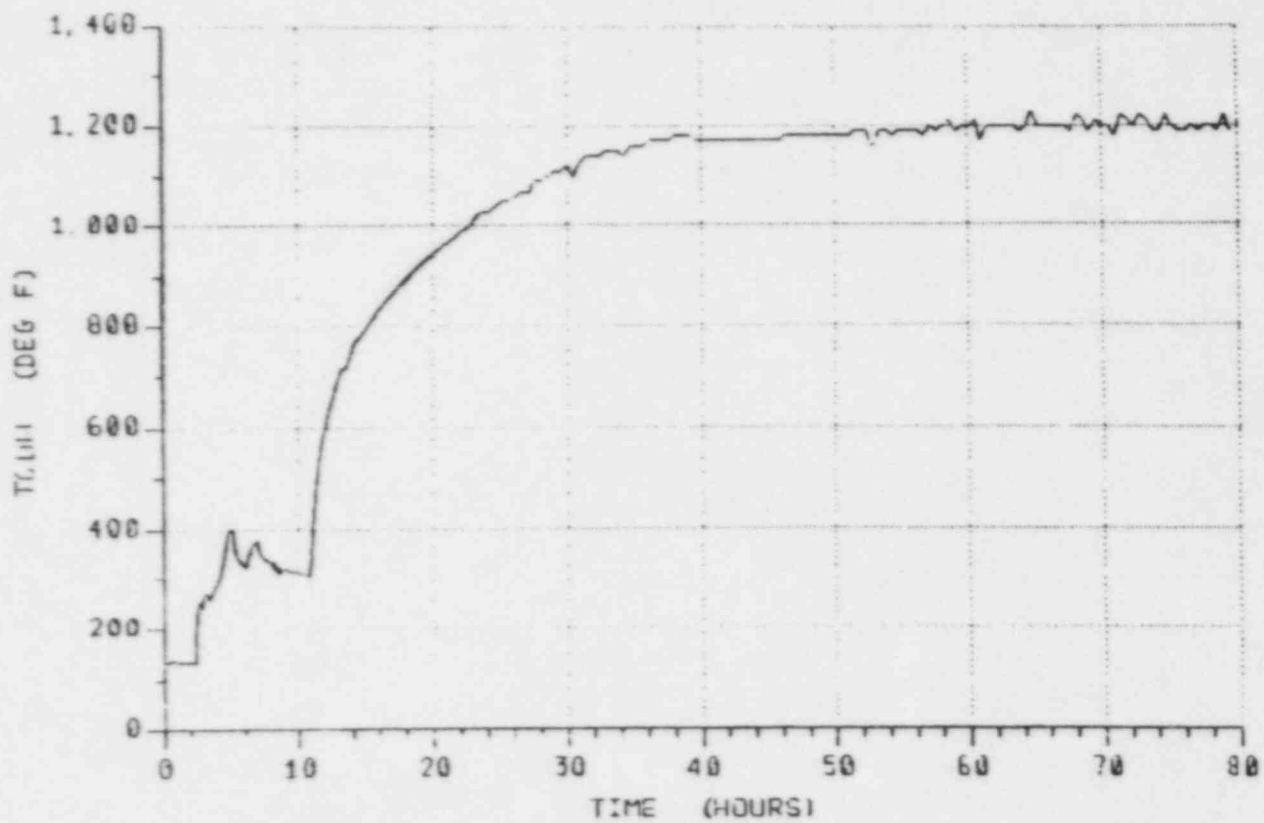


Fig. 4.2 Temperature of gas in the drywell.

T1QUV - GRAND GULF

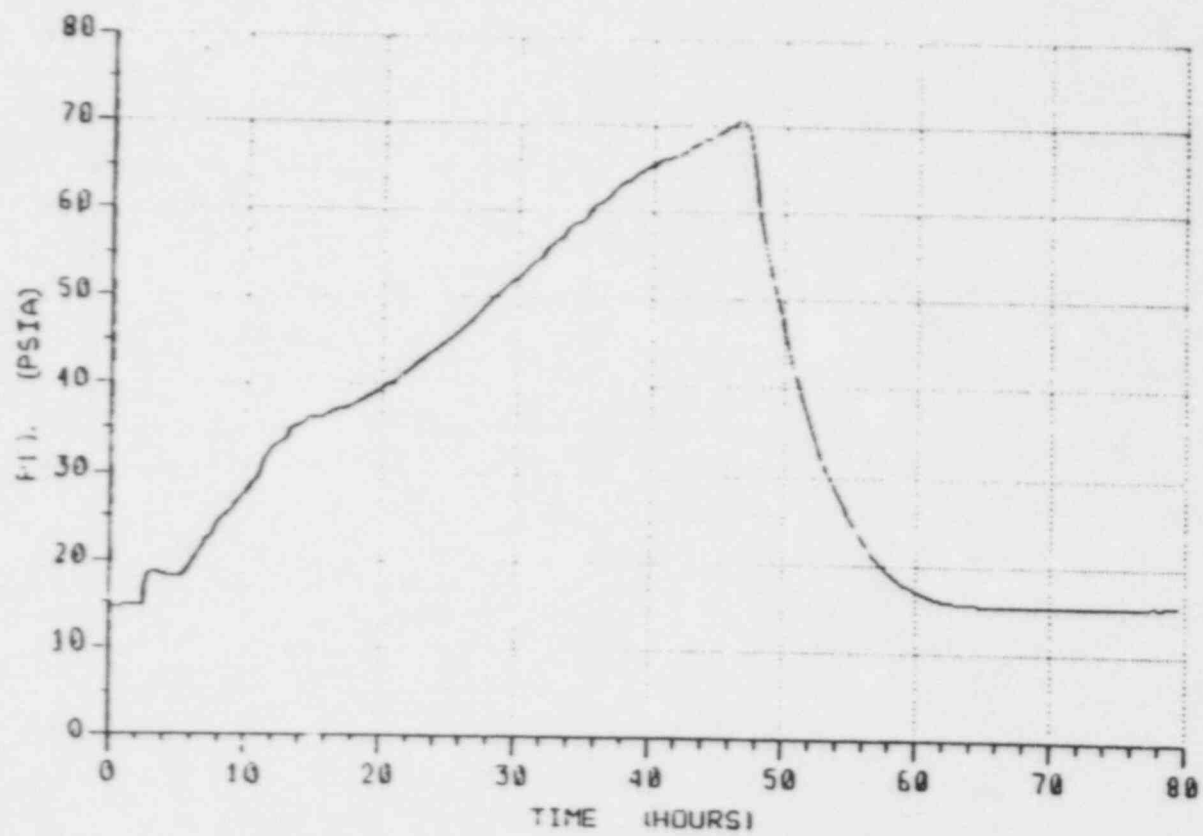


Fig. 4.3 Pressure in Compartment B.

T10UV - GRAND GULF

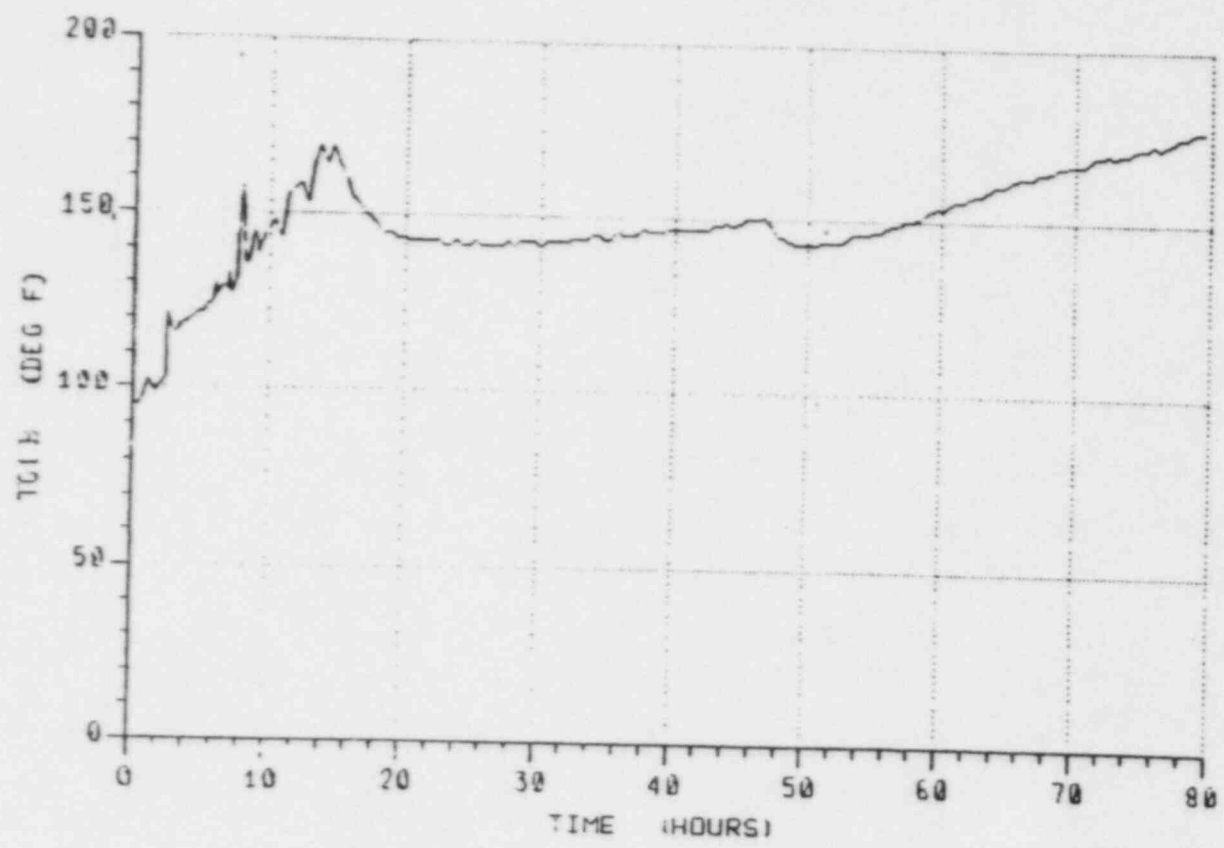


Fig. 4.4 Temperature of gas in Compartment B.

T1QUV - GRAND GULF

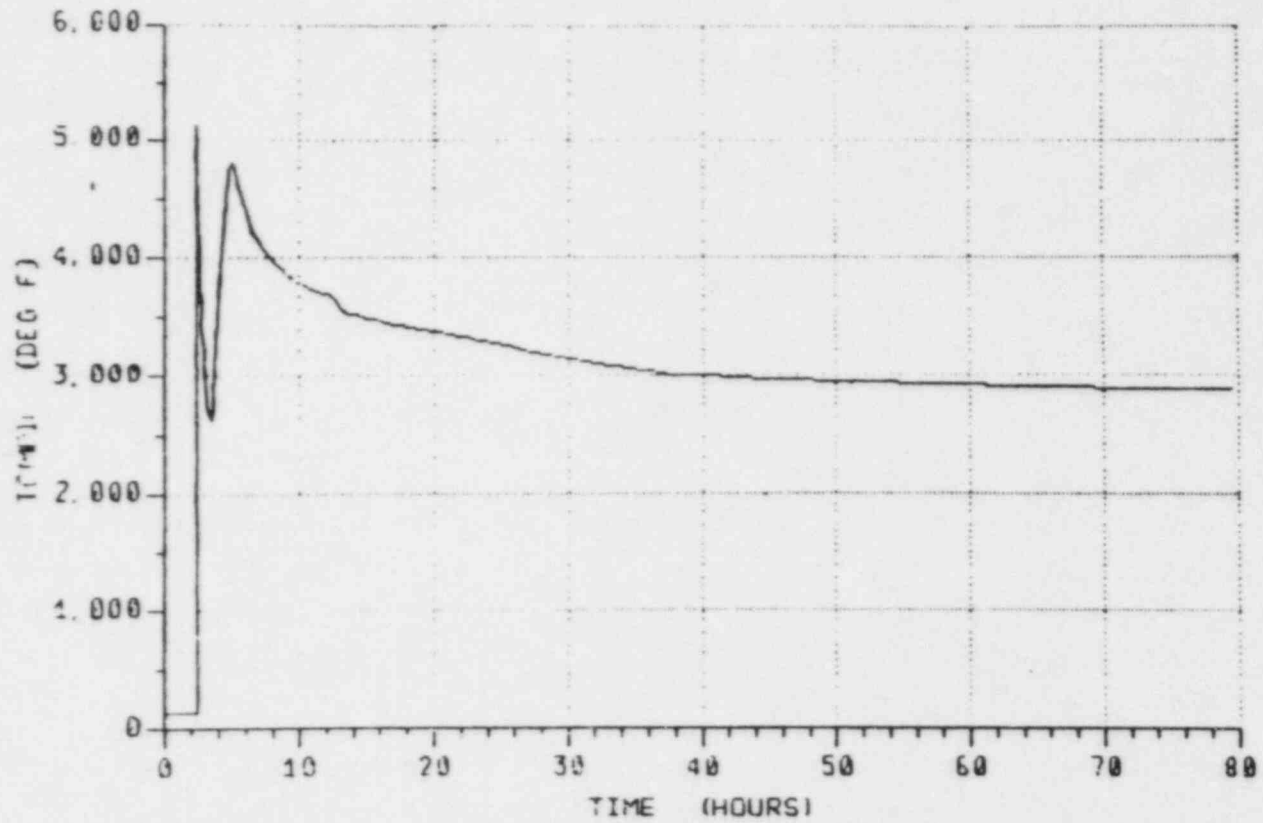


Fig. 4.5 Average corium temperature in the pedestal.

T1QUV - GRAND GULF

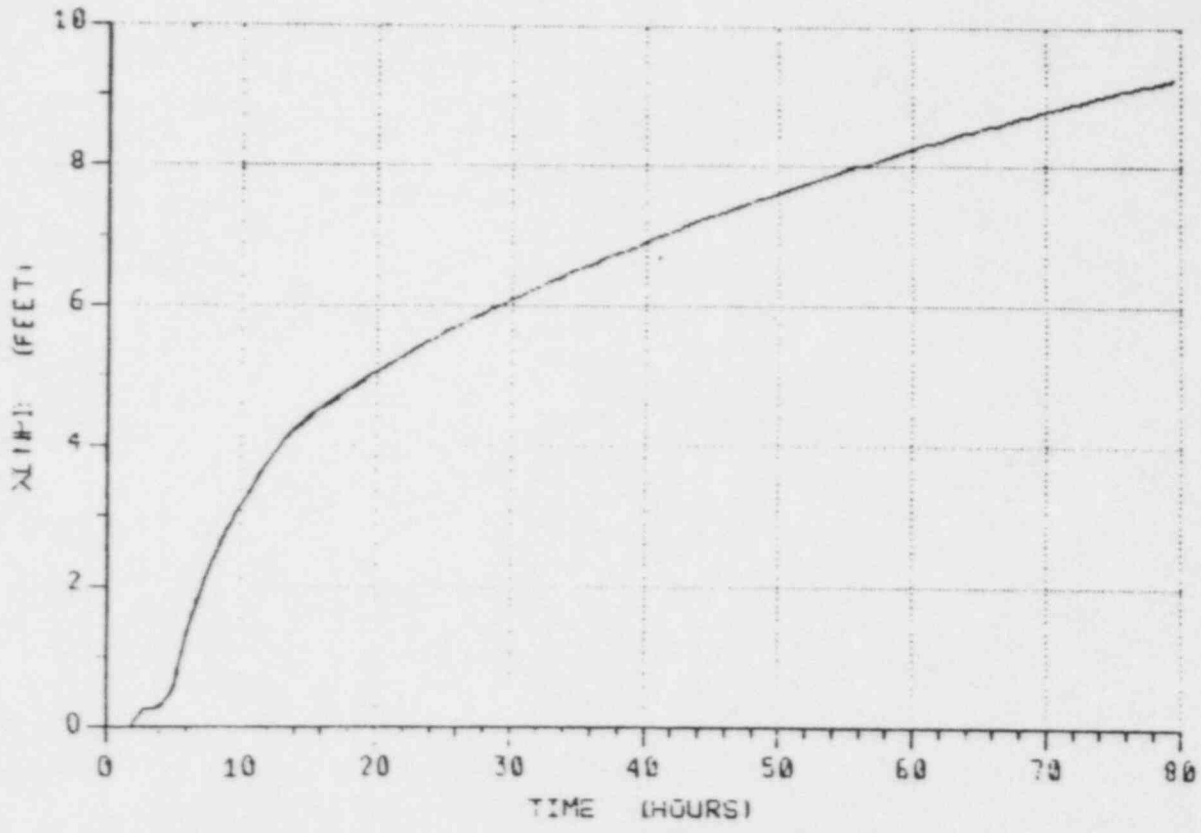


Fig. 4.6 Concrete ablation depth in the pedestal.

hydrogen have been produced and burned to this point. Afterward, the endothermic reactions of elemental carbon with steam and with carbon dioxide begin in the corium debris bed, and hydrogen and carbon monoxide are evolved. At about 15 hours, when the oxygen concentration falls below a combustible level in all containment compartments, burning ceases. At about 38 hr, the corium inventory of elemental carbon is exhausted and combustible gas production ceases; steam and carbon dioxide gas production continues. A total of 3000 lb of hydrogen and 75,000 lb of carbon monoxide is calculated to be produced during this accident. Note, however, that less than 100 lb of the hydrogen came from in-vessel production.

Primarily because the primary system was depressurized prior to vessel failure, debris did not disperse from the pedestal to the drywell. Consequently, the temperature and pressure in the drywell behave as shown in Figs. 4.1 and 4.2. Note the rapid pressure rise in the drywell after vessel failure to about 26 psia due to debris entering the pedestal. The drywell temperature rise following vessel failure is due to the corium/concrete attack in the pedestal.

At 47 hr into the event, the GGNS containment reaches 71.3 psia (see Fig. 4.3). The containment is assumed to fail at this pressure at a location just below the junction between the cylinder and the dome [4.1]*. The failure cause is overpressurization by noncondensable gases. A containment breach area of 0.1 ft^2 was selected for modeling the containment depressurization. For this containment failure size and location, the containment depressurizes to within about 0.5 psid of atmospheric pressure in about 10 hours. The suppression pool remains intact following the containment failure event. As can be seen in Fig. 4.7, the pool temperature is less than 200°F at the time of the containment failure. Note that the suppression pool remains subcooled throughout the accident. Appendix B includes additional plots of results for this sequence.

*This is consistent with the analyses reported in Ref. [4.1] which only addressed the ultimate capacity. Consequently, failure modes were not addressed, specifically the effects on penetrations under large deflections.

T100V - GRAND GULF

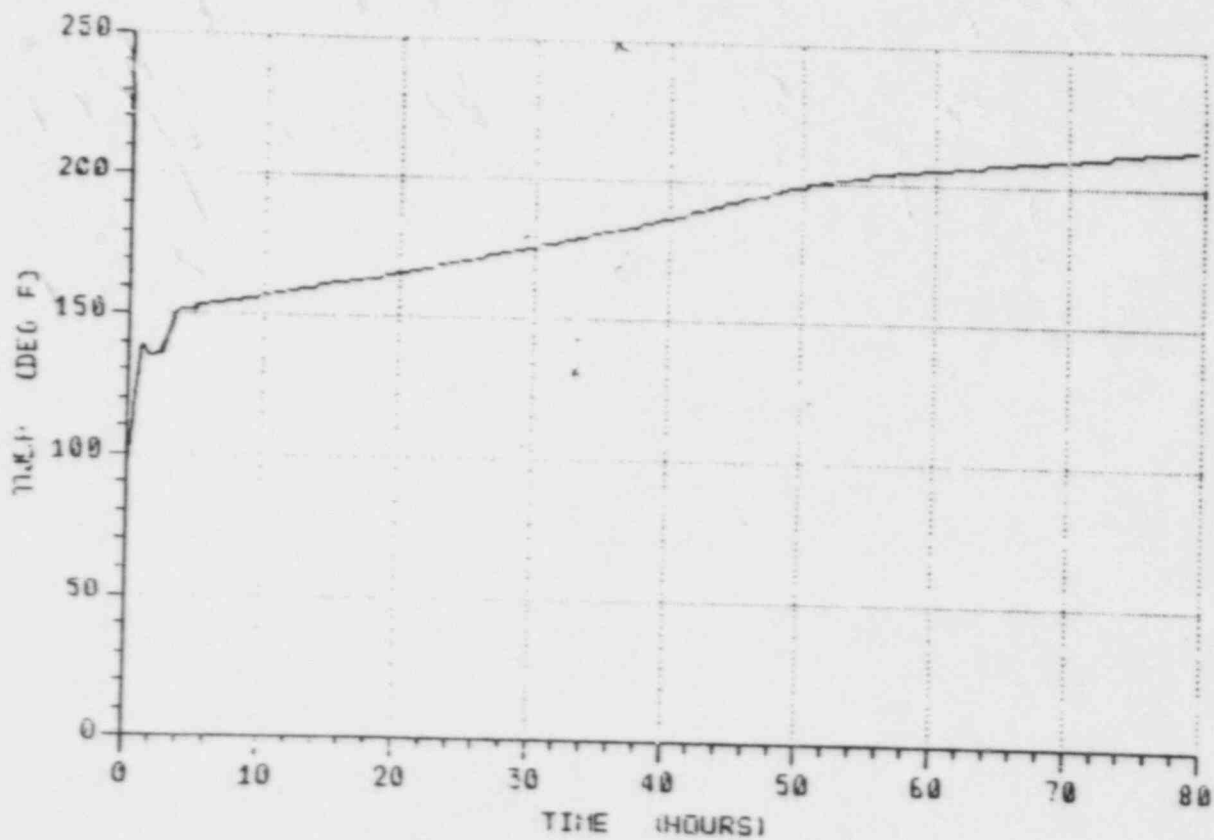


Fig. 4.7 Temperature of the suppression pool.

4.1.3 Manual Depressurization Sensitivity Analysis

In order to assess the sensitivity of the accident response to the assumption of manual vessel depressurization prior to vessel failure, the T₁QUV accident scenario was reanalyzed without vessel depressurization. No major variations in the sequence resulted, although some of the details differed. Key differences between this analysis and the base case are shown in Table 4.2.

For the most part, differences from the base case prior to vessel failure are small, and are due core degradation occurring at an elevated or reduced pressure. The only significant differences are the longer time to vessel failure, the increased in-vessel hydrogen production, and the higher primary system gas temperatures. The first two are due to the slower boiloff of primary system water, and the latter is due to the higher hydrogen generation rates.

Following vessel failure, most of the molten core debris exiting the vessel is dispersed from the pedestal to the drywell, in contrast. No such dispersion occurs into the base case. Despite this difference, Table 4.2 shows that the difference in drywell pressurization from the dispersal is not large between the two cases. Since the core debris in the drywell is well-dispersed, the heat losses are too large for the debris to reach concrete ablation temperatures. The gas and structural temperatures in the drywell rise more quickly than in the base case, however.

There is less concrete attack in the pedestal than in the base case due to the smaller corium inventory in the pedestal. This results in a slower ablation rate, less noncondensable gas generation, and a longer time to containment failure. In summary, while there are minor differences in the accident progression, these would not substantially alter the overall accident response.

Table 4.2

EFFECTS OF DEPRESSURIZATION IN THE T₁QV ACCIDENT

Quantity	Depressurization at 0.43 hr	No Depressurization Until Vessel Failure
Core Uncovery Time, hr	0.47	0.62
Vessel Failure Time, hr	2.35	3.4
Containment Failure Time, hr	47.0	60
In-Vessel Hydrogen Production, lb	10	430
Mass of Core Debris in Dry- well Following Vessel Failure, lb	0	48,000
Pressure in Drywell Follow- ing Vessel Failure, psia	26	45
Gas Temperature in Drywell at Vessel Failure, °F	370	550
Concrete Ablation in Pedestal at 50 hr	7.6	7.2
Total Hydrogen Produced, lb	3,000	3,200
Total Carbon Monoxide Produced, lb	75,000	66,000

4.2 Plant Response to the AE Accident

4.2.1 Sequence Description

The AE accident is assumed to occur during full-power operation. This accident is a large-break loss of coolant accident (LOCA). It is initiated by a 3.14 ft² liquid line break (Event A) in the suction side of the recirculation loop. The accident sequence specifies that neither the high-pressure nor the low-pressure emergency core cooling systems (ECCS) are available at any time during the accident (Event E). The faults in these makeup systems are taken to be such that the systems are unavailable in any of their modes of operation. Thus, for this event, the only water makeup to the reactor pressure vessel (RPV) is due to the control rod drive (CRD) flow; neither the primary system nor containment heat removal is assumed available. All other plant systems are modeled to be available. No credit is taken for any operator action other than to start the containment igniter system at the accident initiation. The AE accident chronology is provided on Table 4.3.

4.2.2 Primary System and Containment Response

The loss of coolant through the primary system break causes a rapid depressurization of the RPV and a rapid pressurization of the drywell (DW). The DW pressure reaches the 1.73 psig and 1.89 psig high drywell pressure LOCA setpoints by 0.2 sec into the accident. The former generates a reactor scram signal; the latter generates actuation signals for the high pressure core spray (HPCS), the low pressure core spray (LPCS), and the low pressure coolant injection (LPCI) systems. The reactor scram is modeled to bring the reactor subcritical by 3.9 sec. The core power remains at decay heat levels for the remainder of the event. Since the HPCS, LPCS and LPCI are assumed unavailable, the RPV level drops to the RPV Level 2 LOCA setpoint. At this point, 5.2 sec into the event, the recirculation pumps are signaled to trip off and the reactor core isolation cooling (RCIC) system is signaled to start. The recirculation pump trips are completed by 5.6 sec; RCIC is assumed unavailable. The RPV water level falls to the RPV Level 1 LOCA setpoint at 6.5 sec. At this point, the main feedwater system trips off and the main steam isolation valves (MSIV) close. In addition, permissive signals are generated for

Table 4.3
GRAND GULF NUCLEAR STATION
AE BASE CASE
ACCIDENT CHRONOLOGY

Time	Event
0.0 sec	Initiating Event: A large break in suction side of a recirculation loop
0.2 sec	High DW pressure LOCA setpoints reached
3.9 sec	Reactor scram completed
5.2 sec	RPV Level 2 LOCA setpoint reached
6.5 sec	RPV Level 1 LOCA setpoint reached; MSIVs close; Main feedwater pumps trip off
45.0 sec	Core begins to uncover
11.6 min	DW purge system actuates
30.4 min	SPMU actuates
1.1 hr	Fuel melting begins
1.4 hr	Core plate failure followed by vessel failure
22.3 hr	CSF drained and CRD flow to vessel ceases
58.0 hr	Containment failure

the suppression pool makeup (SPMU) and the drywell (DW) purge systems. The SPMU system releases the upper containment pool following a programmed 30 minute delay. DW purge actuation is delayed until other permissives are satisfied. Without sufficient water inventory makeup, the core begins to uncover at 45 sec.

Temperatures in the uncovered fuel regions begin to rise and begin to reach 2000°F at about 13 min. The cladding oxidation rate increases rapidly above this point. Oxidation of the Zircaloy cladding, in turn, increases the fuel heatup rate and tends to promote further cladding oxidation. Since the boiloff time is short for the large-break LOCA response, in-vessel Zircaloy oxidation is minimal.

Fuel melting is predicted to begin at 1.1 hr, and relocates to the core plate. By 1.4 hr, sufficient core material is calculated to have fallen onto the RPV core plate to cause it to fail. The core debris then falls to the bottom of the RPV and thirty seconds later, vessel failure occurs at a welded RPV penetration point.

At vessel failure, the molten fraction of the lower plenum core debris falls onto the pedestal floor followed by the saturated lower plenum water. A small steam spike occurs at this point, causing a pressure rise in the pedestal and drywell to about 26 psia. Since the vessel was depressurized prior to failure, no debris is dispersed from the pedestal to the drywell. Drywell leakage flow paths bypassing the suppression pool are modeled to plug with aerosols. These aerosols are released from the vessel when it fails and from the core-concrete interaction in the pedestal. All flow exiting the drywell to the outer containment is afterward forced to pass through the suppression pool.

The debris attacks the concrete until it is cooled below concrete ablation temperatures by the lower plenum water at about two hours. The concrete is ablated to a depth of 2.5 inches up to this time. The remaining water in the pedestal, plus that continually added by the CRD flow, is boiled away while slowly quenching the debris, as can be seen on Figs. 4.8 and 4.9. By about seven hours, the debris and the water are at about the same

AE - GRAND GULF

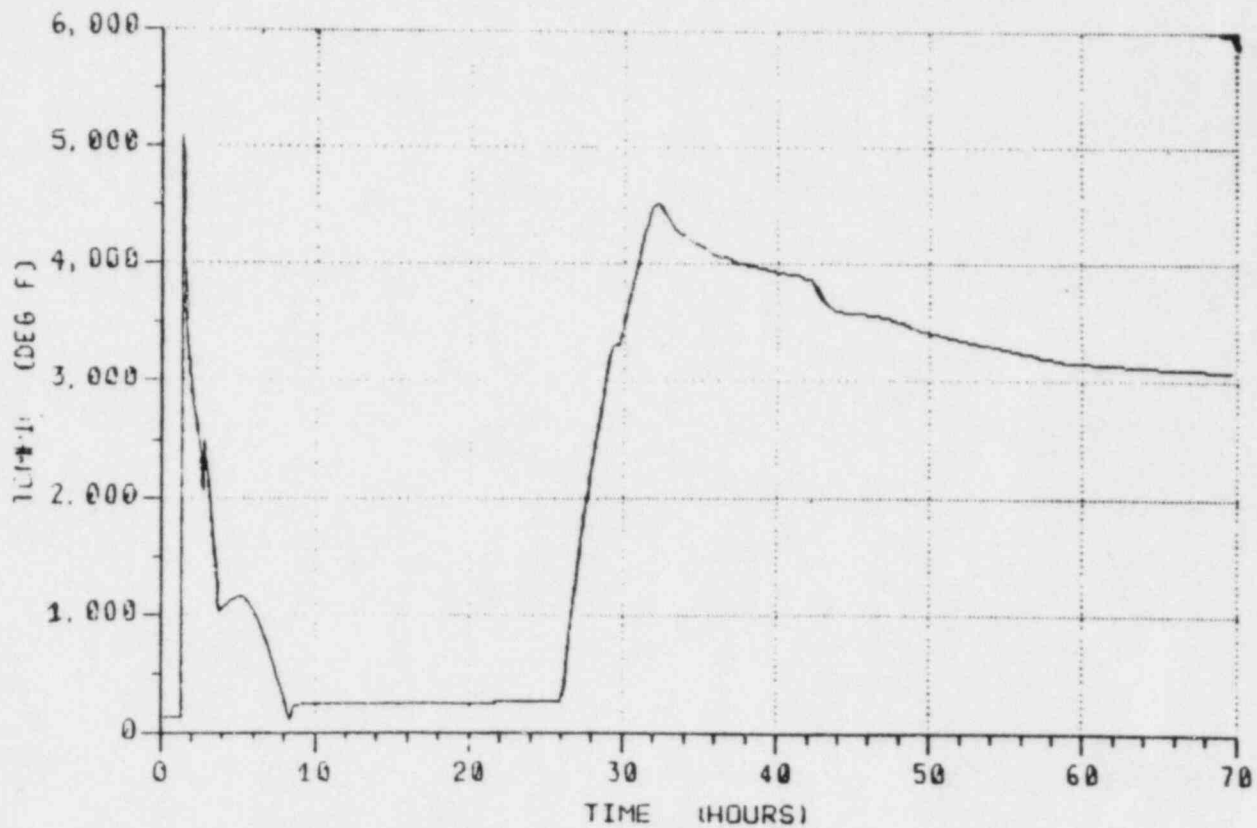


Fig. 4.8 Average corium temperature in the pedestal.

AE - GRAND GULF

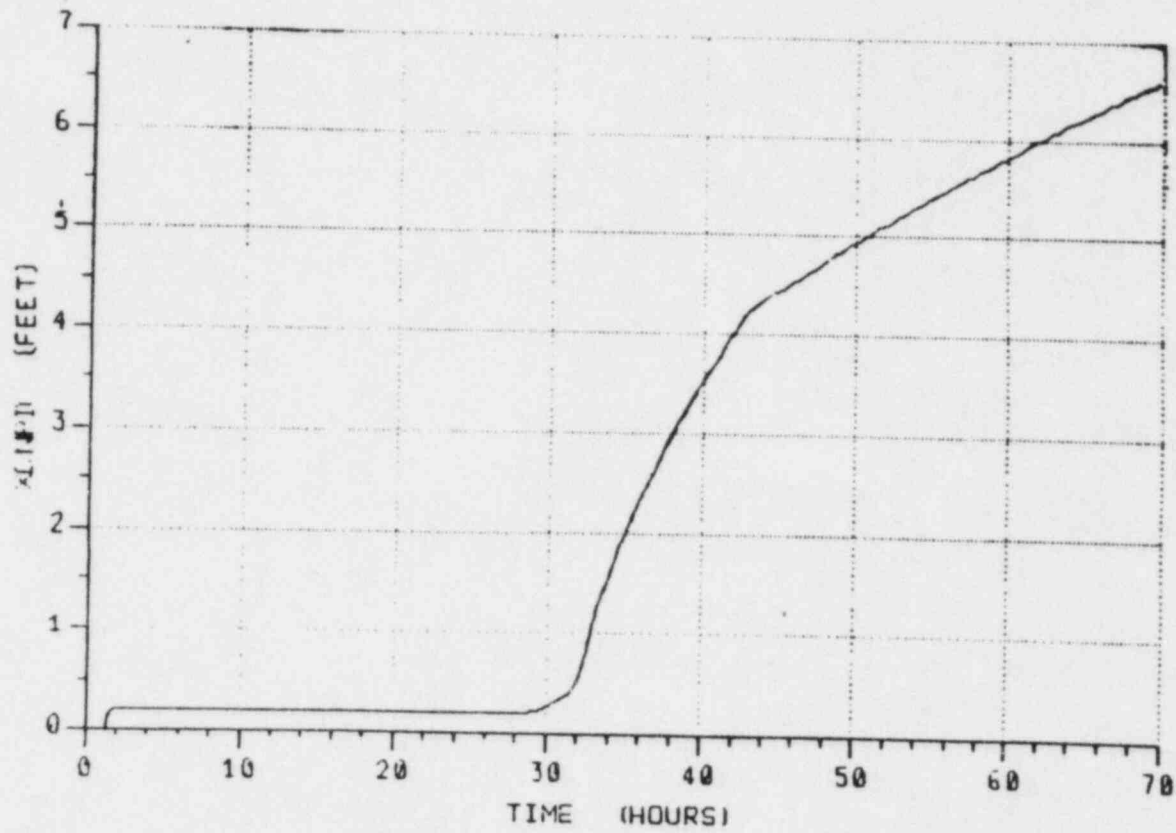


Fig. 4.9 Concrete ablation depth in the pedestal.

temperature. From this point on, the continuing CRD flow into the pedestal refills it to the pedestal doorstep level. Excess water spills into the drywell. The CRD flow keeps the debris quenched until the CST runs out of water at 22.3 hours. Without replenishment, the pedestal water boils away and, by 26 hours the debris begins to reheat. Concrete ablation in the pedestal resumes at 30 hours.

The thermal decomposition of the pedestal concrete floor and walls produces large volumes of carbon dioxide and steam. As these two gases pass through the partially molten corium debris bed in the pedestal, they oxidize the zirconium in the bed to produce hydrogen gas and elemental carbon. The igniters provide for an almost continuous controlled burn-off of all combustible gases being evolved during the accident. The first burn begins at about 35 hours; thereafter, their continuous burn-off prevents high concentrations of combustible gases from occurring. By 43 hr, 100% of the zirconium has been oxidized. At this point, the endothermic reactions of elemental carbon with steam and with carbon dioxide begin in the corium debris bed. Hydrogen and carbon monoxide are evolved in these reactions. At about 45 hours, when the oxygen concentration falls below a combustible level in all containment compartments, burning ceases and the containment becomes self-inerted.

Drywell temperatures rise to about 900°F after the core debris-concrete interaction resumes in the pedestal, as shown on Fig. 4.10. The suppression pool water temperature, shown on Fig. 4.11, reaches saturation due to the large amount of steam generated by quenching the debris in the pedestal prior to dryout. Temperatures in compartment B remain relatively low due to the cooling effect of the suppression pool (as shown in Fig. 4.12).

At 58 hours into the event, the GGNS containment reaches 71.3 psia (see Fig. 4.13). The containment is modeled to fail at this pressure at a location just below the junction between the cylinder and the dome. The cause is overpressurization by steam and by noncondensable gases. A containment breach area of 0.1 ft^2 was selected for modeling the containment depressurization. For this containment failure size and location, the containment depressurizes to within 0.5 psid of atmospheric pressure in about 10 hours. And, the suppression pool remains intact following the containment failure event.

AE - GRAND GULF

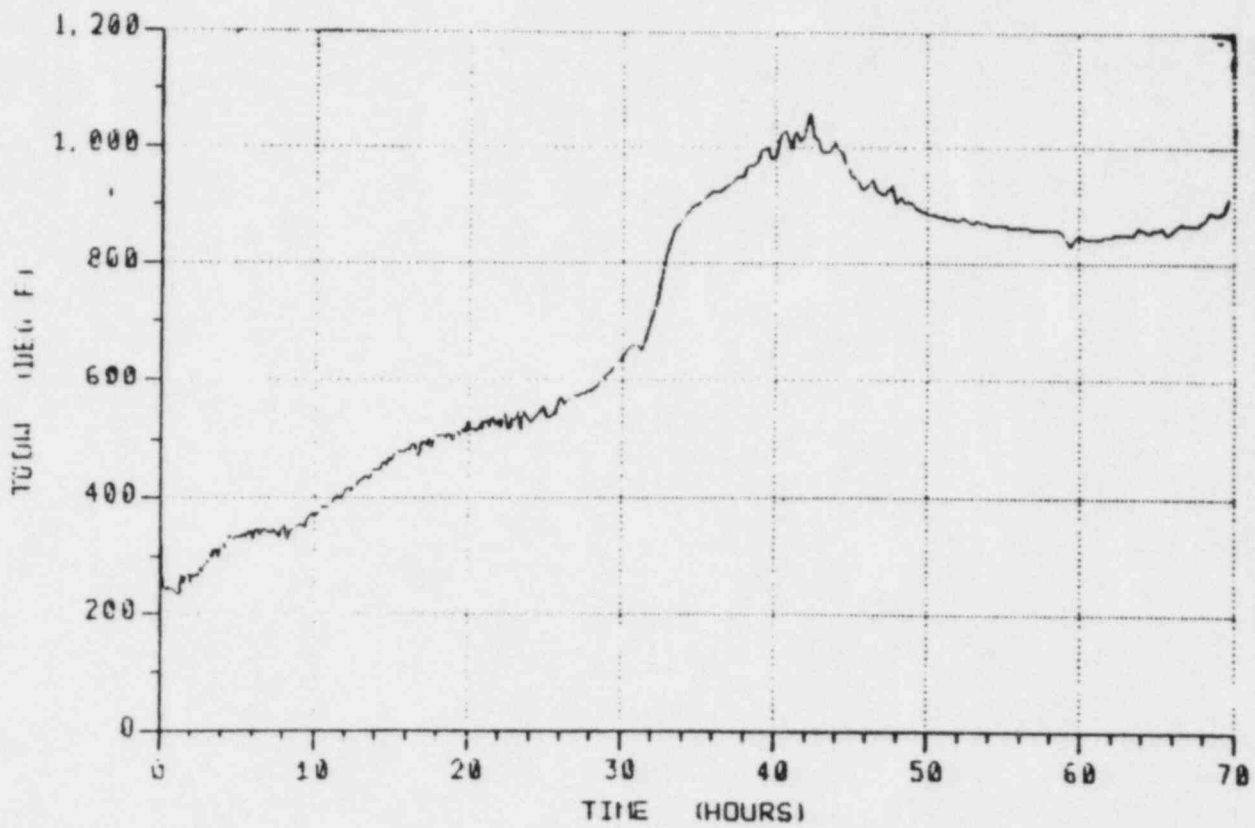


Fig. 4.10 Temperature of gas in the drywell.

AE - GRAND GULF

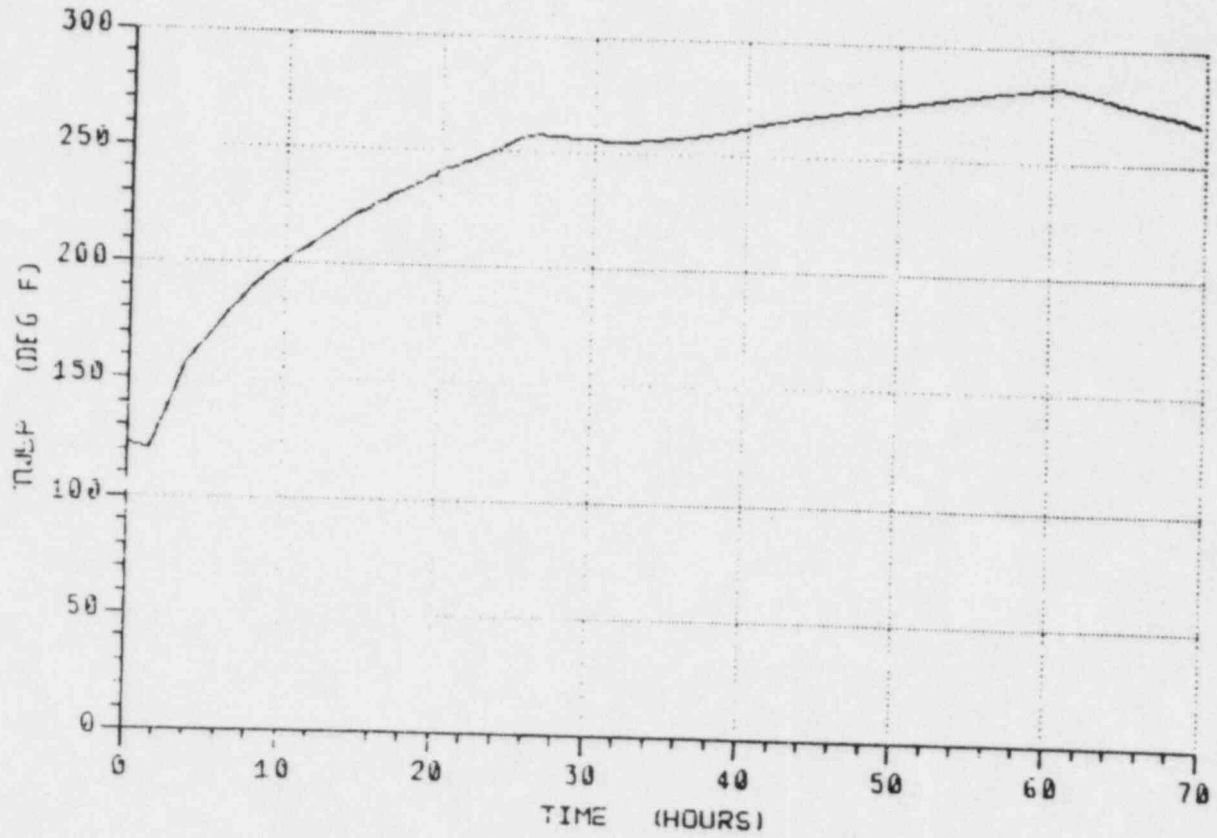


Fig. 4.11 Temperature of the suppression pool.

AE - GRAND GULF

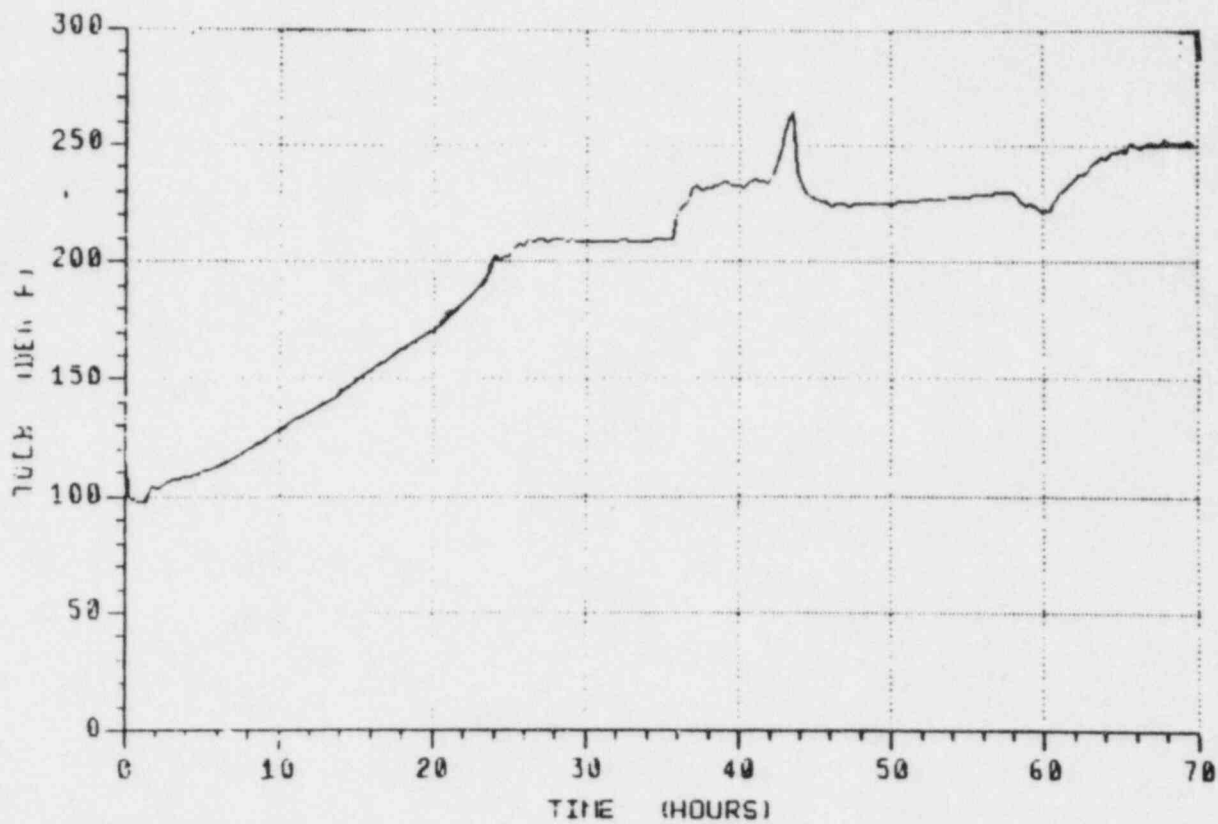


Fig. 4.12 Temperature of gas in Compartment B.

AE - GRAND GULF

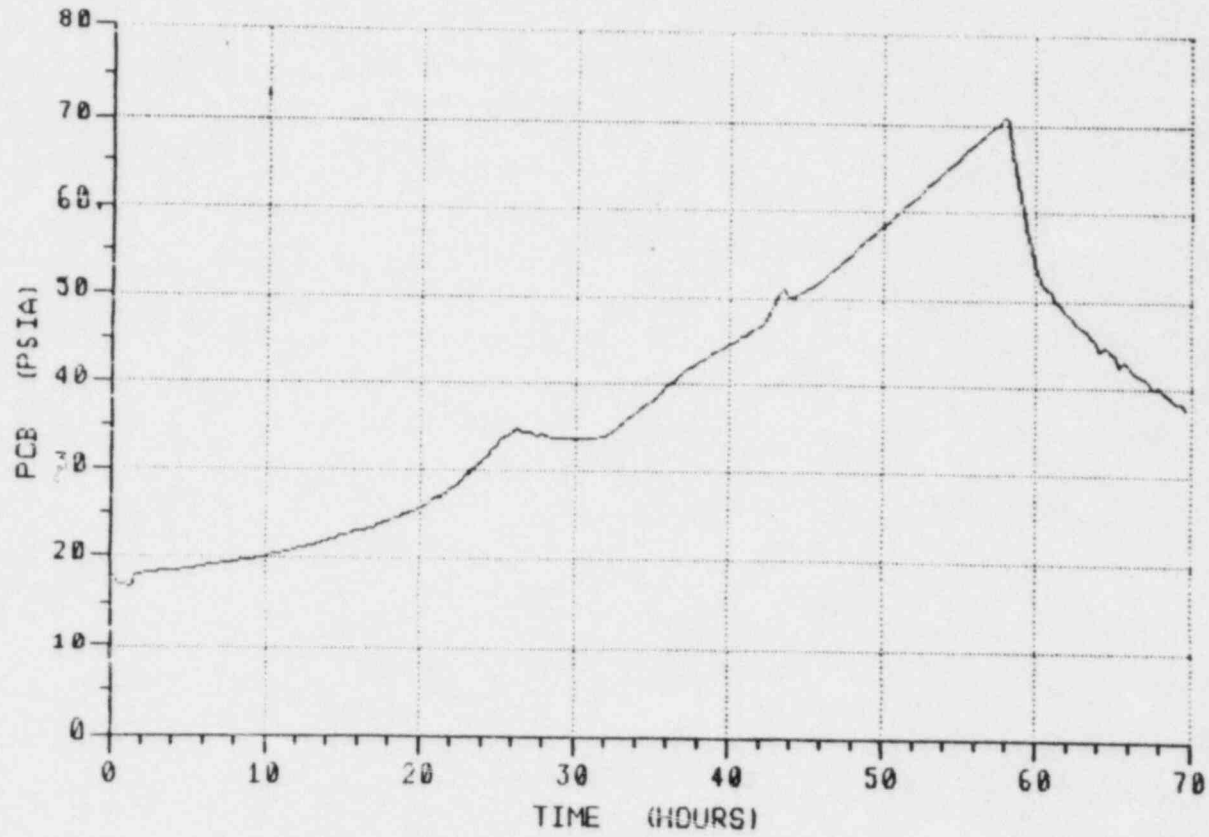


Fig. 4.13 Pressure in Compartment B.

Since the pool temperature is nearly 280°F at the time of the containment failure, about 2% of the pool inventory is calculated to boil away within 10 hrs following failure. Appendix B includes additional plots of results for this sequence.

4.3 Plant Response to the T₂₃QW Accident

4.3.1 Sequence Description

The T₂₃QW accident is assumed to occur during full-power operation. It is initiated by inadvertent main steam isolation valve (MSIV) closures (Event T₂₃). The main feedwater and main condenser are assumed to be unavailable (Event Q) for the entire accident. The accident sequence also specifies that containment heat removal is not available for the entire accident (Event W). Control rod drive (CRD) flow to the reactor pressure vessel (RPV) is modeled to be available. All other plant systems are assumed to be available. However, all emergency core cooling systems (ECCS) are assumed to fail on containment failure. No credit is taken for any operator action other than to start the containment igniter system at the accident initiation and to manually depressurize the RPV when the suppression pool temperature exceeds 145°F. The T₂₃QW accident chronology is provided on Table 4.4.

4.3.2 Primary System and Containment Response

The initiating event, which is inadvertent closure of the MSIV, causes a reactor pressure vessel (RPV) pressure excursion which is relieved by the safety relief valves (SRV). The exiting RPV steam is routed to the suppression pool (SP), where it is quenched. The MSIV closures actuate a reactor scram which is modeled to bring the reactor subcritical by 3.7 sec into the event. The core power remains at decay heat levels for the remainder of the event. At 2.35 hours into the accident the suppression pool temperature exceeds 145°F and an operator intervention occurs to manually initiate ADS.

At 4.1 hr, steam pressurization of the containment building causes a high drywell (DW) pressure LOCA signal. This signal is a permissive signal

DRAFT

4-28

Table 4.4
GRAND GULF NUCLEAR STATION
T₂₃QW - BASE CASE
ACCIDENT CHRONOLOGY

Time	Event
0 sec	Initiating event: MSIV closures; Loss of main feedwater
3.7 sec	Reactor scram completed
28 sec	RPV Level 2 LOCA setpoint reached
1.0 min	HPCS and RCIC systems begin operating
1.1 hr	HPCS and RCIC systems transfer suction from CST to SP
2.35 hr	Suppression pool temperature exceeds 145°C, manual ADS
4.1 hr	High DW pressure LOCA setpoint reached; DW purge system actuates; LPCS and LPCI actuate (but cannot provide makeup without RPV depressurization)
4.6 hr	SPMU actuates
6.3 hr	RCIC pump fails on high suction temperature
22.4 hr	CST empties
23.5 hr	High wetwell pressure setpoint reached; Containment sprays actuate
40.0 hr	Containment failure; All ECCS assumed to fail
48.8 hr	Core begins to uncover
54.1 hr	Fuel melting begins
56.2 hr	Core plate failure followed by vessel failure

for the DW purge system, the SP makeup (SPMU) system, and the automatic depressurization system (ADS); it is an actuation signal for the low pressure core spray (LPCS) and low pressure coolant injection (LPCI) systems. The DW purge system actuates after a 30 sec time delay and the SPMU system actuates the upper containment pool dump following a programmed 30 min delay. The RPV water inventory is maintained by the HPCS and RCIC systems. The high DW pressure LOCA signal is modeled to switch the HPCS and RCIC systems' level control logic to maintain the RPV water level about the RPV Level 8 setpoint.

Because of the assumed unavailability of containment cooling, the SP temperature rises during most of this event (Fig. 4.14). One exception to this trend occurs at 4.6 hr, when the SP makeup system releases relatively cold upper containment pool water into the SP. After the upper pool dump, the SP water temperature continues to rise again. When the SP temperature reaches 200°F at 6.3 hr, the RCIC pump is modeled to fail due to high bearing temperatures. After the loss of the RCIC, the HPCS and the CRD flow continue to maintain adequate RPV inventory. Driven by the steam produced in the core, the containment pressure reaches the 9 psig containment spray actuation pressure setpoint at 23.5 hr into the event. Note that the accident definition assumes that the RHR heat exchangers are unavailable. Thus, the operation of containment sprays removes no heat from the containment; it merely homogenizes temperatures in the outer containment. The effect of this homogenization can be observed in Figs. 4.14, 4.15 and 4.16: the suppression pool temperature decreases, the outer containment air temperatures increase, and, consequently, the outer containment pressure increases slightly. The latter pushes water from the wetwell to the drywell side of the suppression pool and results in a large spill of suppression pool water onto the drywell and pedestal floors. This water plays a key role in quenching the core debris after the vessel fails. At that time, trains A and B of the residual heat removal (RHR) system automatically switch into their spray mode. At 22.4 hr the CST empties and the CRD flow ceases. From this point on, only the HPCS is available to maintain inventory.

At 40 hr into the event, the GGNS containment pressure reaches 71.3 psia. The containment is modeled to fail at this pressure at a location just below the junction between the cylinder and the dome. The failure cause is

T230W - GRAND GULF

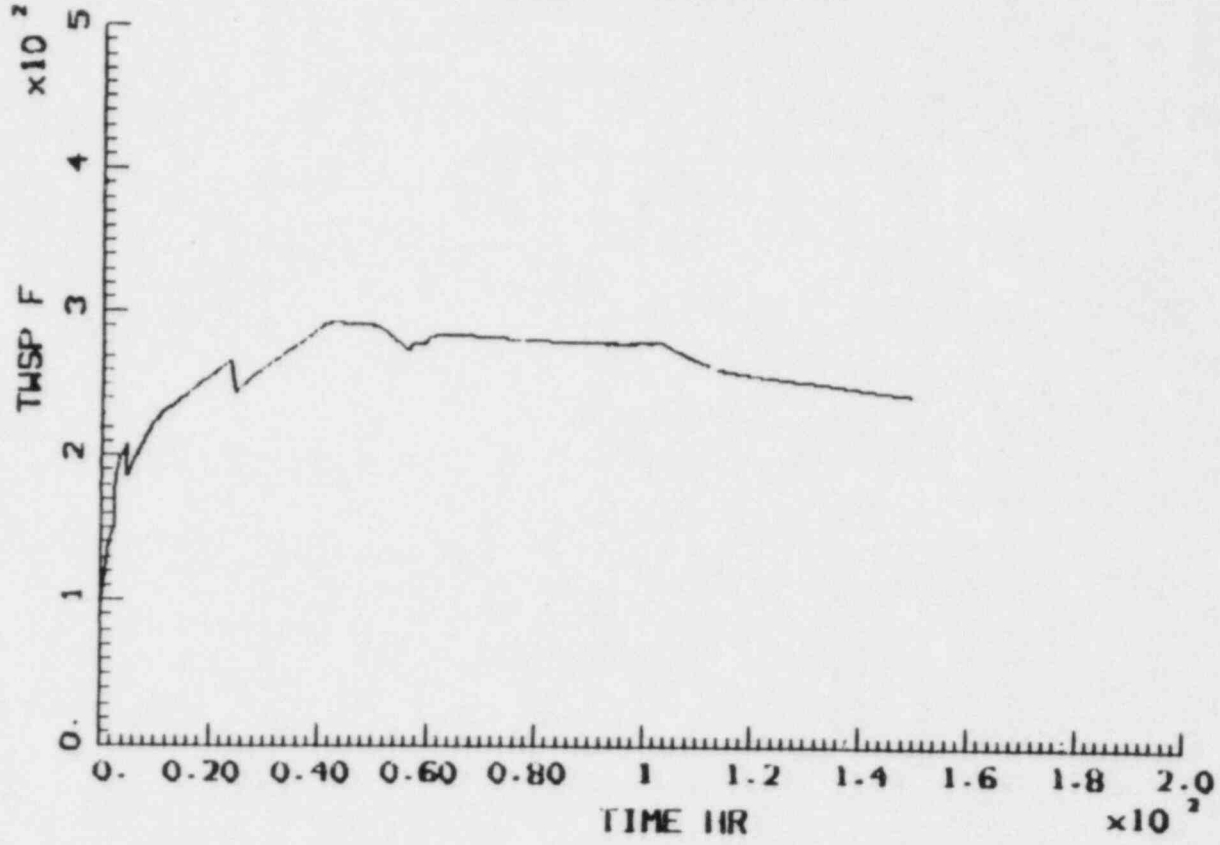


Fig. 4.14 Temperature of the suppression pool.

T230W - GRAND GULF

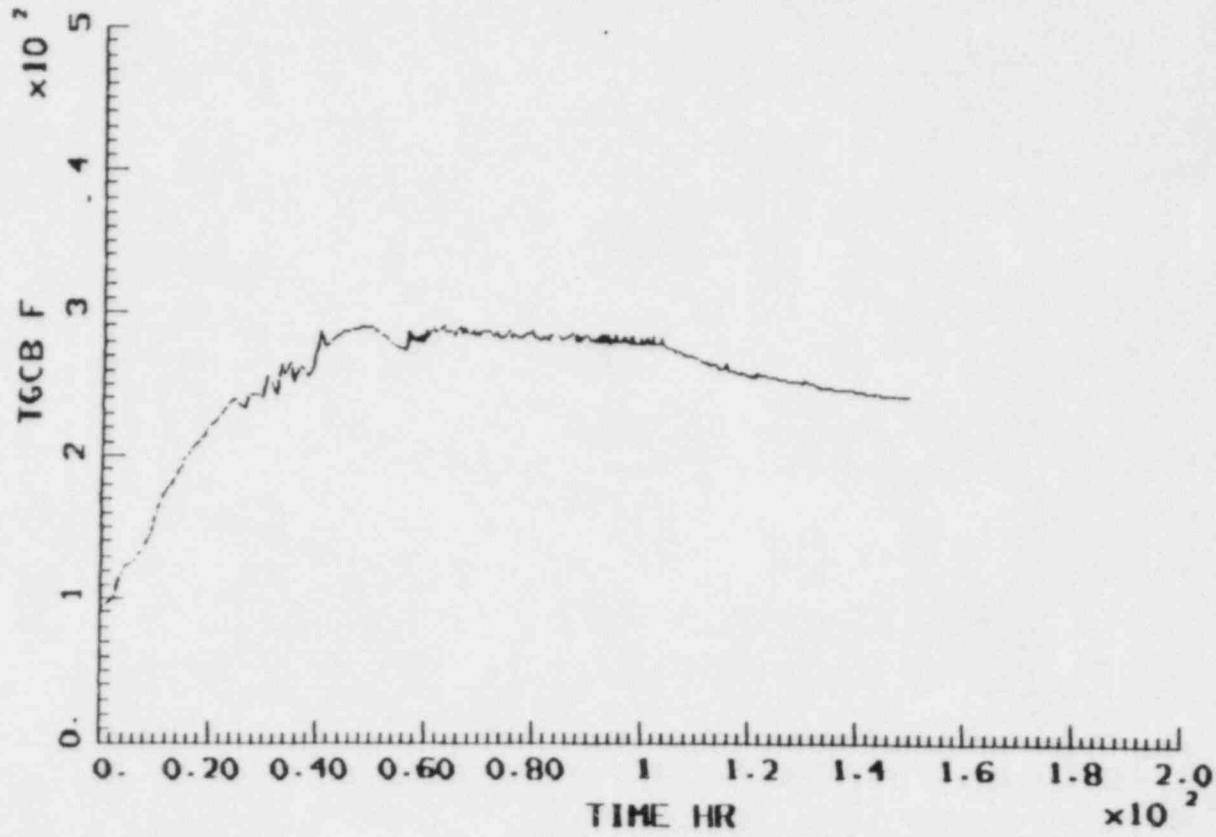


Fig. 4.15 Temperature of gas in Compartment B.

DRAFT

4-32

T236W - GRAND GULF

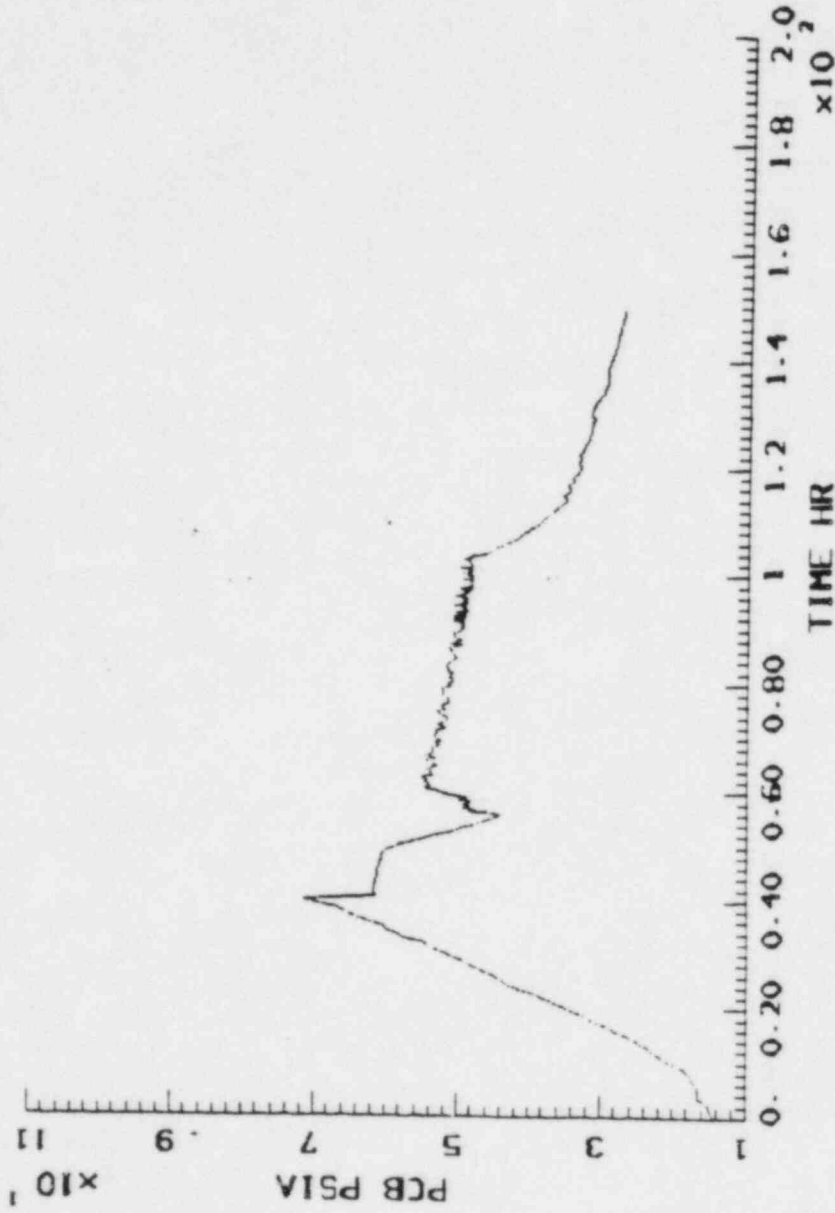


Fig. 4.16 Pressure in Compartment B.

steam overpressurization. A containment breach area of 0.1 ft^2 was modeled. For this containment failure size and location, the containment depressurizes to within about 0.5 psid of atmospheric pressure in about 10 hours. The suppression pool remains intact following the containment failure event. Suppression pool boiloff maintains an elevated containment pressure after the containment fails. Gas temperatures in all outer containment compartments are relatively constant at about 300°F after containment failure. The drywell air temperature is shown on Fig. 4.17.

In order for the $T_{23}\text{QW}$ sequence to result in core damage, it is necessary that all systems supplying or capable of supplying water to the RPV fail at or before containment failure. A realistic mechanism which could cause such a simultaneous failure has not been identified. The accounting of containment failure location, pressure, fluid flow loading, and ECCS pump suction temperature [4.1], pressure, and NPSH limitations [4.2] indicates that at least one GGNS ECCS train should survive a containment failure event. However, for this analysis, the conservative assumption that all ECCS equipment fails on containment failure was made.

Without vessel makeup, the RPV water level falls. The decrease is relatively slow in comparison with the $T_1\text{QUV}$ and AE events, since decay heat levels in the $T_{23}\text{QW}$ accident are relatively low. Core uncover takes place about 8 hours after containment failure, and fuel heatup begins thereafter. Fuel temperatures in the uncovered region of the core begin rising above 2000°F at 51 hr. The clad oxidation rate increases rapidly above the 2000°F fuel temperature point. Since the oxidation of the Zircaloy fuel cladding is an exothermic reaction, its occurrence increases the fuel heatup rate and thus tends to promote further cladding oxidation. About 5% of the total Zircaloy was oxidized at vessel failure.

Fuel melting is predicted to begin at about 54 hr into the event. After melting, the fuel moves to the core plate. By 56.2 hr, sufficient core material is calculated to have fallen onto the RPV core plate to cause it to fail. The core debris then falls to the bottom of the RPV and, about 30 sec later, vessel failure occurs at a welded RPV penetration. At vessel failure,

T230W - GRAND GULF

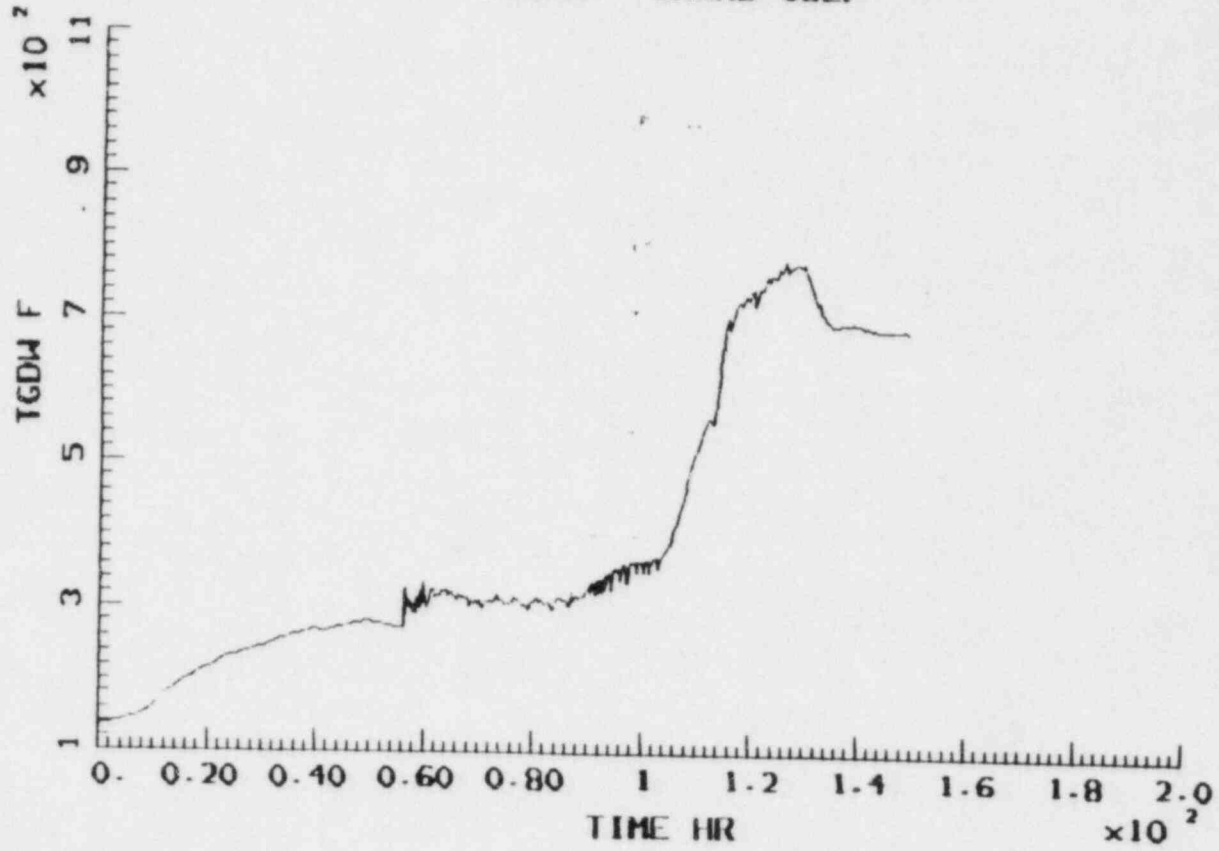


Fig. 4.17 Temperature of gas in the drywell.

the molten fraction of the lower plenum core debris falls onto the pedestal floor followed by the flashing high-pressure lower plenum water.

Since the containment failure size was 0.1 ft^2 , the suppression pool remains saturated at about 280°F , passing the steam entering it through to the upper compartment. The containment pressure remains high, gradually diminishing as the heat load diminishes, as shown in Fig. 4.16. The gas temperatures in all of the containment compartments are relatively constant at about 300°F during the period of interest. The drywell temperature variation is shown on Fig. 4.17.

Since the containment has such large amounts of steam, it is effectively inerted when the hydrogen leaving the vessel enters the wetwell (prior to vessel failure) and the drywell (after vessel failure). Hence, no burning is predicted to occur. For the same reason, any noncondensable gases that may be generated at very late times (beyond 100 hours) from core debris-concrete attack would not burn. The average corium temperature and penetration depth histories are shown in Figs. 4.18 and 4.19. Appendix B includes additional plots of results for this sequence.

4.4 Plant Response to the $T_{23}C$ Accident

4.4.1 Sequence Description

The $T_{23}C$ accident is assumed to occur during full-power operation. It is initiated by inadvertent main steam isolation valve (MSIV) closures (Event T_{23}). The accident sequence specifies that the control rod drive (CRD) system fails to automatically bring the reactor subcritical (Event C). This analysis assumes that no control rods were inserted into the core. All other plant systems are assumed to be available. No credit is taken for any operator action other than to start the containment igniter system at the accident initiation and to manually initiate ADS when the suppression pool temperature exceeds 145°F . The $T_{23}C$ accident chronology is provided on Table 4.5.

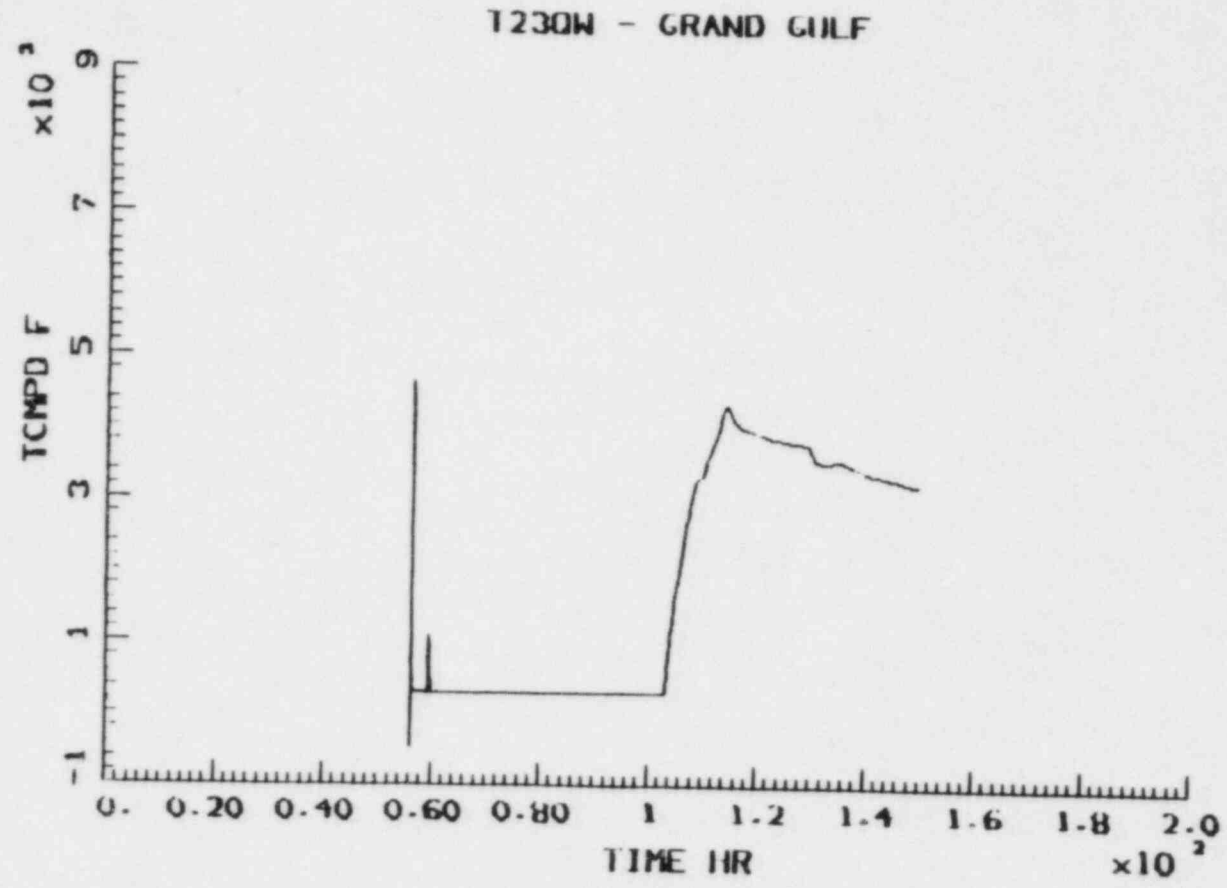


Fig. 4.18 Average corium temperature in the pedestal.

T230W - GRAND CULF

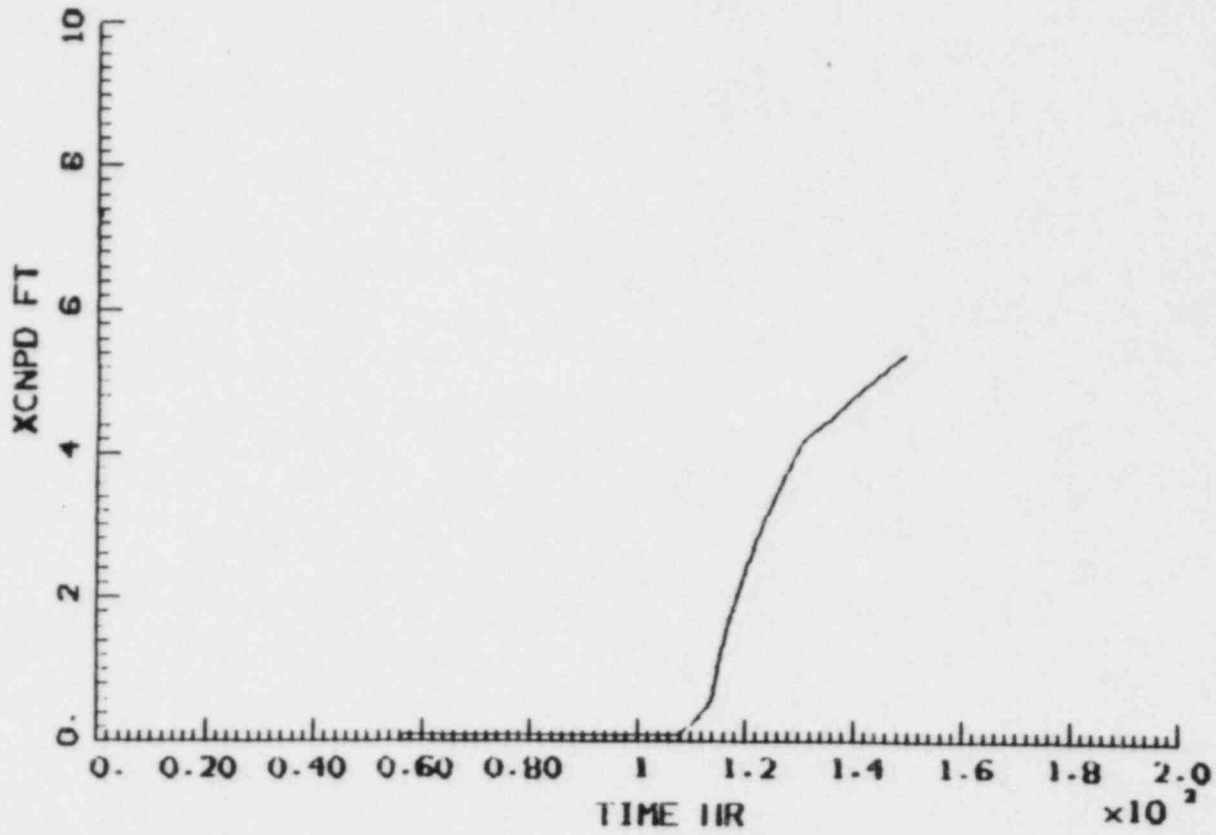


Fig. 4.19 Concrete ablation depth in the pedestal.

Table 4.5
GRAND GULF NUCLEAR STATION
T₂₃C BASE CASE
ACCIDENT CHRONOLOGY

Time	Event
0 sec	Initiating events: MSIV closures; Failure to scram; Loss of main feedwater
33 sec	RPV Level 2 LOCA setpoint reached
49 sec	HPCS begins operating
52 sec	RCIC begins operating
4.5 min	HPCS/RCIC systems transfer suction from CST to SP
8 min	ADS manually initiated
18.3 min	RCIC pump fails on high suction temperature
23.0 min	High JW pressure LOCA setpoint reached; Post-LOCA DW vacuum breakers open
23.6 min	Drywell purge system actuates
23.8 min	LPCS and LPCI actuate
26.2 min	High wetwell pressure setpoint reached
33.8 min	Containment sprays actuate
53.1 min	SPMU actuates
1.0 hr	Containment failure and subsequent ECCS failure
1.3 hr	Core begins to uncover
3.0 hr	Fuel melting begins
3.8 hr	Core plate failure followed by vessel failure

4.4.2 Primary System and Containment Response

The MSIV closures are modeled to actuate a reactor scram which fails to insert the control rods into the core. Despite this failure to scram, the core power is modeled to decrease from its initial full-power level to about 20% of full power level within seconds. This power reduction simulates the thermal-hydraulic reactivity feedback effects which are expected to occur as a result of the initiating MSIV closure event, the resultant recirculation and feedwater trips, and the ensuing high pressure core spray (HPCS) and reactor core isolation cooling (RCIC) systems actuations. The estimate of 20% of full power is based on the assumption that the core power will equilibrate at a level which just equals the power needed to boil all incoming coolant flow. In addition, core power is assumed to linearly decrease from 18% to 6% of full power as the downcomer water level decreases from 7.2 ft above the active core to the top of the jet pumps. Decay heat power levels are assumed for uncovered fuel nodes. The $T_{23}C$ core power history is provided in Fig. 4.20.

The MSIV closures cause a reactor pressure vessel (RPV) pressure excursion which is relieved by the SRVs. The vessel remains at the SRV relief setpoint pressure. The exiting RPV steam is routed to the suppression pool (SP), where it is quenched. By 33 sec into the event, sufficient RPV water inventory has been lost through the cycling SRVs to drop the RPV water level to the RPV Level 2 LOCA setpoint. At that point, signals are automatically generated to actuate the HPCS and RCIC systems. The HPCS begins injecting water into the RPV at 49 sec; the RCIC begins at 52 sec. These systems maintain RPV inventory between RPV Levels 2 and 8. At 4.5 min, suction for these systems is transferred from the condensate storage tank (CST) to the SP on a high SP water level signal. At 8 min, when the suppression pool temperature reaches 145°F, the RPV is manually depressurized according to emergency procedure guidelines. Because the core power generation rate is much greater than the decay heat level, the SP water temperature rises very rapidly. When the SP temperature reaches 200°F at 18.3 min, the RCIC pump is assumed to fail due to high bearing temperatures. The HPCS is unable to maintain sufficient RPV inventory at SRV setpoint pressures and at a 20% of full power level. As a result, the RPV water level decrease to a new equilibrium state. These can be seen in Fig. 4.21.

DRAFT

T230 - GRAND GULF



4-40

Fig. 4.20 Average core power.

T23C - GRAND GULF

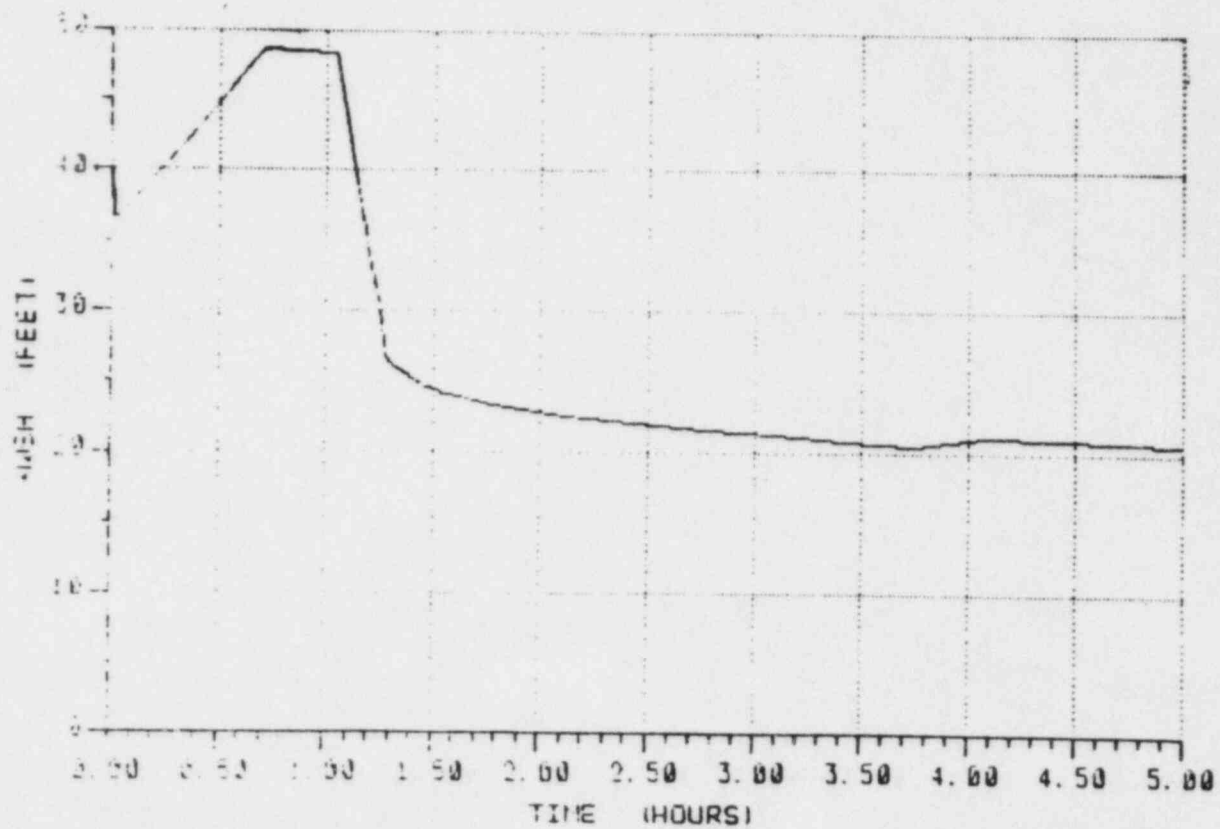


Fig. 4.21 Reactor vessel water level.

The SP reaches saturation conditions and is no longer able to completely quench the steam exiting the RPV through the cycling SRVs; a steam-pressurization of the containment ensues. The rising suppression pool water temperature and the resulting rise in pressures and temperatures in both the drywell and outer containment can be seen in Figs. 4.22 through 4.25. The rising pressure actuates the 1.89 psig high DW pressure LOCA signal at 23.0 min. This signal is a permissive signal for the DW purge system, the post-LOCA DW vacuum breakers, and the SP makeup (SPMU) system; it is an actuation signal for the low pressure core spray (LPCS) and low pressure coolant injection (LPCI) systems. Since the post-LOCA DW vacuum breaker permissive requiring a 0.87 psid drywell vacuum relative to the wetwell is already satisfied, the vacuum breakers open immediately. The DW purge system actuates after a 30 sec time delay and the SPMU system actuates the upper containment pool dump following a programmed 30 min delay. The continuing HPCS injection maintains RPV level. At 26.2 min into the event, the containment pressure reaches the 9 psig containment spray actuation pressure setpoint. At that time, trains A and B of the residual heat removal (RHR) system automatically switch into their spray mode and eight minutes later begin to spray SP water into the upper containment volume. Since the containment spray water cooling requires manual alignment, which was not modeled in this analysis, the containment spray system is unable to effect a containment pressure reduction.

At 53.1 min into the event, the SPMU system releases, as designed, approximately half of the upper containment pool volume into the suppression pool. This action brings the suppression pool to a subcooled state. Consequently, the containment steam pressurization ceases and, in fact, reverses. The former is due to the renewed ability of the suppression pool to quench the SRV steam discharge. The rapid outer containment depressurization is due to the action of the containment sprays which draw suction from the suppression pool. Within 15 minutes of the upper pool release, the continued core power generation reheats the suppression pool to a saturated state and outer containment pressurization resumes. The additional pool inventory begins to spill onto the drywell and pedestal floors at that time. This spill has a large mitigative effect if this accident proceeds beyond vessel failure. At 1.0 hrs into the accident, only minutes after the renewed pressurization, the containment is modeled to fail at this pressure at a failure location just

T23C - GRAND GULF

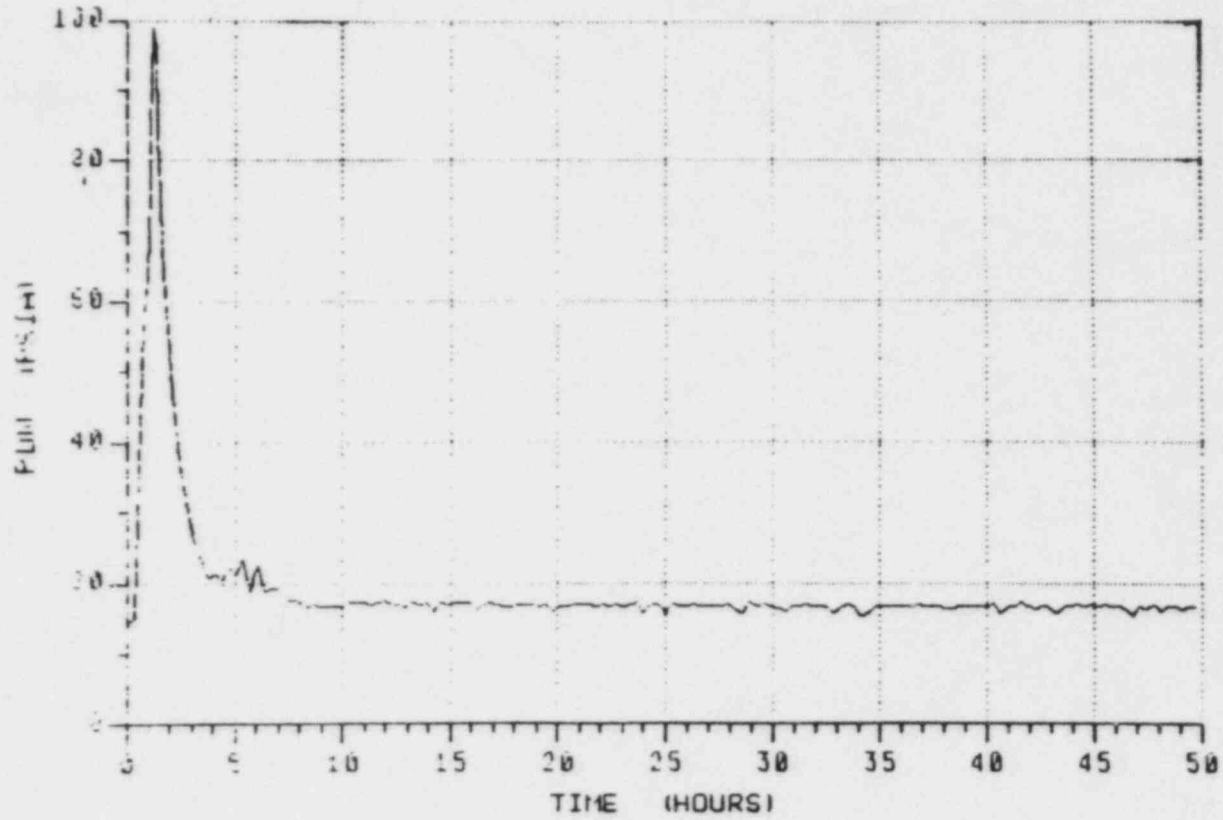


Fig. 4.22 Pressure in the drywell.

T23C - GRAND GULF

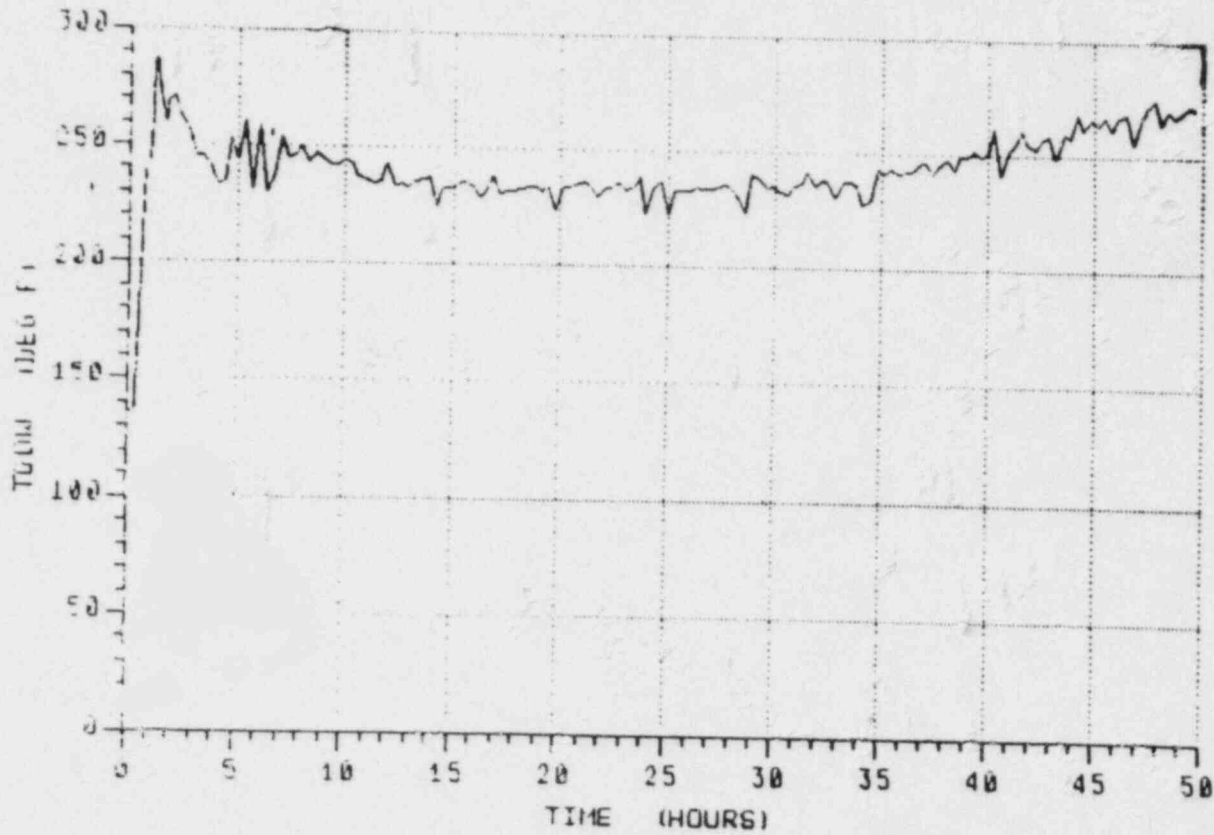


Fig. 4.23 Temperature of gas in the drywell.

T23C - GRAND GULF

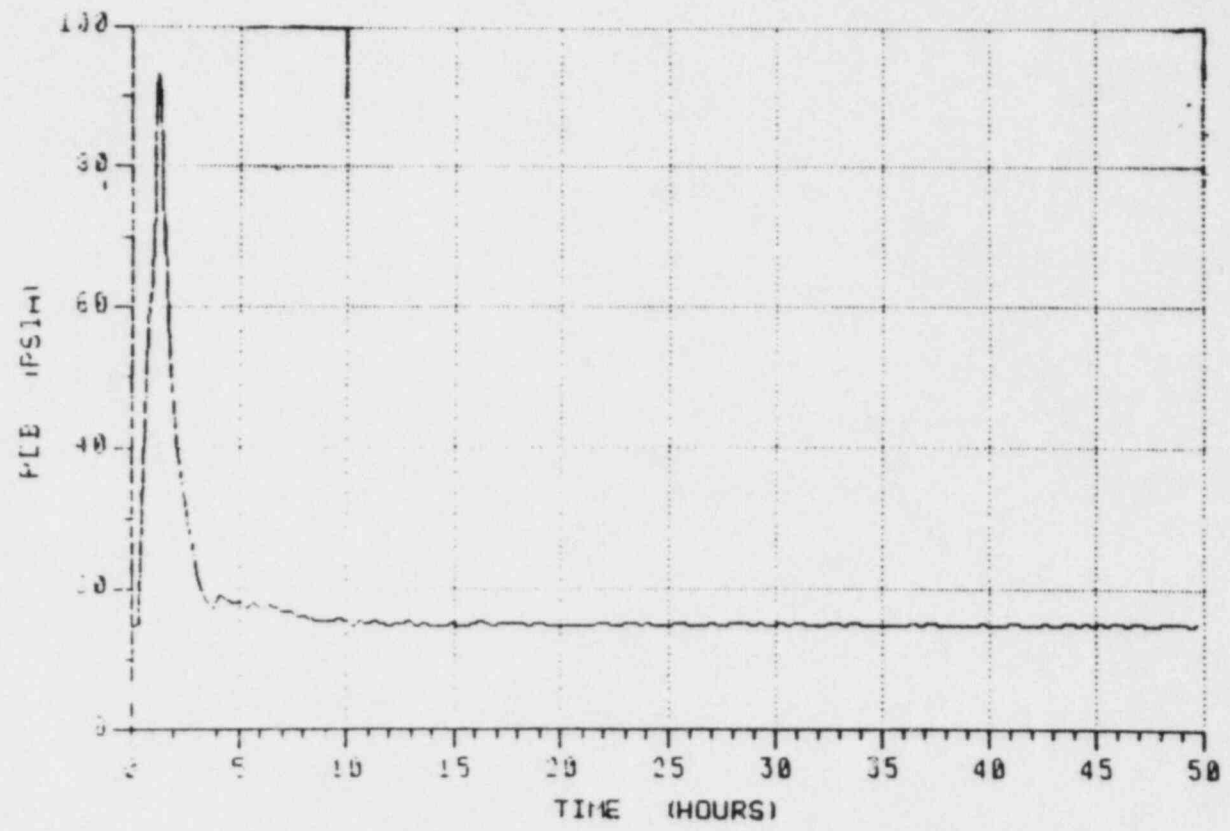


Fig. 4.24 Pressure in Compartment B.

4-45

DRAFT

T23C - GRAND GULF

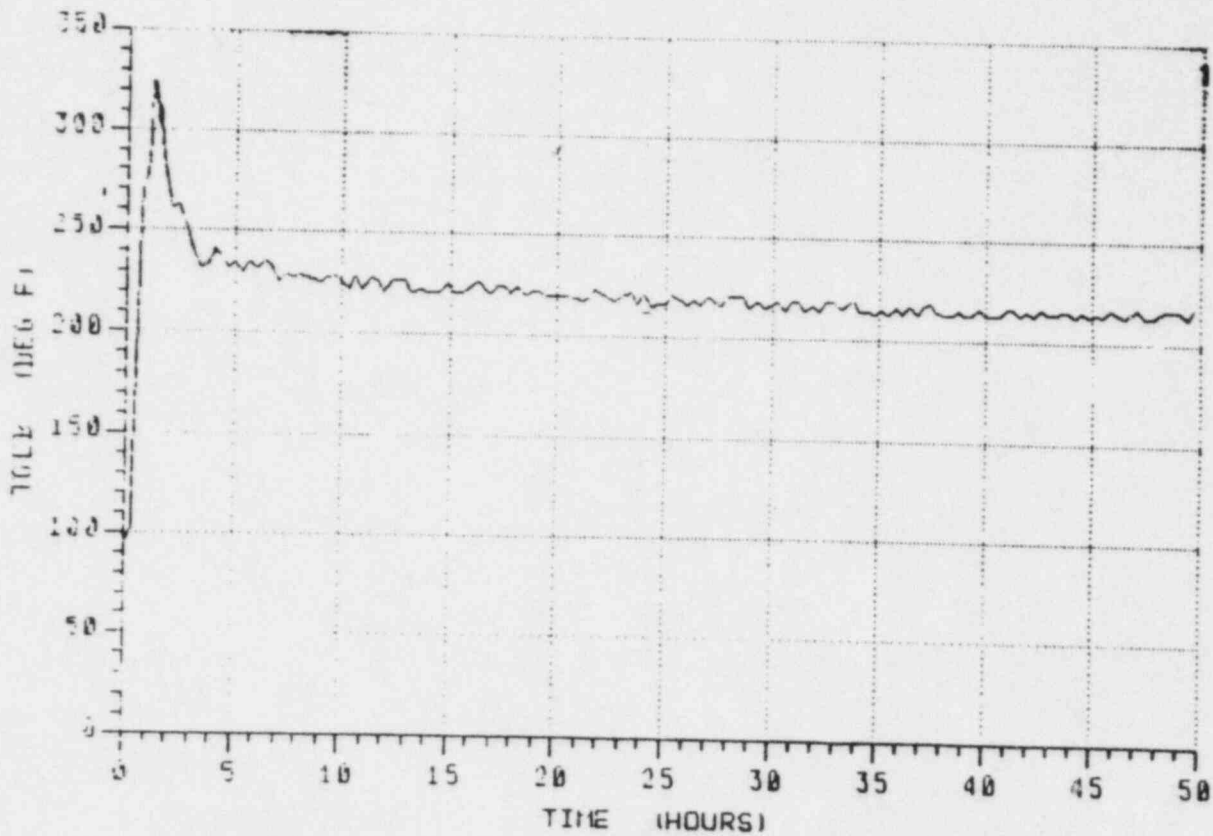


Fig. 4.25 Temperature of gas in Compartment B.

below the junction between the cylinder and the dome. The failure cause is steam overpressurization. A containment breach of 1.5 ft² was modeled.

In order for the T₂₃C sequence to result in core damage, it is necessary that all systems supplying or capable of supplying water to the RPV fail at or before containment failure. A realistic mechanism which could cause such a simultaneous failure has not been identified. The accounting of containment failure location, pressure, fluid flow loading, and ECCS pump suction temperature, pressure, and NPSH limitations indicates that at least one GGNS ECCS train should survive a containment failure event. However, for this analysis, the conservative assumption that all ECCS equipment fails on containment failure was made. The CRD flow was assumed to continue, at the rate of approximately 90 gpm.

Given that all ECCS fail on containment failure, the RPV water level begins to fall sharply as shown in Fig. 4.21. As the water level continues to fall, the power level decreases to 6% of full power. As a fuel node is uncovered, its power level is modeled to decrease to its decay heat level.

Fuel temperatures in the uncovered regions of the core begin rising above 2000°F at about 1.9 hr. The oxidation of the Zircaloy fuel cladding by steam increases rapidly above the 2000°F point. About 530 lb of hydrogen is produced in the vessel.

Fuel melting is predicted to begin at 3.0 hr. After melting, fuel moves from the core to the core plate. By 3.8 hr, sufficient core material is calculated to have fallen onto the RPV core plate to cause it to fail. The core debris then falls to the bottom of the RPV; shortly thereafter, the vessel fails at a welded penetration. At vessel failure, the molten fraction of the lower plenum core debris falls onto the pedestal floor followed by the lower plenum water.

Since the vessel had been depressurized previously, the debris does not disperse from the pedestal to the drywell upon vessel failure. Furthermore, the remainder of the core material gradually enters the pedestal from the vessel and also stays in the pedestal. The debris attacks the pedestal

concrete as it is being quenched (see Fig. 4.26) until about three inches of concrete have been ablated. Once the core debris bed in the pedestal is cooled to below concrete ablation temperatures by the lower plenum water, it remains quenched since its blanket of water is boiled away. As can be seen from Fig. 4.27, this would not occur for a very long time, if ever. Consequently, no appreciable quantities of noncondensable gases are generated.

Subsequent to vessel failure steam flows steadily from the pedestal, to the drywell, to the suppression pool at a rate of roughly 2×10^6 ft³/hr. The flow is due to the fact that the CRD water is continuing to quench the debris in the pedestal, and producing steam.

No hydrogen burning was predicted to occur in this sequence. By the time the hydrogen produced from Zircaloy oxidation in the core reached the wetwell, all of the oxygen had been depleted from the wetwell atmosphere, as well as from the upper containment atmosphere. Furthermore, there are no appreciable quantities of hydrogen or carbon monoxide generated from core debris-concrete attack. Appendix B includes additional plots of results for this sequence.

T23C - GRAND GULF

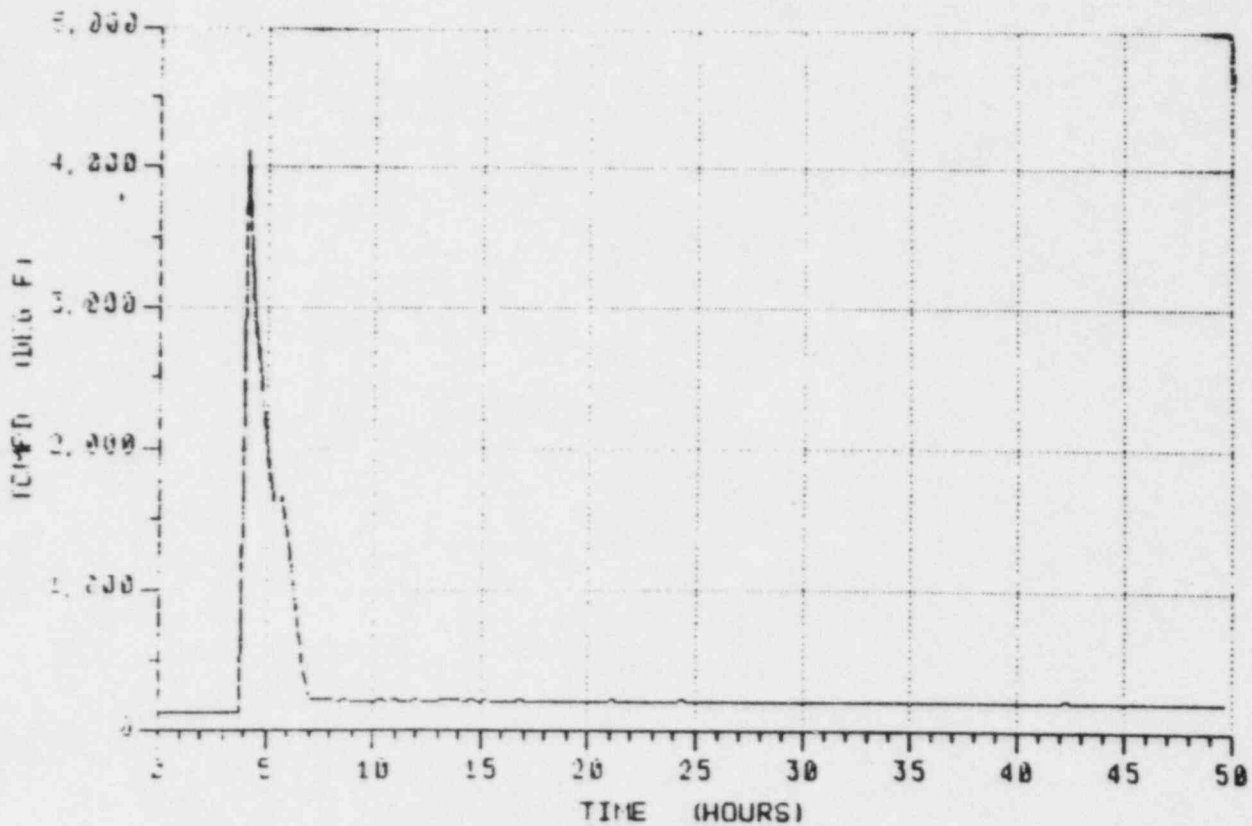


Fig. 4.26 Average corium temperature in the pedestal.

T23C - GRAND GULF

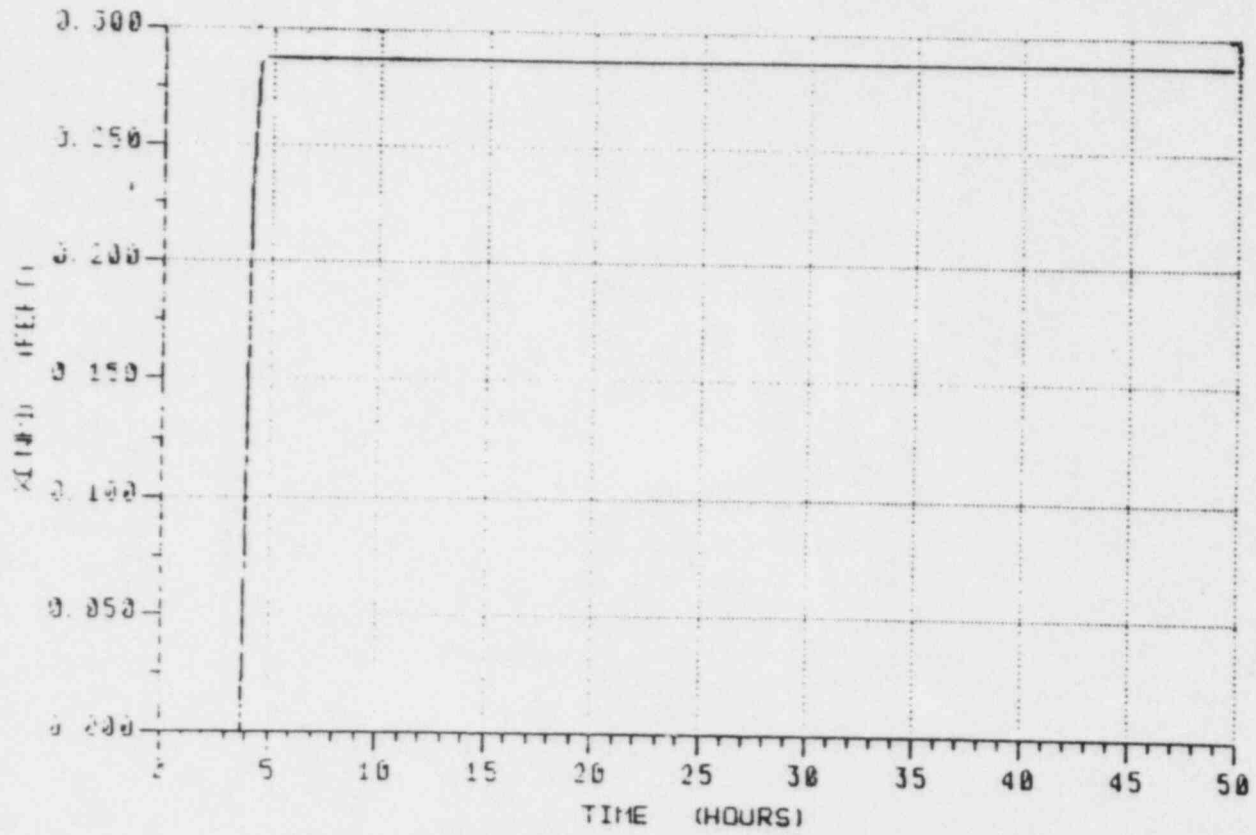


Fig. 4.27 Concrete ablation depth in the pedestal.

DRAFT

Grand Gulf Section 5 to be supplied later.

6.0 FISSION PRODUCT RELEASE, TRANSPORT AND DEPOSITION

6.1 Introduction

The phenomena of fission product release from the fuel matrix, its transport within the primary system, their release from the primary system into the containment, their deposition within the containment and the subsequent release of some fission products from the containment are treated through the use of MAAP [6.1]. Release of fission products from the fuel matrix and their transport to the top of the core are treated by a subroutine in MAAP which is based on the FPRAT code [6.2]. Transport of fission products outside the core boundaries is determined by the natural and forced convection flows modeled in MAAP with the gravitational sedimentation described in Ref. [6.3] and other deposition processes described in Ref. [6.4]. Fission product behavior is considered for the best estimate transport, deposition and relocation processes. Influence of surface reactions between chemically active substances like cesium hydroxide and other uncertainties are considered in subtask 23.4. The best estimate calculation, assuming cesium iodide and cesium hydroxide are the chemical state of cesium and iodine, is discussed below.

6.2 Modeling Approach

Evaluations of the dominant chemical species in Ref. [6.5] show the states of the radionuclides (excluding noble gases) which dominate the public health risk to be cesium iodide and cesium hydroxide, tellurium oxide and strontium oxide. These and others are considered in the code when calculating the release of fission products from the fuel matrix. Vapors of these dominant species form dense aerosol clouds in the upper plenum, in some cases approaching 100 g/m^3 for a very short time, which agglomerate and settle onto surfaces. Depending upon the chemical compound and gas temperature, these deposited aerosols can be either solid or liquid. At the time of reactor vessel failure, some material remains suspended as airborne aerosol or vapor and would be discharged from the primary system into the containment. The rate of discharge is determined by the gaseous flow between the primary system and containment which is sequence specific. (It should be noted that some

fission products can be discharged into the containment before vessel failure through relief valves or through breaks in the primary system. This is also sequence specific.) This set of inter-related processes are treated in MAAP and essentially result in a release of all airborne aerosol and vapor from the primary system into containment immediately following vessel failure.

As a result of the dense aerosols formed when fission products are released from the fuel, considerable deposition occurs within the primary system prior to vessel failure. For some accident sequences, the primary system may be at an elevated pressure at the time of core slump and reactor vessel failure. Resuspension of these aerosol deposits during the primary system blowdown is assessed in Ref. [6.6] in terms of the available experimental results and basic models. It is concluded that resuspension immediately following reactor vessel failure would not be significant, less than 1% of the deposited materials, even for depressurizations initiated from the nominal operating pressure. For delayed containment failure, this small fraction of material is depleted by in-containment mechanisms.

Therefore, a major fraction of the volatile fission products are retained within the primary system following vessel failure, the distribution being determined by the MAAP calculations prior to vessel failure. Natural circulation through the primary system after vessel failure is analyzed using MAAP which allows for heat and mass transport in various nodes of the reactor vessel and the steam generators including heat losses from the primary system as dictated by the reflective insulation. Material transport is due to aerosols and vapors as governed by the heatup of structures due to radioactive decay of deposited fission products. This heatup is principally determined by the transport of cesium iodide and cesium hydroxide by the natural circulation flows. In this regard, the vapor pressure of cesium hydroxide is applied to both the cesium iodide and cesium hydroxide chemical species. In essence, this assumes that the solution of cesium iodide and cesium hydroxide has a vapor pressure close to that of cesium hydroxide, which is a conservatism in the calculations. In carrying out these calculations, the pressurization of the primary system is dependent upon the pressurization of the containment and the heating within the primary system. These determine the in- and out-flows between the primary system and containment.

Deposition within the containment is calculated using thermal hydraulic conditions determined by MAAP. The major aerosol sources are the releases prior to vessel failure (sequence specific), the airborne aerosols and vapors transferred from the primary system at the time of vessel failure, the subsequent releases from the primary system due to long term heatup, and concrete attack. At the time of containment failure, the remaining airborne aerosol and vapor can be released to the environment. Assessments of the potential for resuspension of deposited aerosols following containment failure [6.6] show this to be negligible.

6.3 Sequences Evaluated

The use of MAAP in the manner indicated above leads to the release fractions shown in Tables 6.1 through 6.5. Four sequences are analyzed, including: transient with failure of injection (T_1QUV); large LOCA with failure of injection (AE); transient followed by loss of containment heat removal ($T_{23}QW$); and transient with failure to scram ($T_{23}C$). Thermal-hydraulic behavior for these sequences is described in Section 4. In this section it is shown that, for $T_{23}QW$ and $T_{23}C$, the containment fails before the core is uncovered. Hence, the cesium and iodine are still in the fuel matrix.

6.3.1 T_1QUV Sequence

As indicated in Table 6.1, two percent of the volatile fission product inventory is swept from the vessel to the suppression pool via the SRV lines prior to vessel failure. Of the remainder, 2% is still in the fuel matrix, 95% is in the upper plenum area, 1% is in the downcomer.

During the time between vessel breach and containment failure, revaporization and relocation of material within the primary system occurs, due to the continuing natural circulation flows. Some material continually flows to the pedestal and drywell as vapor, and from there some of the material flows to the suppression pool. After about a day, the drywell is hot enough that revaporization begins there, and flow to the suppression pool is increased. The pool itself is highly effective in scrubbing the fission

DRAFT

6-4

Table 6.1
DISTRIBUTION OF CsI IN PLANT AND ENVIRONMENT
(FRACTION OF CORE INVENTORY)

	At Vessel Failure			
	T_{23}^{QW}	T_{23}^C	AE	T_1^{QUV}
RPV	.90	.68	.98	.98
Drywell	0.0	0.0	.02	0.0
Suppression Pool	.10	.32	0.0	.02
Primary Containment	5.3×10^{-5}	2.2×10^{-5}	0.0	0.0
Environment	3.2×10^{-5}	2.6×10^{-4}	0.0	0.0

	At Containment Failure			
	T_{23}^{QW}	T_{23}^C	AE	T_1^{QUV}
RPV	1.00	1.00	.91	.46
Drywell	0.0	0.0	.03	.20
Suppression Pool	0.0	0.0	.06	.34
Primary Containment	0.0	0.0	0.0	0.0
Environment	0.0	0.0	0.0	0.0

	Ultimate Distribution			
	T_{23}^{QW}	T_{23}^C	AE	T_1^{QUV}
RPV	.50	.26	.90	.33
Drywell	.12	.05	.03	.02
Suppression Pool	.38	.69	.07	.645
Primary Containment	2.1×10^{-4}	1.1×10^{-4}	5.11×10^{-4}	7.3×10^{-4}
Environment	2.6×10^{-4}	7.6×10^{-4}	$< 1 \times 10^{-5}$	7.3×10^{-5}

Table 6.2

T₁QV FISSIION PRODUCT RELEASE

Assumptions
Containment Failure Location - Compartment B, 237' 9" Containment Failure Size - .1 ft ²

Fission Product Group	Release Fraction to Environment
Cs, I	7.3×10^{-5}
Te, Sb	3.2×10^{-5}
Sr, Ba	$< 1 \times 10^{-5}$
Ru, Mo	$< 1 \times 10^{-5}$

DRAFT

Table 6.3
AE FISSION PRODUCT RELEASE

Assumptions
Containment Failure Location - Compartment B, 237' 9" Containment Failure Size - .1 ft ²

Fission Product Group	Release Fraction to Environment
Cs, I	$< 1 \times 10^{-5}$
Te, Sb	1.1×10^{-5}
Sr, Ba	$< 1 \times 10^{-5}$
Ru, Mo	$< 1 \times 10^{-5}$

Table 6.4

 T_{23}^{QW} FISSION PRODUCT RELEASE

Assumptions
Containment Failure Location - Compartment B, 237' 9"
Containment Failure Size - .1 ft ²

Fission Product Group	Release Fraction to Environment
Cs, I	2.6×10^{-4}
Te, Sb	2.2×10^{-4}
Sr, Ba	$< 1 \times 10^{-5}$
Ru, Mo	$< 1 \times 10^{-5}$

DRAFT

6-8

Table 6.5

$T_{23}C$ FISSION PRODUCT RELEASE

Assumptions
Containment Failure Location - Compartment B, 237' 9"
Containment Failure Size - 1.5 ft ²

Fission Product Group	Release Fraction to Environment
Cs, I	7.6×10^{-4}
Te, Sb	7.5×10^{-4}
Sr, Ba	$< 1 \times 10^{-5}$
Ru, Mo	$< 1 \times 10^{-5}$

products. A decontamination factor of 600 is associated with passage from the drywell to the pool through the vents [6.7].

Table 6.1 also shows the volatile fission product inventories in the various compartments at the time of containment failure. Only the airborne material in the upper compartment and that portion of the material still to be revolatilized in the vessel that would not be scrubbed in the suppression pool is available for release to the environment. As can be seen in Table 6.2, the release fractions to the environment for this case are low. Long term releases subsequent to containment failure occur but at extremely slow rates.

Considerable concrete ablation takes place in the pedestal following vessel failure and subsequent flowing of molten core debris into the pedestal. By 24 hr the ablation depth is more than 5 ft.

6.3.2 AE Sequence

The use of MAAP leads to the release fractions shown in Tables 6.1 and 6.3. The thermal-hydraulic analysis is described in Section 4.2.

Table 6.1 shows the distribution of cesium and iodine through the various regions, at vessel failure and 70 hr, when the calculation was terminated. Due to the very low steam flow in the vessel after the initial LOCA blowdown, nearly all of the material is initially deposited in the upper plenum. Hence, very little material enters the suppression pool through the break (less than 1 kg by the time of vessel breach). At the time of vessel breach, only about 1 kg is airborne. This material can leave the vessel. The deposited material (about 229 kg) remains in the vessel at this time.

Following vessel failure, the remainder of the volatile fission products are released from the fuel as it melts. This material, along with that already deposited, moves around the vessel, being deposited, heating up, revaporizing, moving to cooler regions and redepositing, etc. Drywell pressurization from the very hot gases in the pedestal cavity prevents materials from escaping the vessel until containment failure at 58 hr. As can be inferred from Table 6.1 about 1% of cesium and iodine are relocated from the

vessel to the suppression pool during the period following containment failure. Of this, only one part in 600 escapes the pool to the outer containment [6.7].

Release fractions to the environment are very low, as can be seen in Table 6.3. As for the T_1 QUV sequence, however considerable concrete ablation occurs, although it does not occur for the first 30 hr of the event. By 50 hr the ablation depth is approximately 5 ft.

6.3.3 T_{23} QW Sequence

The use of MAAP leads to the release fractions shown in Tables 6.1 and 6.4. The thermal-hydraulic analysis was described in Section 4.3.

Table 6.1 shows the distribution of the volatile fission products (cesium and iodine) through the various regions, at vessel failure and at 150 hr when the calculation was terminated. At vessel failure, nearly all of the volatiles (90%) in the vessel are deposited in the upper structures. The remainder (10%) are in the suppression pool. Only negligible quantities are present elsewhere. The decontamination factor associated with passage through the SRVs and spargers, and subsequent pool scrubbing, is 1000 [6.7].

Since the containment is already failed prior to core uncover there is no rapid depressurization as in the T_1 QUV and AE sequences. Furthermore, there is no large scale concrete attack in the pedestal. Thus the ultimate fission product distribution is such that the release to the environment is very small, as indicated in Table 6.4.

6.3.4 T_{23} C Sequence

The use of MAAP leads to the release fractions shown in Tables 6.1 and 6.5. The MAAP thermal-hydraulic analysis is described in Section 4.4.

Table 6.1 shows the distribution of cesium and iodine through the various regions both at vessel failure and at 50 hr, when the calculation was terminated. At vessel failure 139 kg are deposited in the upper plenum, 10 kg

are in the downcomer, 14 kg are in the core region, and 76 kg have left the vessel through the SRVs to the suppression pool. Only negligible quantities are present elsewhere. The decontamination factor associated with passage through the SRVs and spargers is 1000 [6.7].

The fission products tend not to exit the vessel but rather transfer their heat to gas and structures and move about the primary system. The reflective insulation is very effective in transferring a considerable portion of the heat to the drywell as temperatures rise.

Since the containment is already failed prior to core uncover there is no rapid depressurization. Furthermore, there is no large scale concrete attack in the pedestal. Thus the ultimate fission product distribution is such that the release to the environment is very small, as indicated in Table 6.5.

6.4 References

- 6.1 MAAP - Modular Accident Analysis Program, User's Manual, August, 1983.
- 6.2 IDCOR Technical Report 15.1B, "Analysis of In-Vessel Core Melt Progression," Vol. IV (User's Manual) and Modeling Details for the Fission Product Release and Transport Code (FPRAT), September, 1983.
- 6.3 Draft IDCOR Technical Report, "FAI Aerosol Correlation," July, 1984.
- 6.4 IDCOR Technical Report on Task 11.3, "Fission Product Transport in Degraded Core Accidents," December, 1983.
- 6.5 IDCOR Technical Report on Tasks 11.1, 11.4 and 11.5, "Estimation of Fission Product and Core-Material Source Characteristics," October, 1982.
- 6.6 IDCOR Technical Report on Task 11.6, "Resuspension of Deposited Aerosols Following Primary System or Containment Failure," July, 1984.
- 6.7 K. Holtzclaw, Personal Communication, 1984.

7.0 SUMMARY OF RESULTS

As outlined in Section 2 of this report, the IDCOR Subtask 23.1 Integrated Containment Analysis of the Grand Gulf Nuclear Station (GGNS) consisted of base case accident analyses and operator action case accident analyses.

The accident sequences selected for analysis represent a majority of previously-assessed risk and demonstrate a variety of initiating events, a variety of system failures combinations, and a diversity of accident phenomenology. The primary system and containment thermal-hydraulic response analyses and fission product transport were performed via the MAAP code. Fission product release was performed via the FPRAT code which has been integrated into MAAP. Detailed descriptions of each of these analyses are provided in Sections 4 through 7 of this report, respectively. This section of the report summarizes the major results of each of these analyses.

7.1 Base Case Analyses

The base case analyses establish a reference system response during these accidents by assuming a minimum of operator intervention during the accident progression. As such, these analyses do not realistically account for the mitigative response of the trained operating staff and, thus, should not be considered as representative of realistic plant response analyses. The base case fission product transport results are summarized on Table 7.1. A discussion of these results follows.

Accidents involving demand-type failures of all automatically-actuated high and low pressure reactor pressure vessel (RPV) makeup systems, namely those accident sequences containing events UV or E, result in core damage unless an appropriate operator response is taken. For accidents which involve relatively small RPV coolant inventory loss rates and decay power levels, such as T₁QUV and T₂₃PQE, the core is predicted to begin to uncover within about half an hour of the initiating event. Within about one hour, significant fuel cladding degradation is predicted, and fuel melting is calculated to begin about two hours after the initiating event. Vessel

Table 7.1
SUMMARY OF FRACTIONAL RADIONUCLIDE RELEASES TO THE ENVIRONMENT

Accident	Fission Product Group				
	Xe and Kr	Cs and I	Te	Sr and Ba	Ru and Mo
T ₁ QUV	1.0	7.3 E-5	3.2 E-5	< 1 x 10 ⁻⁵	< 1 x 10 ⁻⁵
AE	1.0	< 1 x 10 ⁻⁵	1.1 E-5	< 1 x 10 ⁻⁵	< 1 x 10 ⁻⁵
T ₂₃ ^C	1.0	7.6 E-4	7.5 E-4	< 1 x 10 ⁻⁵	< 1 x 10 ⁻⁵
T ₂₃ ^{QW}	1.0	2.6 E-4	2.2 E-4	< 1 x 10 ⁻⁵	< 1 x 10 ⁻⁵
BWR-4	0.6	5.0 E-3*	4.0 E-3	6.0 E-4	6.0 E-4

*Iodine release fraction is 0.8 E-4.
Cesium release fraction is 5.0 E-3.

failure will follow within another half-hour. For accidents with large RPV inventory loss rates, such as AE, these events occur sooner. For the large-break LOCA case analyzed, the AE accident, fuel melting was predicted to occur within 0.7 hours of the initiating event and was closely followed by vessel failure.

Accidents involving successful RPV makeup but inadequate containment cooling, such as T_{23}^{QW} and T_{23}^C , will result in containment failure unless appropriate operator action is taken. Previous studies have postulated that all ECCS injection into the RPV will fail on containment failure. With this assumption, and without appropriate operator action, fuel melting will inevitably follow. The results of this study indicate that the assumption that all ECCS equipment fails on containment failure has no mechanistic basis and thus is extremely conservative. Without the containment-failure-induced ECCS failure assumption, many of the previously-postulated dominant GGNS accidents sequences do not lead to core melt and, thus, can no longer be considered risk significant. The T_{23}^{QW} and T_{23}^C sequences are all among these accidents.

The mass of hydrogen produced via steam oxidation of fuel cladding in the core was calculated to be significantly lower than that prescribed by the NRC for interim rule on hydrogen control for Mark III containments. The MAAP predictions demonstrate that less than about 10% fuel cladding oxidation prior to fuel melting for severe GGNS accidents. The NRC cladding oxidation rule specifies a 75% cladding reaction. Even if the accidents were to progress unmitigated to vessel failure, the maximum fraction of cladding oxidized is predicted at only 35%. Judicious misaction is necessary to generate cladding reactions of higher magnitudes. Specifically, a low vessel makeup flow or an orchestrated termination and restart of emergency core cooling would be necessary. The rate of hydrogen production calculated for the GGNS severe accident analyses is also substantially lower than those used in previous studies. The maximum average sustained rate observed in the MAAP calculations was less than 0.5 lb/sec lasting for about less than twenty minutes.

For accidents which proceed beyond vessel failure, the molten core debris is calculated to fall onto the pedestal floor. No core debris is

DRAFT

7-4

calculated to exit the pedestal volume. Thus, concrete attack is limited to the pedestal floor and walls. Without core-debris cooling, substantial erosion of the pedestal floor and walls is calculated to occur.

Three containment failure modes were observed in the GGNS Mark III containment analysis. They were overpressurization by steam, by noncondensable gases, and/or by hydrogen combustion. The dominant failure mode was found to be accident dependent. All three modes result in long-delayed containment failure events for the GGNS accidents analyzed, the MAAP code predicts no steam explosions large enough to fail either the reactor pressure vessel or the containment. Thus, no prompt containment failures were observed. It is noteworthy to state that the containment failure times predicted in this study are long compared to those of previous studies. This is primarily due to the higher ultimate containment capacity (56.6 psig) used in this study.

For the GGNS Mark III design, the suppression pool was observed to exert a dominant influence on the accident progression. There are a number of reasons that the suppression pool displays this behavior. First, overpressurization of the containment by steam can occur only if the suppression pool is heated to high temperatures or if the suppression pool is by-passed. The former requires a substantial energy deposition and inadequate suppression pool heat removal. The latter has been evaluated to be a very low probability occurrence. Secondly, the suppression pool controls the temperature of the noncondensable gases which are calculated to be evolved in sequences heading to core degradation, core melting and core-concrete attack. By cooling these gases, as they enter the outer containment volume, the suppression pool substantially slows the rate of pressurization within the containment building. Thirdly, for accident sequences which have proceeded past vessel failure, the suppression pool water can, in general, be supplied to the debris to provide either temporary or potentially long term debris bed cooling. Lastly, it is significant to recognize that the suppression pool can retain substantial quantities of noninert fission product material which would be released by the fuel during a core meltdown event. With the location of the suppression pool in the Mark III design, these materials cannot be

exhausted through a containment breach without first being highly decontaminated by the suppression pool.

Fission product release and transport calculations were performed with FPRAT and MAAP for the T₁QUV, T₂₃QW, AE, and T₂₃C base case sequences. A summary of the final airborne fission product releases to the environment for the accident sequences analyzed are presented in Table 7.1. The BWR-4 release category from the Reactor Safety Study is also presented for comparison. The data presented on this table shows that for the accidents analyzed the fractional fission product releases to the environment were generally significantly less severe than those associated with the BWR-4 release category. Since the accidents analyzed represent a majority of public health risk, the present analysis indicates that the risk associated with the operation of GGNS is substantially lower than that previously assessed.

The lower fission product release terms produced in this study as compared to previous studies are principally due to the higher suppression pool decontamination factor and the relatively late containment failure time. Other factors which were found to influence the amount of fission product escaping the containment system during the severe accident scenarios analyzed were the duration of the melt releases, the time of the vessel failure, the fission product transport pathway, and the assumed fraction of fission product resuspension at the time of containment failure. A specific finding of these analyses is that accidents which involve rapid core heatups or which display a high RPV pressure until the vessel failure result in rapid releases of volatile fission products from the fuel immediately after the vessel fails. Another finding is that nonvolatile fission product release rates due to core-concrete interaction are small beyond about 20 hours after vessel failure. Lastly, the majority of fission product retention was calculated to occur in the suppression pool and in the drywell.

7.2 Operator Action Analyses

The major results of the operator action case thermal-hydraulics analyses are summarized in Section 5. They demonstrate that a safe stable state can be achieved in the vessel if injection can be restored prior to core

DRAFT

7-6

plate failure. There are many means available to the operator for providing sufficient makeup flow to the reactor vessel. The time available for aligning and actuating these RPV makeup systems prior to core damage and/or fuel melting was evaluated in the base case analyses to be accident dependent. Once actuated, the operator case analyses indicate that these systems are capable of reflooding the core within minutes. These analyses also demonstrate that given the existence of a safe stable state for the core, a safe stable state for the containment can be achieved by restoring adequate containment cooling. Peak containment temperatures and pressures occur from minutes to hours after such restoration, depending on the core heat level and on the mode and magnitude of containment heat removal.

Debris coolability and the maintenance of containment integrity was demonstrated as possible via the restoration of an emergency core cooling system to flood the pedestal and a containment cooling system to cool the suppression pool.

8.0 CONCLUSIONS

Based on the results of the severe accident analyses performed in this study, a number of conclusions can be drawn regarding the progression and consequences of such severe accidents for plant designs similar to that of the Grand Gulf Nuclear Station.

The analytical tools employed in this study, namely MAAP, is a viable means of analyzing both the thermal-hydraulic and the radiological response of the Grand Gulf Nuclear Station primary system and containment to severe accident scenarios.

The most significant conclusions which can be drawn from this integrated containment analysis of the Grand Gulf Nuclear Station are itemized below. The first refers to the analytical tools used in this study. The next set are thermal-hydraulic related conclusions. And, the last and probably most significant conclusion relates to the radiological results of this study.

- The MAAP code is a viable means of analyzing both the thermal-hydraulic and the radiological response of the Grand Gulf Nuclear Station primary system and containment to severe accident scenarios.
- For accidents postulated to lead to core damage, fuel melting, and/or containment failure, there are sufficient time and means available to the operating staff to place the plant into a safe stable state.
- Containment failure should no longer be considered a cause for the failure of all ECCS flow to the reactor vessel. Thus, containment failure should no longer be considered a cause for core melt.
- The mass and rate of hydrogen calculated to be produced in the vessel prior to fuel melting is substantially less than that predicted by previous studies.

DRAFT

8-2

- If successful fuel cooling is delayed beyond the point of significant core damage and/or vessel failure, the core debris coolability is possible.
- The suppression pool exerts a dominant thermal-hydraulic and radiological influence on the containment response to a severe accident.
- The GGNS Mark III containment failure modes are overpressurization via steam, noncondensable gas generation, and/or hydrogen combustion. Containment failure times are long compared to previous studies. No prompt containment failures due to steam explosions or steam spiking were calculated.
- The overall containment response is much more sensitive to whether continuous hydrogen combustion occurs than to the details of how incomplete combustion progresses within the containment.
- Through continuous burning of the containment combustible gas, the GGNS containment hydrogen igniters can significantly delay containment failure during a severe accident.
- Decontamination of the fission product releases by the suppression pool and their condensation and gravitational settling in the drywell were found to be the two most important fission product removal mechanisms.
- The public health consequences of the severe accidents are substantially less than those of previous assessments.

APPENDIX A

Grand Gulf Parameter File

GULEFP.DAT;14

6-JUL-1984 14:29

Page 1

```

**MARK III BWR PLANT PARAMETER VALUES-- TYPICAL OF GRAND GULF
**SI UNITS (M-KG-SEC-DEGK)
** 7-22-83
**
**PRIMARY SYSTEM
01 13.521D0 AFLCOR FLOW AREA OF REACTOR CORE
** ALSH IS CALCULATED BY TAKING THE VOLUME OF WATER IN THE LOWER
** DOWNCOMER+JET PUMP AND DIVIDING BY (ZTOAF-ZBJET)
02 8.57D0 ALSH FLOW AREA IN LOWER SHROUD
03 5.695D0 AFLBYP CORE BYPASS FLOW AREA
** AUSH IS CALCULATED BY TAKING THE VOLUME OF WATER IN THE UPPER
** DOWNCOMER ABOVE TOAF AND DIVIDING BY THE WATER HEIGHT ABOVE TOAF
04 2.644D1 AUSH FLOW AREA IN UPPER SHROUD
05 1.116D5 HCRD SPECIFIC ENTHALPY OF FLOW IN CRD TUBES
06 9.248D5 HEW SPECIFIC ENTHALPY OF FEEDWATER
07 1.65697D5 MU2PS TOTAL MASS OF UO2 IN CORE
08 8.0D2 MASS NUMBER OF FUEL ASSEMBLIES IN REACTOR CORE
09 6.2D1 NPINS NUMBER OF FUEL RODS IN A FUEL ASSEMBLY
10 1.93D2 NCRD NUMBER OF CRD TUBES
11 4.5D0 NGEPS SENSIBLE ENERGY STORED IN FUEL (FULL POWER SECONDS)
12 4.0D0 IDMSIV DELAY TIME FOR MSIV CLOSURE
13 3.5D0 IDSCRM DELAY TIME FOR FULL SCRAM
14 5.976D7 TIRRAD TOTAL EFFECTIVE IRRADIATION TIME FOR CORE
** ALL PUMP CURVES ASSOCIATE THE FIRST FLOW RATE WITH THE FIRST PRESSURE
** FOR THAT SPECIFIC PUMP
15 7.0-3 WVCRDI CRD FLOW RATE PUMP CURVE FOR CRD FLOW
16 1.12D-2 WVCRDI CRD FLOW RATE PPS VS WVCRDI
17 1.12D-2 WVCRDI CRD FLOW RATE M3/S
18 1.12D-2 WVCRDI CRD FLOW RATE
19 1.12D-2 WVCRDI CRD FLOW RATE
20 1.12D-2 WVCRDI CRD FLOW RATE
21 1.12D-2 WVCRDI CRD FLOW RATE
22 1.12D-2 WVCRDI CRD FLOW RATE
23 6.894D6 PCRD PPS FOR CRD PUMP
24 1.0134D5 PCRD PPS FOR CRD PUMP
25 1.0134D5 PCRD PPS FOR CRD PUMP
26 1.0134D5 PCRD PPS FOR CRD PUMP
27 1.0134D5 PCRD PPS FOR CRD PUMP
28 1.0134D5 PCRD PPS FOR CRD PUMP
29 1.0134D5 PCRD PPS FOR CRD PUMP
30 1.0134D5 PCRD PPS FOR CRD PUMP
31 3.333D3 WFWMAX MAXIMUM FEEDWATER FLOW RATE (RUN OUT FLOW)
32 6.85D2 WBPMAX MAXIMUM TURBINE BYPASS FLOW RATE
33 1.63D-1 NXCORE EXIT CORE QUALITY AT TIME ZERO
34 5.264D0 XDCORE REACTOR CORE DIAMETER TO INNER SHROUD WALL
35 2.206D1 XHRV INTERIOR HEIGHT OF REACTOR VESSEL
36 3.188D0 XRRV INTERIOR RADIUS OF REACTOR VESSEL
37 41.01D0 ZBJET ELEVATION AT BOTTOM OF JET PUMPS
38 38.77D0 ZBRDT ELEVATION AT BOTTOM OF CRD TUBES
39 50.44D0 ZBSEP ELEVATION AT BOTTOM OF STEAM SEPARATORS
40 37.41D0 ZBV ELEVATION AT BOTTOM OF REACTOR VESSEL
41 42.73D0 ZCPL ELEVATION AT CORE PLATE
42 45.48D0 ZTJET ELEVATION AT TOP OF JET PUMPS
43 1.33D0 AJET TOTAL AREA OF JET PUMPS
44 46.74D0 ZTOAF ELEVATION AT TOP OF ACTIVE FUEL
45 52.65D0 ZTSEP ELEVATION AT TOP OF STEAM SEPARATORS
46 51.91D0 ZWNORM ELEVATION AT NORMAL SHROUD WATER LEVEL
47 41.82D0 ZLOCA ELEVATION AT BREAK
48 .2919D0 ALOCA AREA OF BREAK
49 52.325D0 ZWL8 ELEVATION AT LEVEL 8 TRIP
50 0.0D0 NOT USED

```

DRAFT

A-2

GULFFP.DAT;14

6-JUL-1984 14:29

Page 2

51	51.26D0	ZSCRAM LOW WATER LEVEL SCRAM	PS
52	7.4435D6	PSCRAM HIGH PRESSURE SCRAM SETPOINT	PS
53	.20D0	FQATWS ATWS CONSTANT POWER ASSUMPTION	PS
54	1.2D3	TDSLCTIME FOR SCRAM WITH SLC	PS
55	0.D0	TIRR(1) TIME VS. FRACTION OF TOTAL FLOW FOR RECIRC PUMP	PS
56	2.D0	TIRR(2)	PS
57	4.D0	TIRR(3)	PS
58	6.D0	TIRR(4)	PS
59	8.D0	TIRR(5)	PS
60	10.D0	TIRR(6)	PS
61	15.012D0	TIRR(7)	PS
62	40.D0	TIRR(8)	PS
63	1.D0	EWRR(1)	PS
64	.67D0	EWRR(2)	PS
65	.45D0	EWRR(3)	PS
66	.30D0	EWRR(4)	PS
67	.20D0	EWRR(5)	PS
68	.135D0	EWRR(6)	PS
69	.050D0	EWRR(7)	PS
70	0.D0	EWRR(8)	PS
71	1.18393D5	HSLC INLET ENTHALPY OF SLC	PS
72	0.D0	PSLC(1) PRESSURE POINTS FOR SLC FLOW CURVE	PS
73	7.93D6	PSLC(2)	PS
74	7.93D6	PSLC(3)	PS
75	7.93D6	PSLC(4)	PS
76	7.93D6	PSLC(5)	PS
77	7.93D6	PSLC(6)	PS
78	7.93D6	PSLC(7)	PS
79	7.93D6	PSLC(8)	PS
80	2.713D-3	WVSLC(1) SLC FLOW RATE AT PSLC(1) -- M3/S	PS
81	2.713D-3	WVSLC(2)	PS
82	2.713D-3	WVSLC(3)	PS
83	2.713D-3	WVSLC(4)	PS
84	2.713D-3	WVSLC(5)	PS
85	2.713D-3	WVSLC(6)	PS
86	2.713D-3	WVSLC(7)	PS
87	2.713D-3	WVSLC(8)	PS
88	.2D0	TDRPT DELAY TIME FOR RECIRC PUMP TRIP	PS
89	47.16D0	ZLMSIV LOW WATER LEVEL FOR MSIV CLOSURE	PS
90	49.92D0	ZLRPT LOW WATER LEVEL FOR RECIRC PUMP TRIP	PS
91	7.858D6	PHRPT HIGH VESSEL PRESSURE FOR RECIRC PUMP TRIP	PS
92	1.1327D5	PDWSCM HIGH DRYWELL PRESSURE FOR SCRAM	PS
93	.032D0	FENRCH NORMAL FUEL ENRICHMENT	PS
94	2.D4	EXPO AVERAGE BURNUP IN MWD/TONNE	PS
95	.6D0	FCR PRODUCTION OF U239 TO ABSORPTION IN FUEL	PS
96	1.3D0	FEAF RATIO OF FISSION ABSORPTION TO TOTAL FISSION	PS
97	5.D-1	EQFR1 FISSION POWER FRACTION OF U235 AND PU241	PS
98	4.2D-1	EQFR2 FISSION POWER FRACTION OF U239	PS
99	8.D-2	EQFR3 FISSION POWER FRACTION OF U238	PS
100	.3051D0	XPCRDT PITCH OF CRD TUBES	PS
101	.2755D0	XDCRDT OUTER DIAMETER OF CRD TUBE	PS
102	58.D0	MINST NUMBER OF INSTRUMENT TUBES	PS
103	.0044D0	XTHCRD THICKNESS OF CRD TUBE WALL	PS
104	.0508D0	XDINST OUTER DIAMETER OF INSTRUMENT TUBE	PS
105	.0818D0	XDRIVE LOWER CRD DRIVE OUTER DIAMETER	PS
106	1.004D-3	VWCRD SPECIFIC VOLUME OF CRD WATER	PS
107	1.004D-3	VWCST SPECIFIC VOLUME OF SLC WATER	PS
108	5.8167D4	MEQPS MASS OF UPPER PLENUM HEAT SINK	PS
109	1.016D3	AEQPS SURFACE AREA OF UPPER PLENUM HEAT SINK	PS
110	.241D0	XTRV THICKNESS OF LOWER VESSEL HEAD	PS
111	0.D0	TIFWCD TIME SINCE MSIV CLOSURE SIGNAL VS. FEEDWATER	PS

GULFFP.DAT;14

6-JUL-1984 14:29

Page 3

112	0.00	COASIDOWN MASS FLOW RATE	PS
113	0.00		PS
114	0.00		PS
115	0.00		PS
116	0.00		PS
117	0.00		PS
118	0.00		PS
119	0.00	WEWCD	PS
120	0.00		PS
121	0.00		PS
122	0.00		PS
123	0.00		PS
124	0.00		PS
125	0.00		PS
126	0.00		PS
127	5.86D6	PLMSIV LOW RPV PRESSURE FOR MSIV CLOSURE	PS
128	53.9D0	ZMSL ELAVATION AT CENTER LINE OF MAIN STEAM LINE	PS
**			PS
**			HE
*CIRC			
01	0.00	ACSHS(1) CORE + LOWER PLENUM	
**		CARBON STEEL-HEAT SINK HEAT TRANSFER AREA	
02	140.D0	ACSHS(2) UPPER PLENUM	
03	0.00	ACSHS(3) DOWNCOMER	
04	0.00	ACSHS(4)	
05	0.00	ACSHS(5)	
06	50.D3	MCS(1) CORE + LOWER PLENUM CARBON STEEL MASS	
07	100.D3	MCS(2) UPPER PLENUM	
08	350.D3	MCS(3) DOWNCOMER	
09	0.00	MCS(4)	
10	0.00	MCS(5)	
11	0.00	MHS(1) CORE + LOWER PLENUM HEAT SINK MASS	
12	100.D3	MHS(2) UPPER PLENUM	
13	0.00	MHS(3) DOWNCOMER	
14	0.00	MHS(4)	
15	0.00	MHS(5)	
16	0.00	ACSX(1) CORE + LOWER PLENUM CARBON STEEL TO DRYWELL	
**		HEAT TRANSFER ARE	
17	0.00	ACSX(2) UPPER PLENUM	
18	240.D0	ACSX(3) DOWNCOMER	
19	0.00	ACSX(4)	
20	0.00	ACSX(5)	
21	0.00	AHSX(1) CORE + LOWER PLENUM HEAT SINK TO DRYWELL	
**		HEAT TRANSFER AREA	
22	140.D0	AHSX(2) UPPER PLENUM	
23	0.00	AHSX(3) DOWNCOMER	
24	0.00	AHSX(4)	
25	0.00	AHSX(5)	
26	100.D0	AGCS(1) CORE + LOWER PLENUM GAS TO CARBON STEEL	
**		HEAT TRANSFER AREA	
27	5.D3	AGCS(2) UPPER PLENUM	
28	240.D0	AGCS(3) DOWNCOMER	
29	0.00	AGCS(4)	
30	0.00	AGCS(5)	
31	0.00	AGHS(1) CORE + LOWER PLENUM GAS TO HEAT SINK	
**		HEAT TRANSFER AREA	
32	140.D0	AGHS(2) UPPER PLENUM	
33	0.00	AGHS(3) DOWNCOMER	
34	0.00	AGHS(4)	
35	0.00	AGHS(5)	
36	8.0D0	XL(1) CORE + LOWER PLENUM LENGTH	
37	5.D0	XL(2) UPPER PLENUM LENGTH	

DRAFT

A-4

GULFFP.DAT;14

6-JUL-1984 14:29

Page 4

38	10.00	XL(3)	DOWNCOMER LENGTH	
39	0.00	XL(4)		
40	0.00	XL(5)		
41	11.00	AG(1)	CORE + LOWER PLENUM FLOW AREA	
42	11.00	AG(2)	UPPER PLENUM FLOW AREA	
43	10.00	AG(3)	DOWNCOMER FLOW AREA	
44	0.00	AG(4)		
45	0.00	AG(5)		
46	5.00	DH(1)	HYDRAULIC DIAMETER FOR CORE REGION	
47	.1500	DH(2)	HYDRAULIC DIAMETER FOR UPPER PLENUM	
48	.400	DH(3)	HYDRAULIC DIAMETER FOR DOWNCOMER	
49	0.00	DH(4)		
50	0.00	DH(5)		
51	0.00	QCO	RPV CONVECTION LOSSES AT TIME ZERO	
52	8.00	FINPLT	NUMBER OF LAYERS IN REFLECTIVE INSULATION	
**				
*HEATUP				
01	3.8100	XZFUEL	LENGTH OF ACTIVE FUEL	HE
02	5.210-3	XRFUEL	RADIUS OF FUEL PELLET	HE
03	8.130-4	XTCLAD	THICKNESS OF CLADDING	HE
04	5.03304	MZRCAN	TOTAL MASS OF ZR IN ASSEMBLY CAN	HE
05	1.704	MBCR	TOTAL MASS OF CONTROL BLADES IN REACTOR CORE	HE
06	3.0480-3	XZRCAN	CAN WALL THICKNESS	HE
** NODE 1,1 IS BOTTOM-CENTER, 1,10 IS TOP-CENTER, 2,1 IS SECOND RADIAL				
** RING OUT FROM CENTER AT THE BOTTOM OF THE CORE, ETC				
07	6.6800-1	EPEAK(1,1)	PEAKING FACTOR FOR NODE (1,1)	HE
08	7.9100-1	EPEAK(2,1)	PEAKING FACTOR FOR NODE (2,1)	HE
09	4.7000-1	EPEAK(3,1)	PEAKING FACTOR FOR NODE (3,1)	HE
15	1.14500	EPEAK(1,2)	PEAKING FACTOR FOR NODE (1,2)	HE
16	1.46600	EPEAK(2,2)	PEAKING FACTOR FOR NODE (2,2)	HE
17	9.2900-1	EPEAK(3,2)	PEAKING FACTOR FOR NODE (3,2)	HE
23	1.01900	EPEAK(1,3)	PEAKING FACTOR FOR NODE (1,3)	HE
24	1.34300	EPEAK(2,3)	PEAKING FACTOR FOR NODE (2,3)	HE
25	8.9600-1	EPEAK(3,3)	PEAKING FACTOR FOR NODE (3,3)	HE
31	1.02900	EPEAK(1,4)	PEAKING FACTOR FOR NODE (1,4)	HE
32	1.28100	EPEAK(2,4)	PEAKING FACTOR FOR NODE (2,4)	HE
33	8.670-1	EPEAK(3,4)	PEAKING FACTOR FOR NODE (3,4)	HE
39	1.22300	EPEAK(1,5)	PEAKING FACTOR FOR NODE (1,5)	HE
40	1.41400	EPEAK(2,5)	PEAKING FACTOR FOR NODE (2,5)	HE
41	9.4300-1	EPEAK(3,5)	PEAKING FACTOR FOR NODE (3,5)	HE
47	1.23500	EPEAK(1,6)	PEAKING FACTOR FOR NODE (1,6)	HE
48	1.37300	EPEAK(2,6)	PEAKING FACTOR FOR NODE (2,6)	HE
49	9.030-1	EPEAK(3,6)	PEAKING FACTOR FOR NODE (3,6)	HE
55	1.19800	EPEAK(1,7)	PEAKING FACTOR FOR NODE (1,7)	HE
56	1.26900	EPEAK(2,7)	PEAKING FACTOR FOR NODE (2,7)	HE
57	8.090-1	EPEAK(3,7)	PEAKING FACTOR FOR NODE (3,7)	HE
63	1.23500	EPEAK(1,8)	PEAKING FACTOR FOR NODE (1,8)	HE
64	1.24300	EPEAK(2,8)	PEAKING FACTOR FOR NODE (2,8)	HE
65	7.110-1	EPEAK(3,8)	PEAKING FACTOR FOR NODE (3,8)	HE
71	1.33100	EPEAK(1,9)	PEAKING FACTOR FOR NODE (1,9)	HE
72	1.10700	EPEAK(2,9)	PEAKING FACTOR FOR NODE (2,9)	HE
73	5.530-1	EPEAK(3,9)	PEAKING FACTOR FOR NODE (3,9)	HE
79	7.400-1	EPEAK(1,10)	PEAKING FACTOR FOR NODE (1,10)	HE
80	5.640-1	EPEAK(2,10)	PEAKING FACTOR FOR NODE (2,10)	HE
81	2.690-1	EPEAK(3,10)	PEAKING FACTOR FOR NODE (3,10)	HE
87	0.300	XCHIM	UNHEATED FUEL LENGTH AT TOP OF CORE	HE
88	1.0-7	XIZROX	INITIAL CLADDING OXIDE THICKNESS	HE
**				
**				
*ENGINEERED SAFEGUARDS				
01	1.00	NLPC11	NUMBER OF LPCI PUMPS IN LOOP 1	ES
				ES
				ES
				ES

DRAFT

GULFFP.DAT;14

6-JUL-1984 14:29

Page 5

02	1.0D0	NLPCI2 NUMBER OF LPCI PUMPS IN LOOP 2	ES
03	1.0D0	NLPCI3 NUMBER OF LPCI PUMPS IN LOOP 3 (INJECTION ONLY)	ES
04	1.D0	NLPCSP NUMBER OF LPCS PUMPS	ES
05	0.0D0	NOT USED	
06	1.4D1	VMNCST MIN. WATER VOLUME IN CONDENSATE STORAGE TANK	ES
**		FOR HPCI AND RCIC SUCTION SWITCH OVER	ES
07	1.008D-3	VMCST SPECIFIC VOLUME OF CST WATER	ES
**	ALL PUMP CURVES ARE ARRANGED SO THAT THE FIRST FLOW ENTRY CORRESPONDS		
**	TO THE FIRST PRESSURE ENTRY		
24	2.09D6	PLPCI(1) PUMP CURVES FOR ECCS -- LPCI	ES
25	2.D6	PLPCI(2) PPS-PDW VS. VOLUMETRIC FLOW	ES
26	1.896D6	PLPCI(3)	ES
27	1.641D6	PLPCI(4)	ES
28	1.462D6	PLPCI(5)	ES
29	1.1651D6	PLPCI(6)	ES
30	.841D6	PLPCI(7)	ES
31	.4964D6	PLPCI(8)	ES
32	0.0D0	WVLP(1)	ES
33	.1262D0	WVLP(2)	ES
34	.1893D0	WVLP(3)	ES
35	.3155D0	WVLP(4)	ES
36	.3786D0	WVLP(5)	ES
37	.4417D0	WVLP(6)	ES
38	.5048D0	WVLP(7)	ES
39	.5641D0	WVLP(8)	ES
40	3.584D6	PLPCS(1) LPCS PUMP CURVE	ES
41	3.378D6	PLPCS(2)	ES
42	3.06D6	PLPCS(3)	ES
43	2.889D6	PLPCS(4)	ES
44	2.67D6	PLPCS(5)	ES
45	2.392D6	PLPCS(6)	ES
46	2.068D6	PLPCS(7)	ES
47	1.572D6	PLPCS(8)	ES
48	0.D0	WVPCS(1)	ES
49	.1262D0	WVPCS(2)	ES
50	.2524D0	WVPCS(3)	ES
51	.3155D0	WVPCS(4)	ES
52	.3786D0	WVPCS(5)	ES
53	.4417D0	WVPCS(6)	ES
54	.5048D0	WVPCS(7)	ES
55	.5742D0	WVPCS(8)	ES
56	9.892D6	PHPCS(1) HPCS PUMP CURVE	ES
57	8.886D6	PHPCS(2)	ES
58	7.521D6	PHPCS(3)	ES
59	6.749D6	PHPCS(4)	ES
60	5.667D6	PHPCS(5)	ES
61	4.226D6	PHPCS(6)	ES
62	2.296D6	PHPCS(7)	ES
63	0.0D0	PHPCS(8)	ES
64	0.D0	WVHPCS(1)	ES
65	.1262D0	WVHPCS(2)	ES
66	.2524D0	WVHPCS(3)	ES
67	.3155D0	WVHPCS(4)	ES
68	.3786D0	WVHPCS(5)	ES
69	.4417D0	WVHPCS(6)	ES
70	.5048D0	WVHPCS(7)	ES
71	.5742D0	WVHPCS(8)	ES
72	10.341D6	PRCIC(1) RCIC PUMP CURVE	ES
73	10.340D6	PRCIC(2)	ES
74	6.894D6	PRCIC(3)	ES
75	3.447D6	PRCIC(4)	ES

DRAFT

A-6

GULFFP.DAT;14

6-JUL-1984 14:29

Page 6

76	2.758D6	PRCIC(5)	ES
77	2.068D6	PRCIC(6)	ES
78	4.144D5	PRCIC(7)	ES
79	4.137D5	PRCIC(8)	ES
80	0.D0	WVRCIC(1)	ES
81	.0505D0	WVRCIC(2)	ES
82	.0505D0	WVRCIC(3)	ES
83	.0505D0	WVRCIC(4)	ES
84	.0505D0	WVRCIC(5)	ES
85	.0505D0	WVRCIC(6)	ES
86	.0505D0	WVRCIC(7)	ES
87	0.D0	WVRCIC(8)	ES
89	50.D0	ZLHPCI LOW WATER INITIATION FOR HPCI	ES
89	1.D10	PSHPCI HIGH DRYWELL PRESSURE SET POINT FOR HPCI	ES
90	1.D10	IDHPCI TIME DELAY FOR HPCI	ES
91	1.D10	PHHPCI MINIMUM PRESSURE FOR HPCI TURBINE	ES
92	49.92D0	ZLHPCS LOW WATER INITIATION FOR HPCS	ES
93	1.144D5	PSHPCS HIGH DRYWELL PRESSURE SET POINT FOR HPCS	ES
94	27.D0	IDHPCS TIME DELAY FOR HPCS	ES
95	47.16D0	ZLLPCI LOW WATER INITIATION FOR LPCI	ES
96	1.144D5	PSLPCI HIGH DRYWELL PRESSURE SET POINT FOR LPCI	ES
97	40.D0	IDLPCI TIME DELAY FOR LPCI	ES
98	1.D10	PLLPCI LOW VESSEL PRESSURE PERMISSIVE FOR LPCI	ES
99	47.16D0	ZLLPCS LOW WATER INITIATION FOR LPCS	ES
100	1.144D5	PSLPCS HIGH DRYWELL PRESSURE SET POINT FOR LPCS	ES
101	37.D0	IDLPCS TIME DELAY FOR LPCS	ES
** THE NEXT PARAMETER IS A LOCA PERMISSIVE SIGNAL AND IF ONE DOES NOT			
** EXIST THEN ENTER VERY LARGE NUMBER (1.D10 PA)			
102	1.D10	PLLCS LOW VESSEL PRESSURE PERMISSIVE FOR LPCS	ES
103	49.92D0	ZLRCIC LOW WATER INITIATION FOR RCIC	ES
104	1.0D10	PSRCIC HIGH DRYWELL PRESSURE SET POINT FOR RCIC	ES
105	30.D0	IDRCIC TIME DELAY FOR RCIC	ES
106	5.15D5	PHRCIC MINIMUM VESSEL PRESSURE FOR RCIC TURBINE	ES
107	1.70D5	HCST ENTHALPY OF CST	ES
108	498.D0	WSWHX SERVICE WATER FLOW RATE (KG/S) THRU EACH RHR HTX	ES
109	.0119D0	ASRV1 FLOW AREA OF RELIEF VALVE TYPE #1	ES
110	.0119D0	ASRV2 FLOW AREA OF RELIEF VALVE TYPE #2	ES
111	.0115D0	ASRV3 FLOW AREA OF RELIEF VALVE TYPE #3	ES
112	.0119D0	ASRV4 FLOW AREA OF RELIEF VALVE TYPE #4	ES
** IF THE AREA OF GROUP #5 IS INPUT AS A NEGATIVE NUMBER THEN THE VALVE			
** WILL DISCHARGE DIRECTLY INTO THE DRYWELL, IF POSITIVE IT WILL			
** DISCHARGE INTO THE SUPPRESSION POOL			
113	.0D0	ASRV5 FLOW AREA OF RELIEF VALVE TYPE #5	ES
114	1.0D0	NSRV1 NUMBER OF TYPE #1 RELIEF VALVES	ES
115	1.0D0	NSRV2 NUMBER OF TYPE #2 RELIEF VALVES	ES
116	9.0D0	NSRV3 NUMBER OF TYPE #3 RELIEF VALVES	ES
117	9.0D0	NSRV4 NUMBER OF TYPE #4 RELIEF VALVES	ES
118	0.D0	NSRV5 NUMBER OF TYPE #5 RELIEF VALVES	ES
119	0.D0	NADS1 NUMBER OF ADS VALVES IN GROUP 1	ES
120	1.D0	NADS2 NUMBER OF ADS VALVES IN GROUP 2	ES
121	3.D0	NADS3 NUMBER OF ADS VALVES IN GROUP 3	ES
122	4.D0	NADS4 NUMBER OF ADS VALVES IN GROUP 4	ES
123	7.1220D6	PSRV1 PRESSURE SETPOINT FOR #1 RELIEF VALVE	ES
124	7.398D6	PSRV2 PRESSURE SETPOINT FOR #2 RELIEF VALVE	ES
125	7.674D6	PSRV3 PRESSURE SETPOINT FOR #3 RELIEF VALVE	ES
126	7.743D6	PSRV4 PRESSURE SETPOINT FOR #4 RELIEF VALVE	ES
127	1.D10	PSRV5 PRESSURE SETPOINT FOR #5 RELIEF VALVE	ES
128	47.16D0	ZLADS LOW WATER LEVEL FOR INITIATION OF ADS	ES
129	114.37D3	PSADS HIGH DRYWELL PRESSURE SET POINT FOR ADS	ES
130	115.D0	IDADS TIME DELAY FOR ADS ACTUATION	ES
** LPCI,LPCS,HPCS HAVE NPSH REQUIREMENTS			

DRAFT

GULFPP.DAT;14

6-JUL-1984 14:25

Page 7

```

** HPCI AND RCIC WILL TRIP OFF ON USER SUPPLIED TEMPERATURE OF SUPP POOL
131 373.00 TCMPCI INLET TEMP LIMIT FOR HPCI ES
132 31.400 ZCLHPS PUMP CENTER LINE ELAVATION FOR HPCS ES
133 29.300 ZCLLPI PUMP CENTER LINE ELAVATION FOR LPCI ES
134 30.500 ZCLLPS PUMP CENTER LINE ELAVATION FOR LPCS ES
135 366.300 TCRIC INLET TEMP LIMIT FOR RCIC ES
136 305.00 TWSW SERVICE WATER TEMP (RHR HEAT EXCHANGERS, ICOLD) ES
137 13.00 TDDG1 HPCS LOAD DELAY TIME FOR DIESEL ES
138 13.00 TDDG2 LPCI LOAD DELAY TIME FOR DIESEL ES
139 13.00 TDDG3 LPCS LOAD DELAY TIME FOR DIESEL ES
140 2.30-4 XDDROP SRRAY DROPLET DIAMETER FOR CONTAINMENT SPRAYS ES
141 19.600 XHSPWM SPRAY FALL HEIGHT IN WETWELL ES
142 10.00 XHSPDW SPRAY FALL HEIGHT IN DRYWELL ES
** THE HPSW SYSTEM CAN BE USED TO MODEL ANY INJECTION MODE SUCH AS
** SERVICE WATER OR FIRE WATER, THE SYSTEM IS TOTALLY DEFINED BELOW
143 1.83705 HWHPSW ENTHALPY OF HIGH PRES SERVICE WATER (MARK I CI) ES
144 1.0090-3 VWHPSW SPEC VOL OF HIGH PRES SERVICE WATER (MARK I CI) ES
145 6.52505 PHPSW(1) PPS VS. VOLUMETRIC FLOW FOR HPSW CORE INJECTION ES
146 6.52405 PHPSW(2) (MARK I CORE INJECTION) ES
147 6.52305 PHPSW(3) ES
148 6.52205 PHPSW(4) ES
149 6.52105 PHPSW(5) ES
150 6.52005 PHPSW(6) ES
151 6.51905 PHPSW(7) ES
152 0.00 PHPSW(8) ES
153 0.00 WWHPSW(1) ES
154 .75700 WWHPSW(2) ES
155 .75700 WWHPSW(3) ES
156 .75700 WWHPSW(4) ES
157 .75700 WWHPSW(5) ES
158 .75700 WWHPSW(6) ES
159 .75700 WWHPSW(7) ES
160 .75700 WWHPSW(8) ES
161 1.14405 PDWSPR DRYWELL PRES SET PT FOR MARK III CONTAINMNT SPRAYS ES
162 1.633905 PWWSPPR WETWELL DPRES SET PT FOR MARK III CONTAINMNT SPRAYS ES
163 600.00 TDSPPR TIME DELAY FOR MARK III CONTAINMENT SPRAYS ES
164 7.3805 PDSRV1 DEAD BAND FOR CLOSURE OF SRV#1 ES
165 9.4505 PDSRV2 DEAD BAND FOR CLOSURE OF SRV#2 ES
166 1.15106 PDSRV3 DEAD BAND FOR CLOSURE OF SRV#3 ES
167 5.1705 PDSRV4 DEAD BAND FOR CLOSURE OF SRV#4 ES
168 0.00 PDSRV5 DEAD BAND FOR CLOSURE OF SRV#5 ES
** 8 POINTS ARE USED HERE TO DEFINE THE RCIC AND HPCI TURBINE STEAM FLOW
185 8.2206 PTURRI(1) PPS-PWV VS. STEAM FLOW TO RCIC TURBINE ES
186 1.3406 PTURRI(2) ES
187 1.3406 PTURRI(3) ES
188 1.3406 PTURRI(4) ES
189 1.3406 PTURRI(5) ES
190 1.3406 PTURRI(6) ES
191 1.3406 PTURRI(7) ES
192 1.3406 PTURRI(8) ES
193 4.8300 WSTRCI(1) ES
194 1.5600 WSTRCI(2) ES
195 1.5600 WSTRCI(3) ES
196 1.5600 WSTRCI(4) ES
197 1.5600 WSTRCI(5) ES
198 1.5600 WSTRCI(6) ES
199 1.5600 WSTRCI(7) ES
200 1.5600 WSTRCI(8) ES
201 2.73705 PHTURM HIGH TURBINE EXHAUST PRESSURE FOR HPCI ES
202 1.7205 PHTURR HIGH TURBINE EXHAUST PRESSURE FOR RCIC ES
203 4.91605 PCFAIL CONTAINMENT FAILURE PRESSURE ES

```

DRAFT

A-8

GULEFP.DAT;14

6-JUL-1984 14:29

Page 8

```

** THE SHUT OFF HEAD SHOULD APPEAR IN THE PUMP CURVE DEFINITION FOR ECCS
** THE NEXT TWO PARAMETERS ARE PERMISSIVE SIGNALS FOR TRIPPING SYSTEMS
204 1.D10 PHLPCI HIGH VESSEL PRESSURE TRIP FOR LPCI ES
205 1.D10 PHLPCS HIGH VESSEL PRESSURE TRIP FOR LPCS ES
206 34.237D0 ZHISP HIGH SUPP. POOL LEVEL TRIP FOR HP SUCTION ES
207 47.16D0 ZLSPR NOT USED
** ALL OF THE HEAT EXCHANGER DATA MAY BE OMITTED WITH THE EXCEPTION
** OF NTUHX1,NTUHX2,NHX1,NHX2
208 0.D0 NTHX NUMBER OF TUBES IN RHR HTX ES
209 0.D0 NBHX NUMBER OF BAFFLES IN RHR HTX ES
210 0.D0 XIDTHX TUBE ID FOR RHR HTX ES
211 0.D0 XTTHX TUBE WALL THICKNESS FOR RHR HTX ES
212 0.D0 XICHX TUBE CENTER TO CENTER SPACING FOR RHR HTX ES
213 0.D0 XSHX SHELL LENGTH FOR RHR HTX ES
214 0.D0 RGFOL FOULING FACTOR FOR RHR HTX ES
215 0.D0 KTHX THERMAL CONDUCTIVITY FOR TUBE WALL (RHR HTX) ES
216 0.D0 XBCHX BAFFLE CUT LENGTH FOR RHR HTX ES
217 0.D0 XIDSHX SHELL ID FOR RHR HTX ES
218 0.D0 XSTHX BUNDLE TO SHELL GAP LENGTH FOR RHR HTX ES
** NTU VALUES NOT NEEDED IF ABOVE INFORMATION IS DEFINED
219 1.2D0 NTUHX1 NTU FOR RHR HTX #1 ES
220 1.2D0 NTUHX2 NTU FOR RHR HTX #2 ES
221 2.D0 NHX1 NUMBER OF RHR LOOP #1 HTX ES
222 2.D0 NHX2 NUMBER OF RHR LOOP #2 HTX ES
223 2.D0 FHX TYPE OF RHR HTX(1=STRAIGHT TUBE,2=U TUBE) ES
224 14.4D3 TDBATT BATTERY OPERATION TIME FOR STATION BLACK-OUT ES
** THE FOLLOWING ARE NPSH CURVES AND THE FIRST ENTRY FOR THAT SYSTEM
** CORRESPONDS TO THE FIRST FLOW RATE LISTED ABOVE FOR THAT PUMP
225 .518D0 ZHDHPS HPCS NPSH FOR GIVEN FLOWS ES
226 .518D0 (METERS) ES
227 .518D0 ES
228 .549D0 ES
229 .61D0 ES
230 .762D0 ES
231 1.372D0 ES
232 2.226D0 ES
233 2.073D0 ZHDLPI LPCI NPSH FOR GIVEN FLOW ES
234 .671D0 ES
235 .335D0 ES
236 .335D0 ES
237 .335D0 ES
238 .335D0 ES
239 .366D0 ES
240 .396D0 ES
241 2.457D0 ZHDLPS LPCS NPSH FOR GIVEN FLOW ES
242 1.524D0 ES
243 .854D0 ES
244 .854D0 ES
245 .854D0 ES
246 .854D0 ES
247 .854D0 ES
248 .854D0 ES
249 31.4D0 ZCLRCI PUMP CENTER LINE ELAVATION FOR RCIC ES
250 28.35D0 ZCLHPI PUMP CENTER LINE ELAVATION FOR HPCI ES
251 .0093D0 ACVENT AREA OF CONTAINMENT VENT ES
252 0.0D0 ZCFAIL ELEVATION OF CONTAINMENT VENT IN WETWELL (MII ONLY) ES
253 28.35D0 ZSRVD AVERAGE ELEVATION OF SRV DISCHARGE IN SUPP POOL ES
254 0.D0 IGDWHX(1) COOLING CURVE FOR DRYWELL COOLERS
255 0.D0 IGDWHX(2) TEMP IN DRYWELL VS. HEAT LOSS RATE (J/S)
256 0.D0 IGDWHX(3)
257 0.D0 IGDWHX(4)

```


GULFEP.DAT;14

6-JUL-1984 14:29

Page 13

55	880.DO	CPHS7	SPECIFIC HEAT FOR WALL #7	HS
56	880.DO	CPHS8	SPECIFIC HEAT FOR WALL #8	HS
**ALL OF THESE EQUIPMENT HEAT SINKS ARE LOCATED IN GAS VOL. OF COMPARTMENT				
57	0.DO	MEQPD	MASS OF EQUIPMENT IN PEDESTAL	HS
58	151000.DO	MEQDW	MASS OF EQUIPMENT IN DRYWELL	HS
59	0.DO	MEQWW	MASS OF EQUIPMENT IN WETWELL	HS
60	342462.DO	MEQCA	MASS OF EQUIPMENT IN COMPT A	HS
61	1.9581D6	MEQCB	MASS OF EQUIPMENT IN COMPT B	HS
62	0.DO	AEQPD	AREA OF EQUIPMENT IN PEDESTAL	HS
63	4153.DO	AEQDW	AREA OF EQUIPMENT IN DRYWELL	HS
64	0.DO	AEQWW	AREA OF EQUIPMENT IN WETWELL	HS
65	9.7177D3	AEQCA	AREA OF EQUIPMENT IN COMPT A	HS
66	1189.2D0	AEQCB	AREA OF EQUIPMENT IN COMPT B	HS
67	50.DO	HTOUTW	HEAT TRANSFER COEFF. AT OUTER WALL	HS
68	0.DO	RGAP	INNER LINER TO WALL GAP RESISTANCE #1	HS
69	0.DO	RGAP	INNER LINER TO WALL GAP RESISTANCE #2	HS
70	0.DO	RGAP	INNER LINER TO WALL GAP RESISTANCE #3	HS
71	0.DO	RGAP	INNER LINER TO WALL GAP RESISTANCE #4	HS
72	0.DO	RGAP	INNER LINER TO WALL GAP RESISTANCE #5	HS
73	0.DO	RGAP	INNER LINER TO WALL GAP RESISTANCE #6	HS
74	0.DO	RGAP	INNER LINER TO WALL GAP RESISTANCE #7	HS
75	0.DO	RGAP	INNER LINER TO WALL GAP RESISTANCE #8	HS
76	0.DO	RGAP	OUTER LINER TO WALL GAP RESISTANCE #1	HS
77	0.DO	RGAP	OUTER LINER TO WALL GAP RESISTANCE #2	HS
78	0.DO	RGAP	OUTER LINER TO WALL GAP RESISTANCE #3	HS
79	0.DO	RGAP	OUTER LINER TO WALL GAP RESISTANCE #4	HS
80	0.DO	RGAP	OUTER LINER TO WALL GAP RESISTANCE #5	HS
81	0.DO	RGAP	OUTER LINER TO WALL GAP RESISTANCE #6	HS
82	0.DO	RGAP	OUTER LINER TO WALL GAP RESISTANCE #7	HS
83	0.DO	RGAP	OUTER LINER TO WALL GAP RESISTANCE #8	HS
84	0.DO	MEQWWS	MASS OF EQUIP. HEAT SINK WETWELL (SUBMERGED)	HS
85	0.DO	AEQWWS	AREA OF EQUIP. HEAT SINK WETWELL (SUBMERGED)	HS
86	1.45D2	AHSPS1	AREA OF RPV IN GAS SPACE OF VESSEL	HS
87	1.75D2	AHSPS2	AREA OF RPV IN DOWNCOMER REGION	HS
88	6.5D0	AHSPS3	AREA OF RPV IN LOWER PLENUM	HS
89	2.24D5	MRPV1	RPV WALL MASS IN UPPER DOME REGION	HS
90	2.22D5	MRPV2	RPV WALL MASS IN DOWNCOMER REGION	HS
91	9.D4	MRPV3	RPV WALL MASS IN LOWER PLENUM REGION	HS
**				HS
**				HS
*MODEL PARAMETERS FOR BWR				
01	.005D0	FRCOEF	FRICTION COEFFICIENT FOR CORIUM IN VEAIL	MO
02	2.0D-1	EMAXCP	FRACTION OF TOTAL CORE MASS WHICH MUST MELT TO FAIL THE CORE PLATE	MO
**				MO
03	50.DO	HTBLAD	FUEL CHANNEL TO CONTROL BLADE HEAT TRANS. COEFF	MO
04	300.DO	HIEB	FILM BOILING HEAT TRANS. COEFF.	MO
05	0.DO	FBLOCK	FUEL CHANNEL BLOCKAGE PARAMETER	MO
**			0=BLOCKAGE AT TZOOFF,1=NO BLOCKAGE	MO
06	2300.DO	TZOOFF	OXIDATION CUT-OFF TEMPERATURE	MO
07	.3D0	FACPE	FRACTION OF CORE PLATE AREA THAT FAILS	MO
08	5.DO	CDBPD	FLAME BUOYANCY DRAG COEFFICIENT IN THE PEDESTAL	MO
09	5.DO	CDBDW	FLAME BUOYANCY DRAG COEFFICIENT IN THE DRYWELL	MO
10	5.DO	CDBWW	FLAME BUOYANCY DRAG COEFFICIENT IN THE WETWELL	MO
11	5.DO	CDBCA	FLAME BUOYANCY DRAG COEFFICIENT IN COMPARTMENT A	MO
12	5.DO	CDBC B	FLAME BUOYANCY DRAG COEFFICIENT IN COMPARTMENT B	MO
13	.10D0	XCNREE	CORIUM REFERENCE THERMAL BOUNDARY LAYER THICKNESS	MO
14	1.D3	HTCMCR	CORIUM-CRUST HEAT TRANSF. COEFF. USED IN DECOMP	MO
15	0.05D0	XCMX	MINIMUM CORIUM THICKNESS ON DRYWELL FLOOR AND PED FLOOR (MARK II ONLY)	MO
**				MO
16	0.01D0	XDCMSP	PARTICLE SIZE (DIAMETER) FOR CORIUM AS IT FALLS INTO SUPPRESSION POOL (MARK II ONLY)	MO
**				MO

DRAFT

A-14

GULFEP.DAT;14

6-JUL-1984 14:29

Page 14

17	983.DO	TCFLAM	CRITICAL FLAME TEMPERATURE	MO
18	1.53DO	FCMTUR	CHURN-TURBULENT CRITICAL FLOW PARAMETER	MO
19	3.7DO	FDROP	DROPLET CRITICAL FLOW PARAMETER	MO
20	3.DO	FFLOOD	FLOODING FLOW PARAMETER	MO
21	1.DO	FSPAR	PARAMETER FOR BOTTOM-SPARGED STEAM VOID FRACTION	MO
22	2.DO	FVOL	PARAMETER FOR VOLUME SOURCE VOID FRACTION MODEL	MO
23	5.0-1	TTENTR	ENTRAINMENT EFFECTIVE EMPTYING TIME	MO
24	.9DO	EW	EMISSIVITY OF WATER	MO
25	.85DO	EWL	EMISSIVITY OF WALL	MO
26	.85DO	ECM	EMISSIVITY OF CORIUM	MO
27	.6DO	EG	EMISSIVITY OF GAS	MO
28	.85DO	EEQ	EMISSIVITY OF EQUIPMENT	MO
29	0.5DO	FOVER	FRACTION OF CORE SPRAY FLOW ALLOWED TO BYPASS CORE	MO
30	1.DO	NPF	NUMBER OF PENETRATIONS FAILED IN LOWER HEAD	MO
31	2.DO	FCDCDW	DOWNCOMER PERIMETER PER METER FROM PEDESTAL DOOR (MARK II ONLY)	MO
**				
32	0.14DO	FCHE	COEFFICIENT FOR CHE CORRELATION IN PLSTM	MO
33	.75DO	FCDBRK	DISCHARGE COEFFICIENT FOR PIPE BREAK	MO
34	.33DO	FENTR	NUMBER TO MULTIPLY KUTATELADZE CRITERION BY TO REPRESENT DIFFICULTY (GT 1.DO) OR EASE (LT 1.DO)	MO
**				
**			FOR MATERIAL TO BE BLOWN OUT OF CAVITY	MO
35	1.00	SCALU	SCALING FACTOR FOR ALL BURNING VELOCITIES	MO
36	1.00	SCALH	SCALING FACTOR FOR HT COEFFICIENTS TO PASSIVE HEAT SINKS	MO
**				
37	2.000	FUMIN	CLADDING SURFACE MULTIPLIER	MO
**				
**				CN
*CONCRETE PROPERTIES				
01	56.DO	MOLWCM	MOLECULAR WEIGHT OF CONCRETE	CN
02	1743.DO	TCMMP	MELTING TEMPERATURE OF CONCRETE	CN
03	.8DO	LHRCN	REACTION ENERGY FOR CONCRETE DECOMPOSITION	CN
04	65.DO	DCFWCM	FREE WATER DENSITY IN CONCRETE	CN
05	65.DO	DCCWCM	COMBINED WATER DENSITY IN CONCRETE	CN
06	572.DO	DCC2CN	CO2 DENSITY IN CONCRETE	CN
07	1.06	LHCM	LATENT HEAT TO MELT CONCRETE	CN
**				
*FISSION PRODUCTS				
01	.028DO	FQP(1)	PERCENT POWER IN FISSION PRODUCT GROUP 1	FI
02	.176DO	FQP(2)	PERCENT POWER IN FISSION PRODUCT GROUP 2	FI
03	.019DO	FQP(3)	PERCENT POWER IN FISSION PRODUCT GROUP 3	FI
04	0.00	FQP(4)	PERCENT POWER IN FISSION PRODUCT GROUP 4	FI
05	0.00	FQP(5)	PERCENT POWER IN FISSION PRODUCT GROUP 5	FI
06	439.3	MFP(1)	MASS OF FISSION PRODUCT GROUP 1 -NOBLES	FI
07	237.7	MFP(2)	MASS OF FISSION PRODUCT GROUP 2 -CS+I	FI
08	37.1	MFP(3)	MASS OF FISSION PRODUCT GROUP 3 -TE	FI
09	178.7	MFP(4)	MASS OF FISSION PRODUCT GROUP 4 -SR	FI
10	435.0	MFP(5)	MASS OF FISSION PRODUCT GROUP 5 -RU	FI
11	1190.DO	MSMO(1)	MASS OF SM IN CORE REGION	FI
12	268.DO	MSMO(2)	MASS OF MN IN CORE REGION	FI
13	0.000	EDSP(1)	SPRAY REMOVAL LAMDA FOR EP GROUP 1	FI
14	0.000	EDSP(2)	SPRAY REMOVAL LAMDA FOR EP GROUP 2	FI
15	0.000	EDSP(3)	SPRAY REMOVAL LAMDA FOR EP GROUP 3	FI
16	0.000	EDSP(4)	SPRAY REMOVAL LAMDA FOR EP GROUP 4	FI
17	0.000	EDSP(5)	SPRAY REMOVAL LAMDA FOR EP GROUP 5	FI
18	600.DO	EDFSP(1)	DRYWELL VENTS DECON. FACTOR FOR EP GROUP 1	FI
19	600.DO	EDFSP(2)	DRYWELL VENTS DECON. FACTOR FOR EP GROUP 2	FI
20	600.000	EDFSP(3)	DRYWELL VENTS DECON. FACTOR FOR EP GROUP 3	FI
21	600.000	EDFSP(4)	DRYWELL VENTS DECON. FACTOR FOR EP GROUP 4	FI
22	600.000	EDFSP(5)	DRYWELL VENTS DECON. FACTOR FOR EP GROUP 5	FI
23	1000.DO	EDERV(1)	SRV DECON. FACTOR FOR EP GROUP 1	FI
24	1000.DO	EDERV(2)	SRV DECON. FACTOR FOR EP GROUP 2	FI
25	1000.000	EDERV(3)	SRV DECON. FACTOR FOR EP GROUP 3	FI

DRAFT

GULFFP.DAT;14

6-JUL-1984 14:29

Page 15

26 1000.000 FDERV(4) SRV DECON. FACTOR FOR FP GROUP 4
27 1000.000 FDERV(5) SRV DECON. FACTOR FOR FP GROUP 5
** 28 - 31 ARE FOUR CONSTANTIS IN HENRY-EPSTEIN MODEL
**
*BR

FI
FI
FI

DRAFT

APPENDIX B

Supplemental Plots for the Base Accident Sequences

DRAFT

B-2

DRAFT

SUPPLEMENTAL PLOTS FOR SEQUENCE T_1 QUV

DRAFT

B-4

T1QUV - GRAND GULF

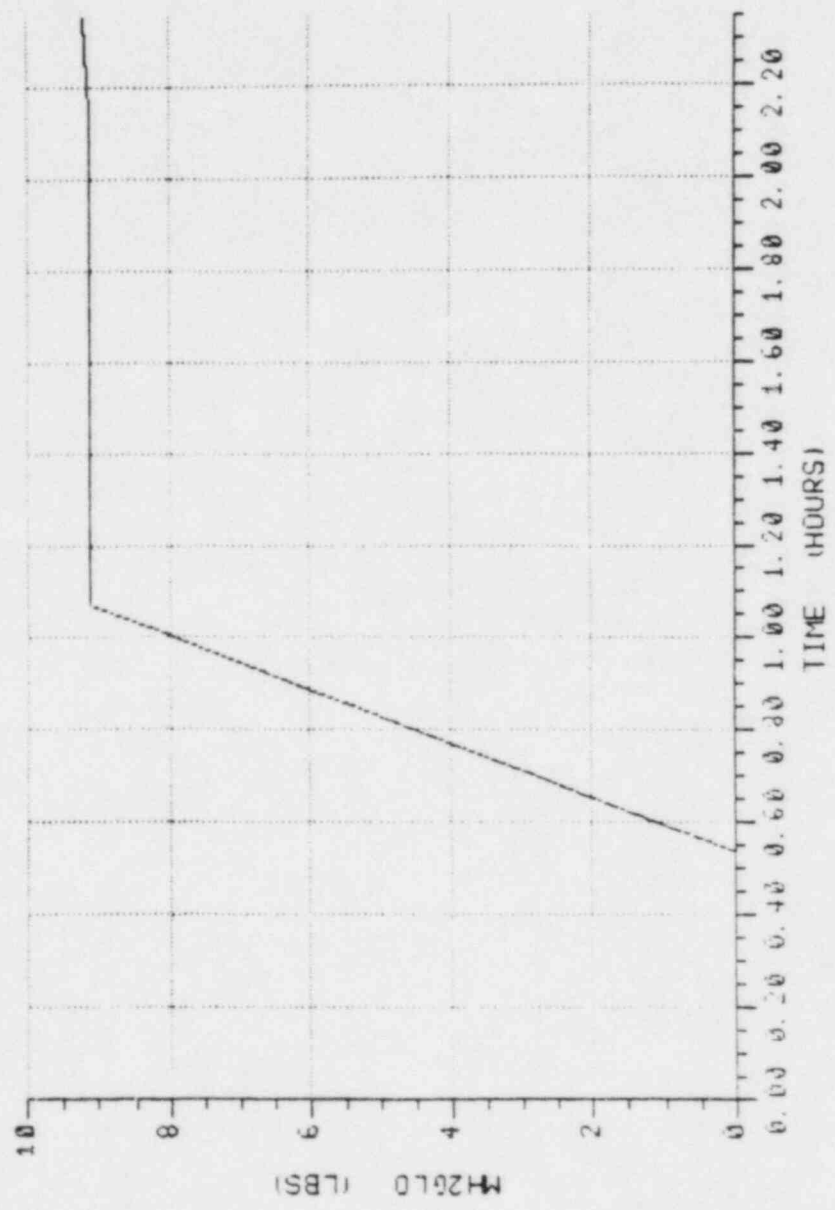


Fig. B.1 Total H₂ generated.

T10UV - GRAND GULF

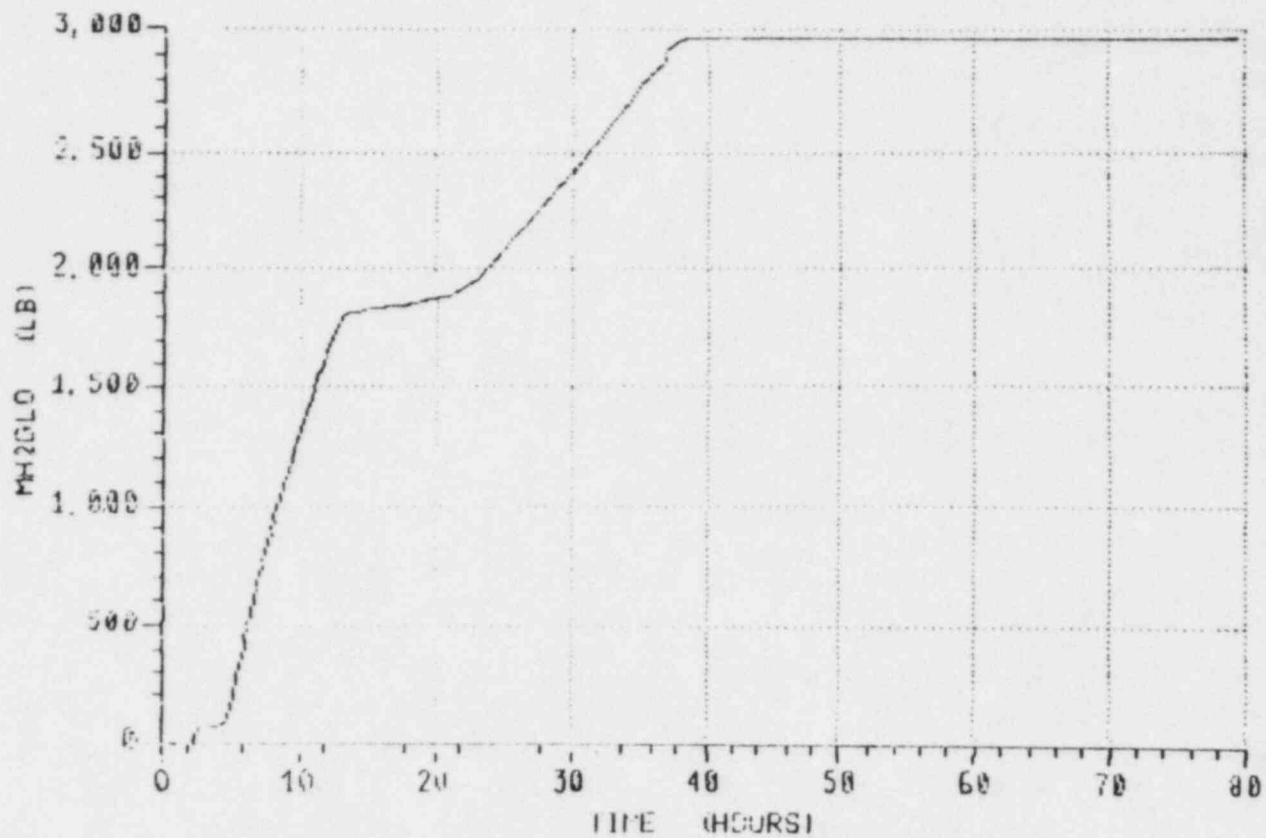


Fig. B.2 Total H₂ generated.

B-5

DRAFT

T1QUV - GRAND GULF

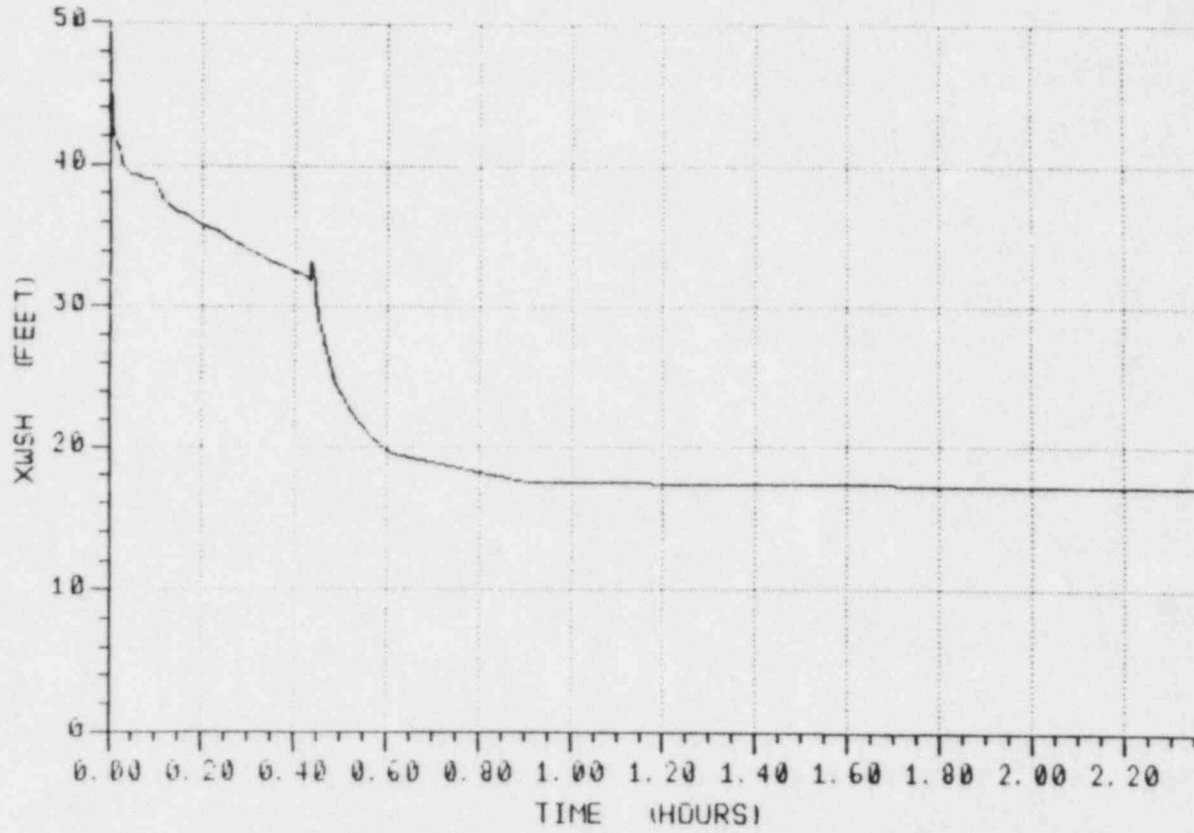


Fig. B.3 Reactor vessel water level.

T1QUV - GRAND GULF

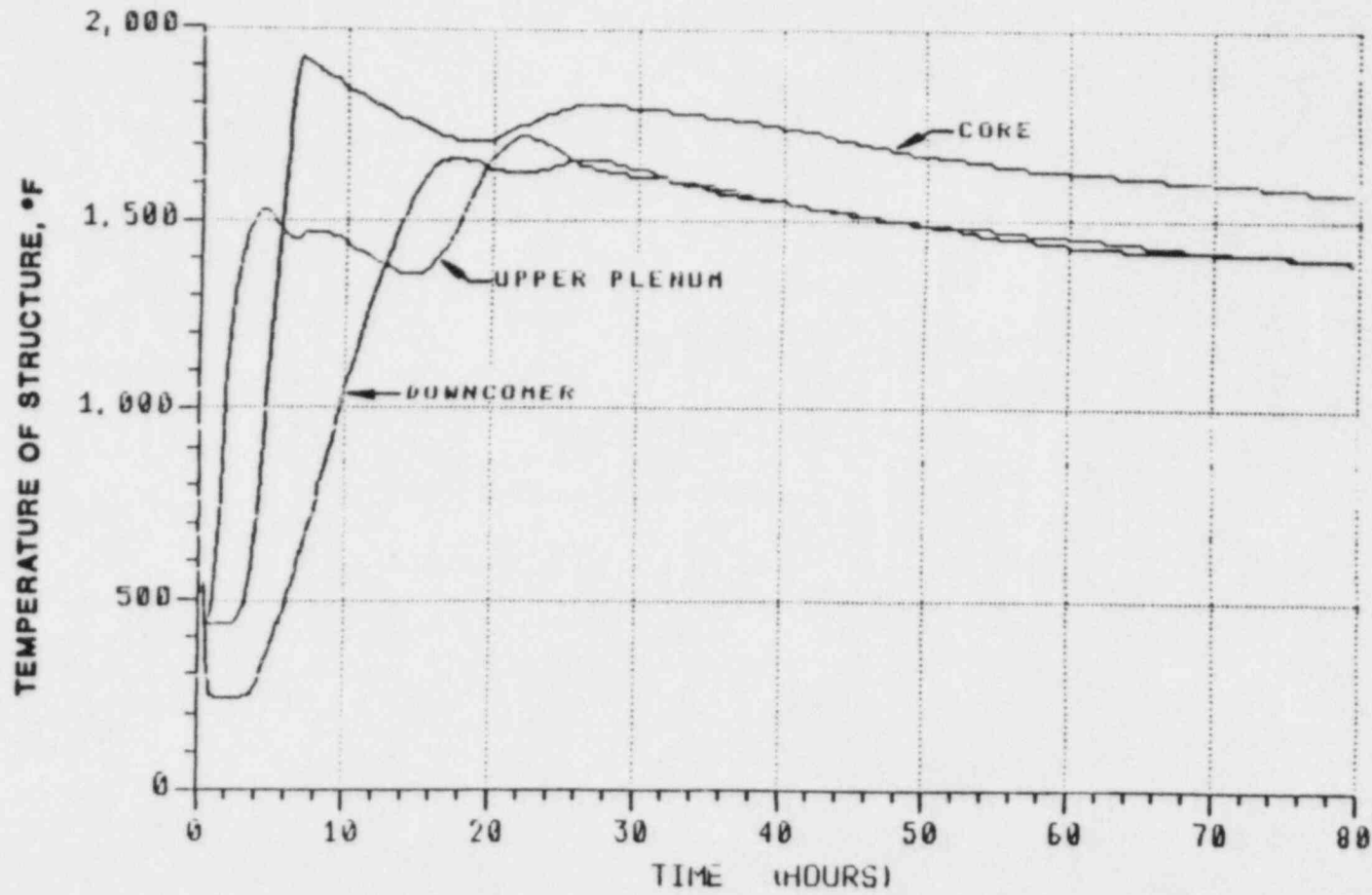


Fig. B.4 Temperature of structure, °F.

T1QUV - GRAND GULF

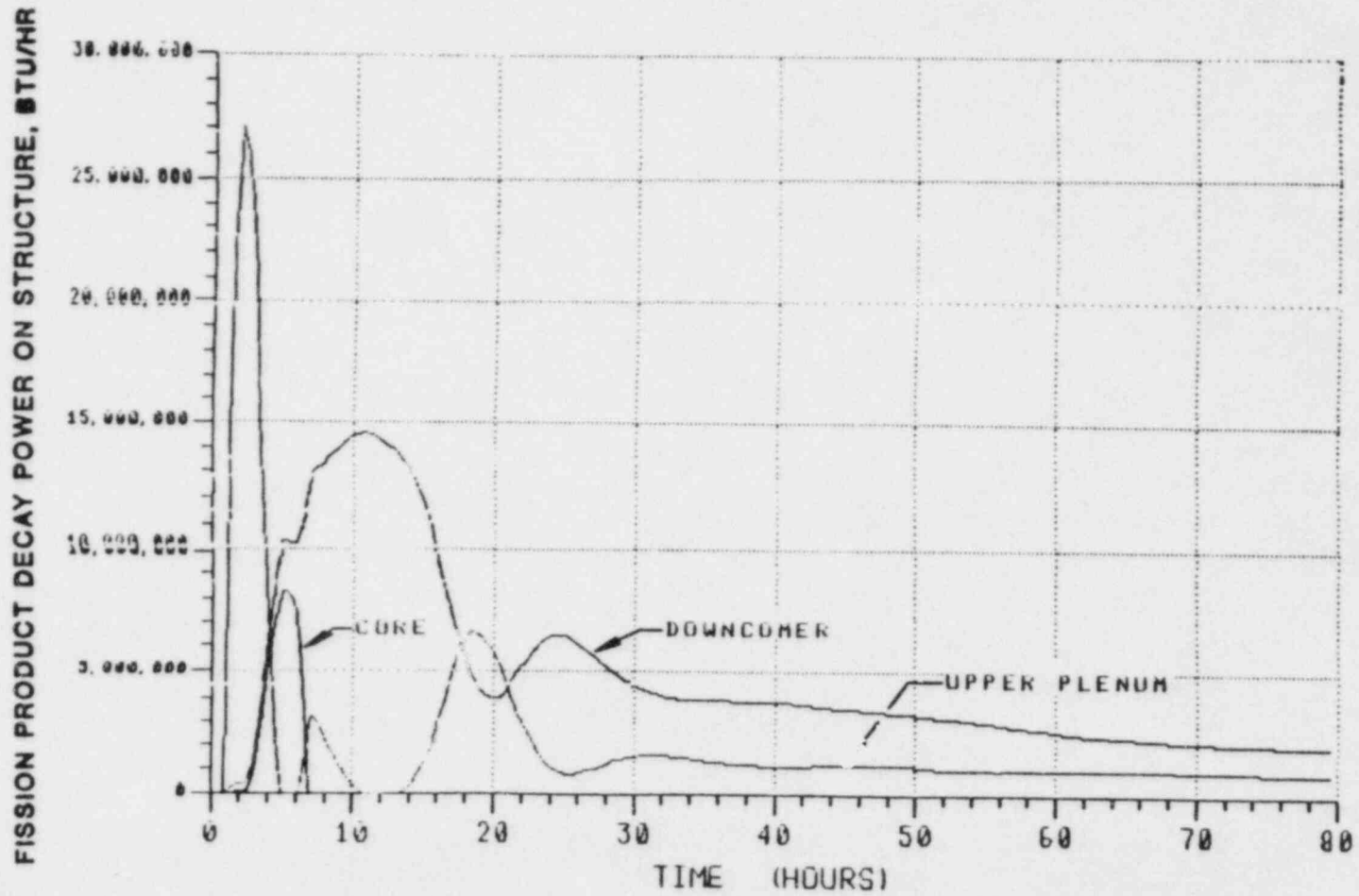


Fig. B.5 Fission product decay power on structure, Btu/hr.

T1QUV - GRAND GULF

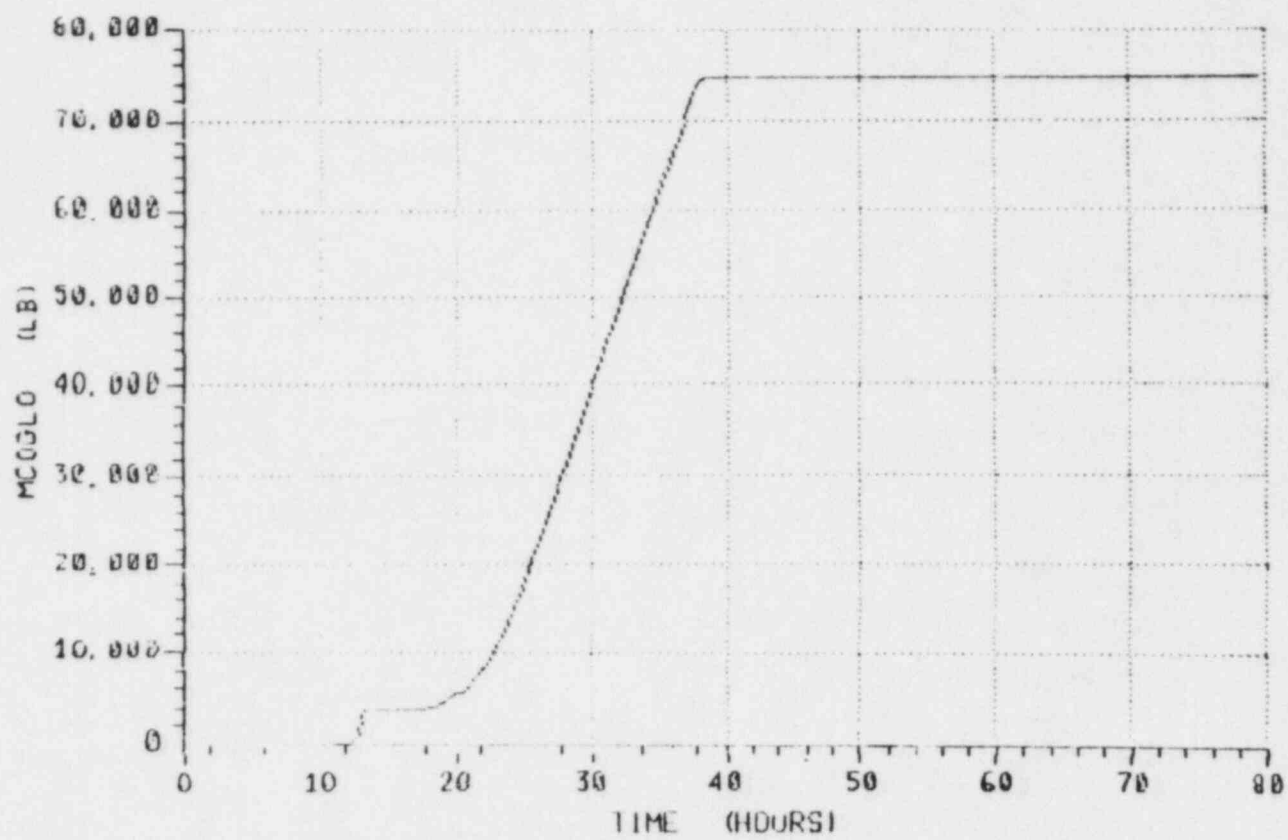


Fig. B.6 Total CO generated.

DRAFT

DRAFT

T1QUV - GRAND GULF

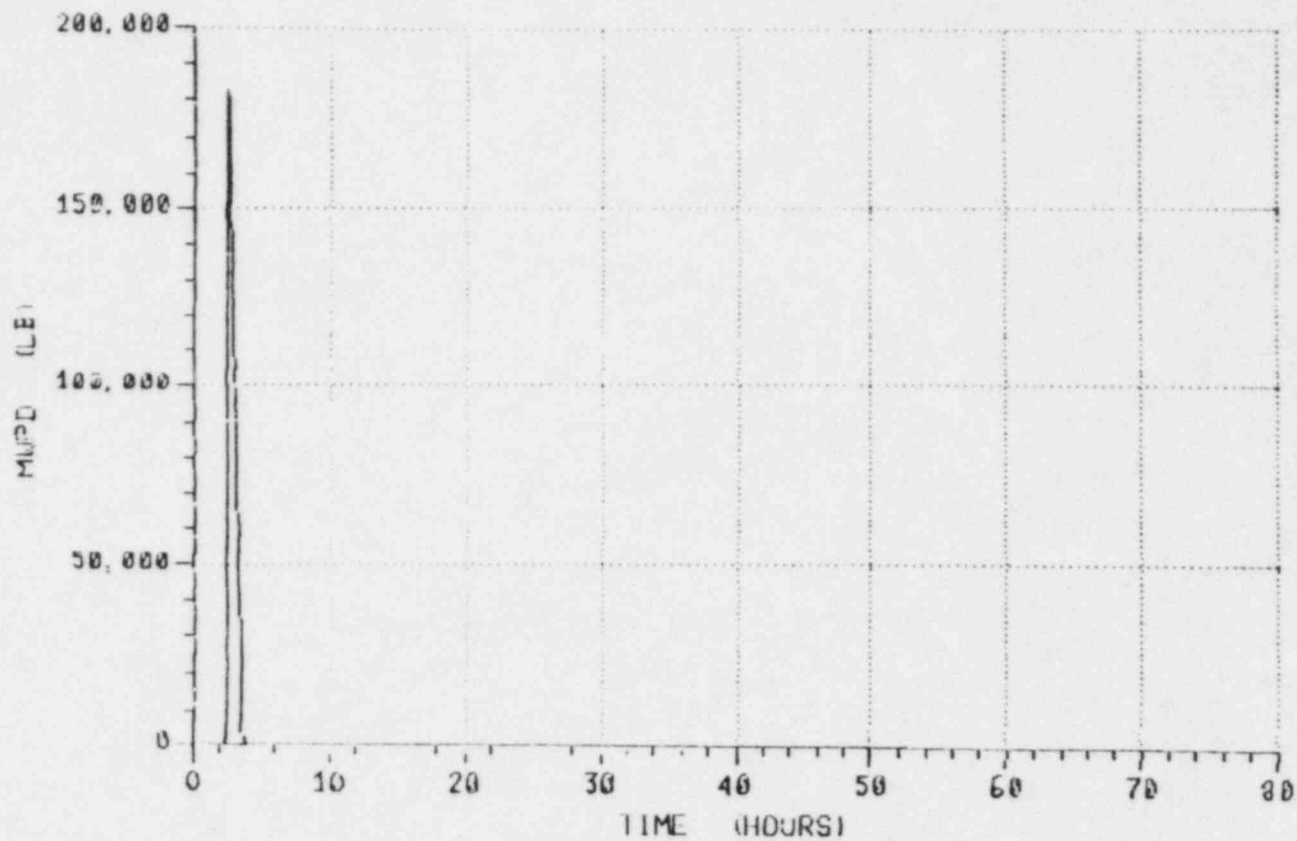


Fig. B.7 Mass of water in the pedestal.

T10UV - GRAND GULF

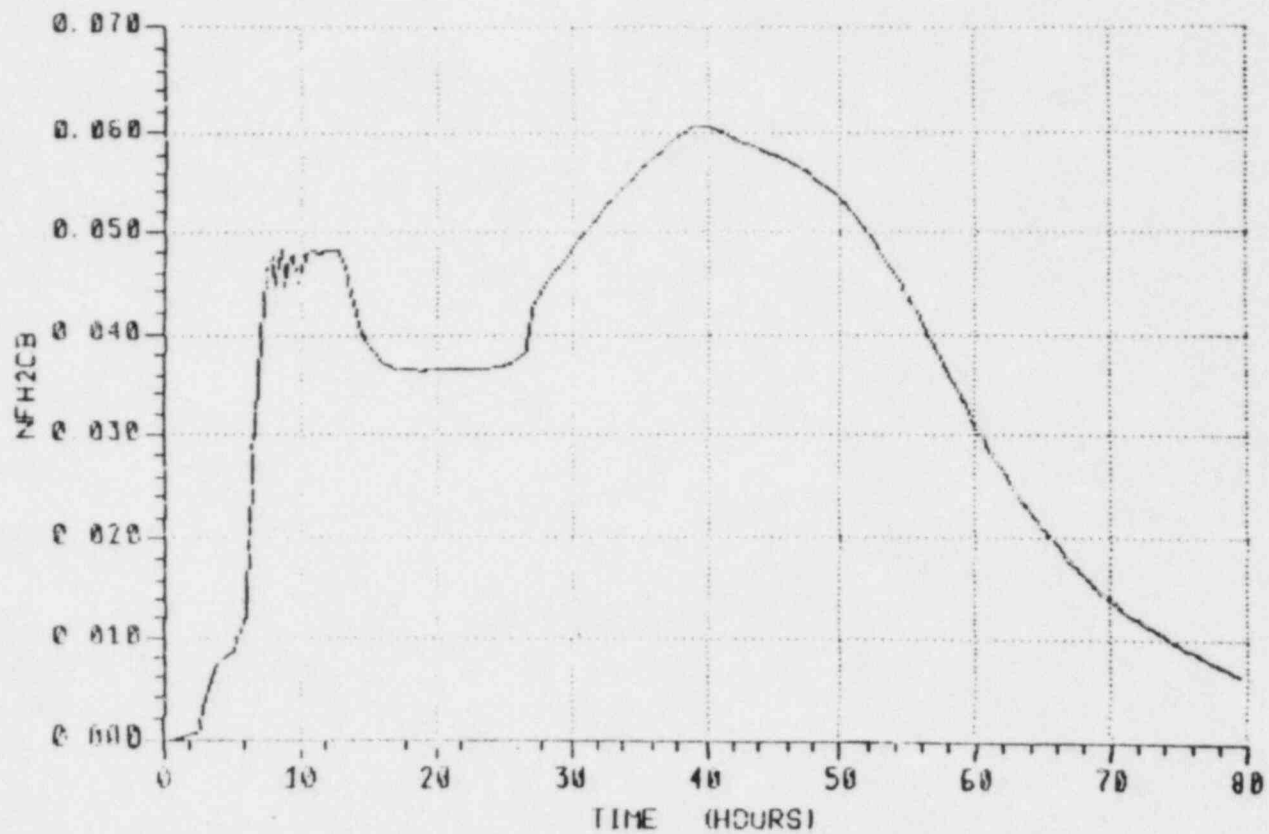


Fig. B.8 Mole fraction of H₂ in Compartment B.

B-11

DRAFT

T1QUV - GRAND GULF

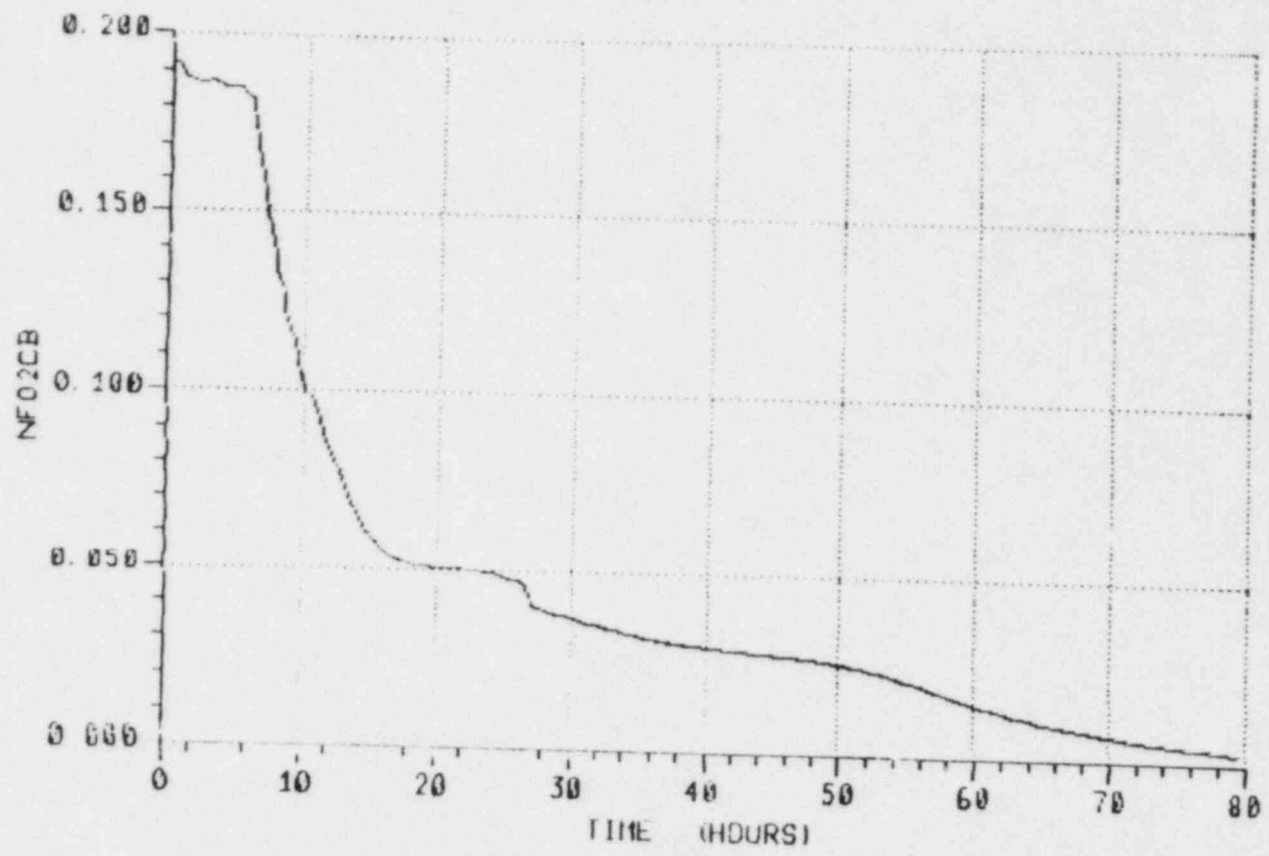


Fig. B.9 Mole fraction of O₂ in Compartment B.

T1QUV - GRAND GULF

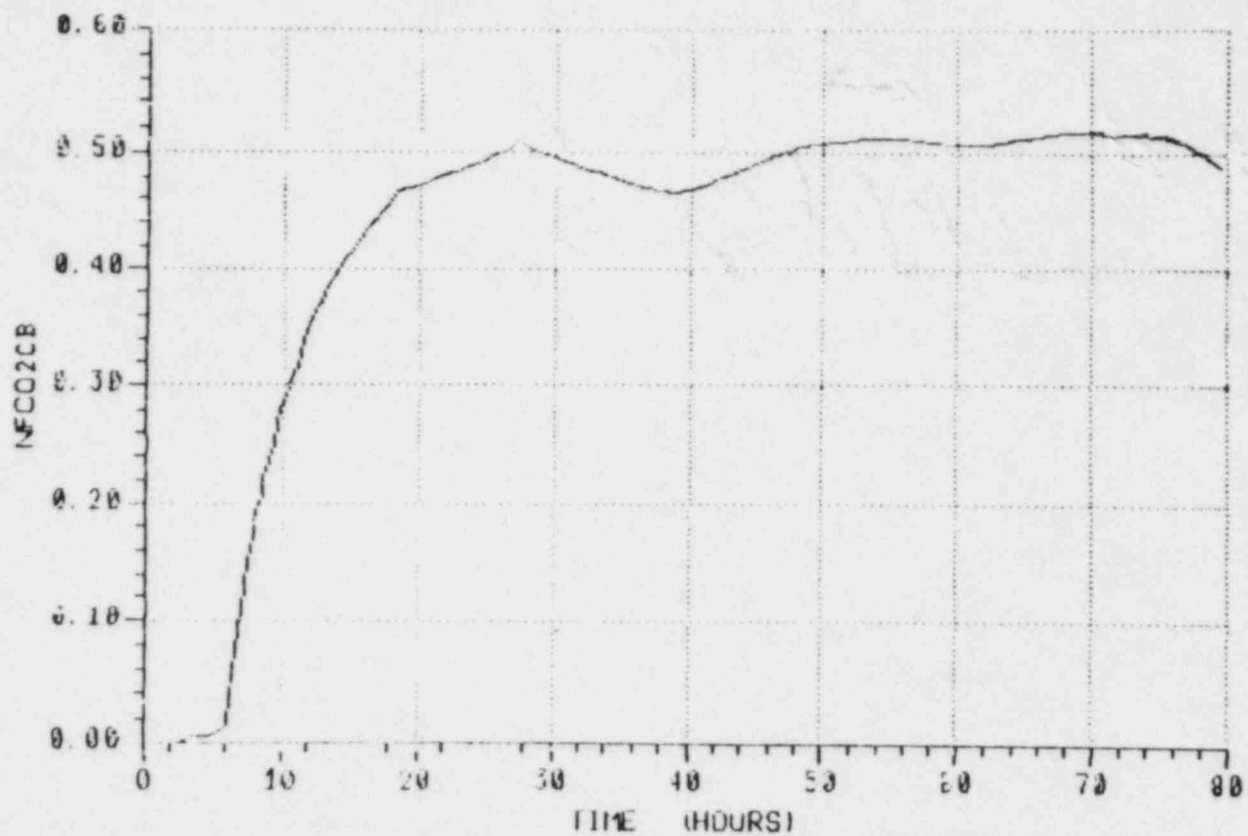


Fig. B.10 Mole fraction of CO₂ in Compartment B.

T1QUV - GRAND GULF

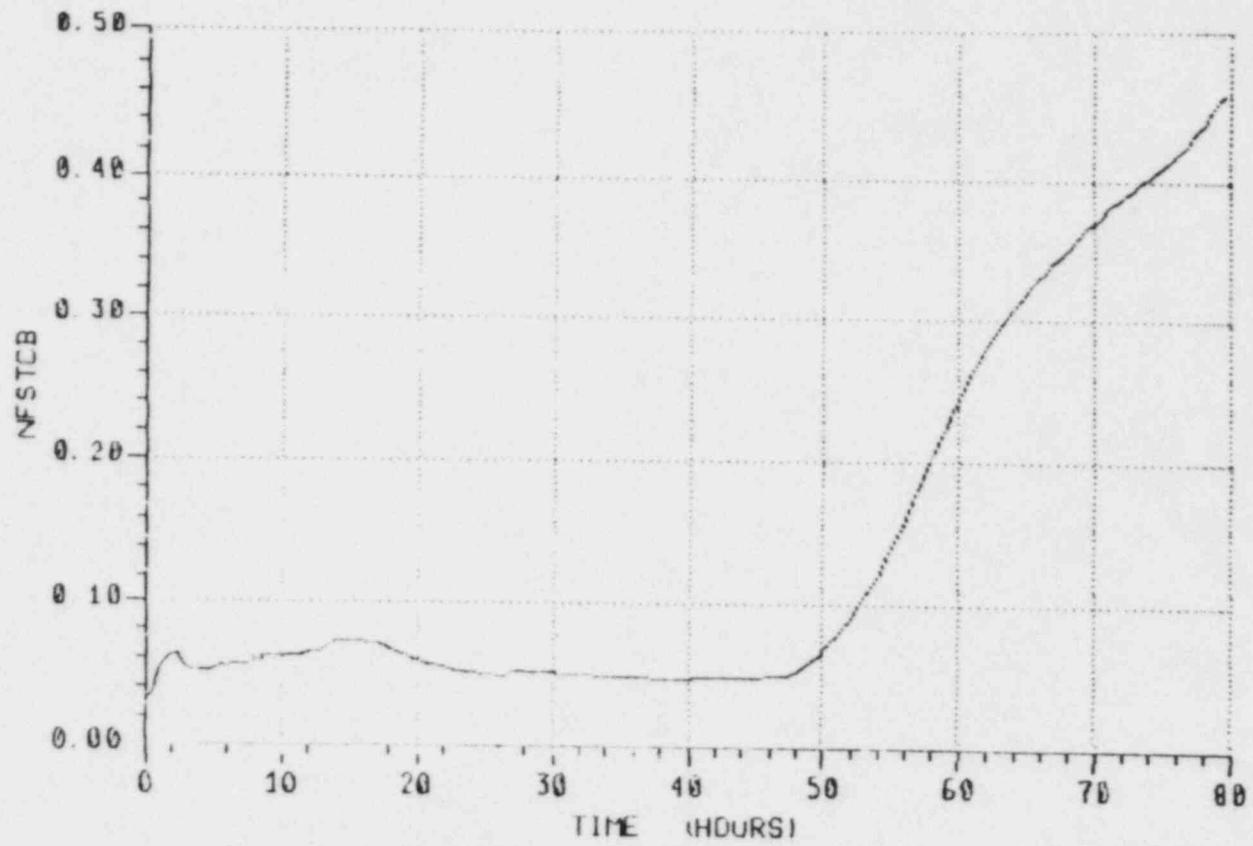


Fig. B.11 Mole fraction of steam in Compartment B.

T10UV - GRAND GULF

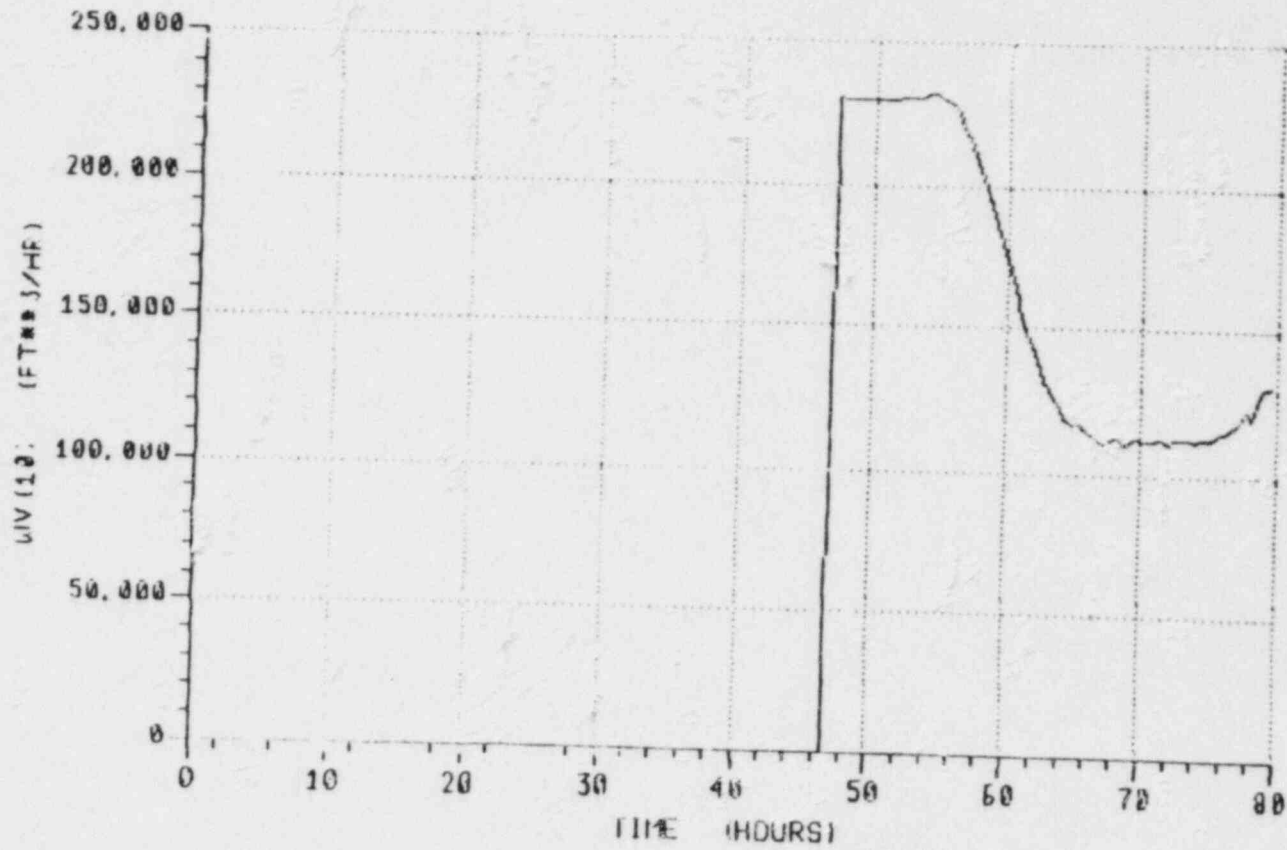


Fig. B.12 Volumetric flow out of containment.

T1QUV - GRAND GULF

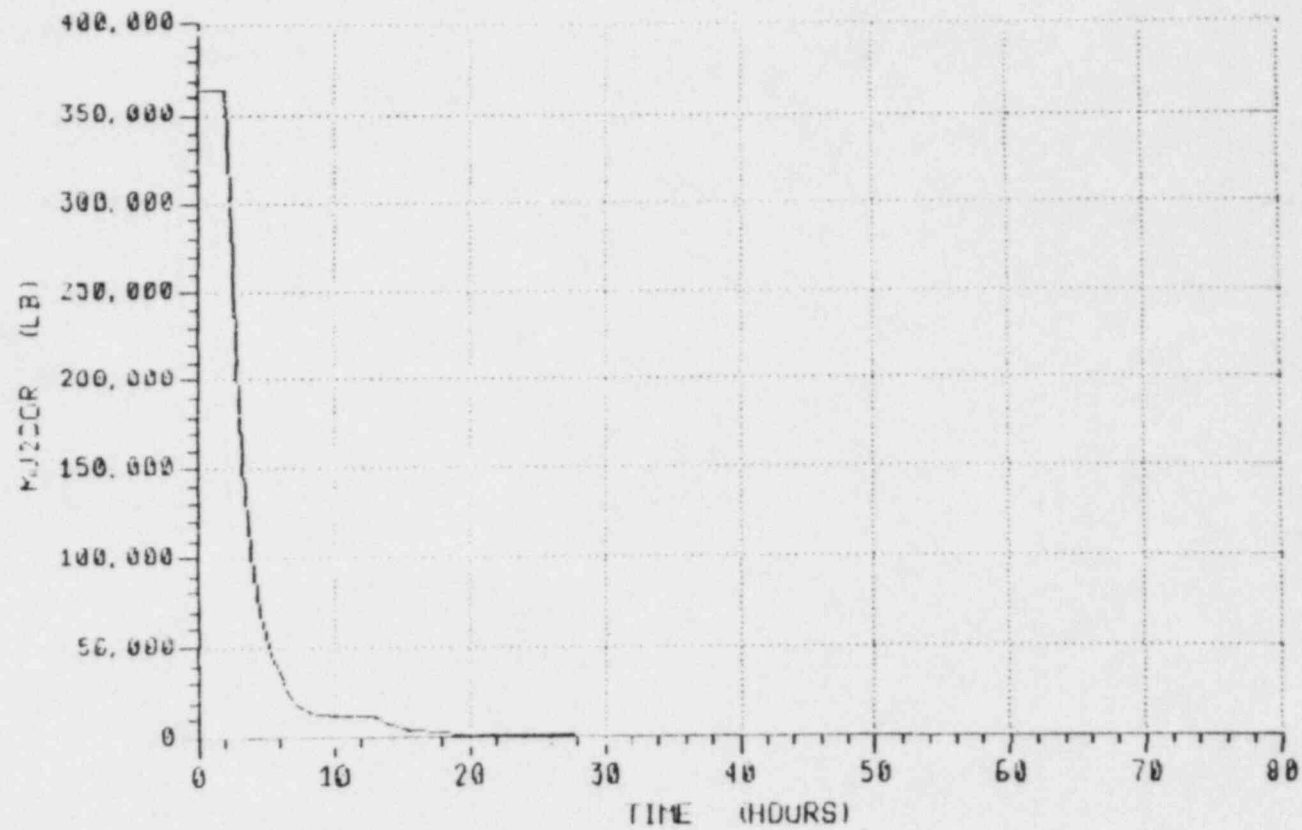


Fig. B.13 Mass of UO₂ in core region.

DRAFT

SUPPLEMENTAL PLOTS FOR SEQUENCE AE

AE - GRAND GULF

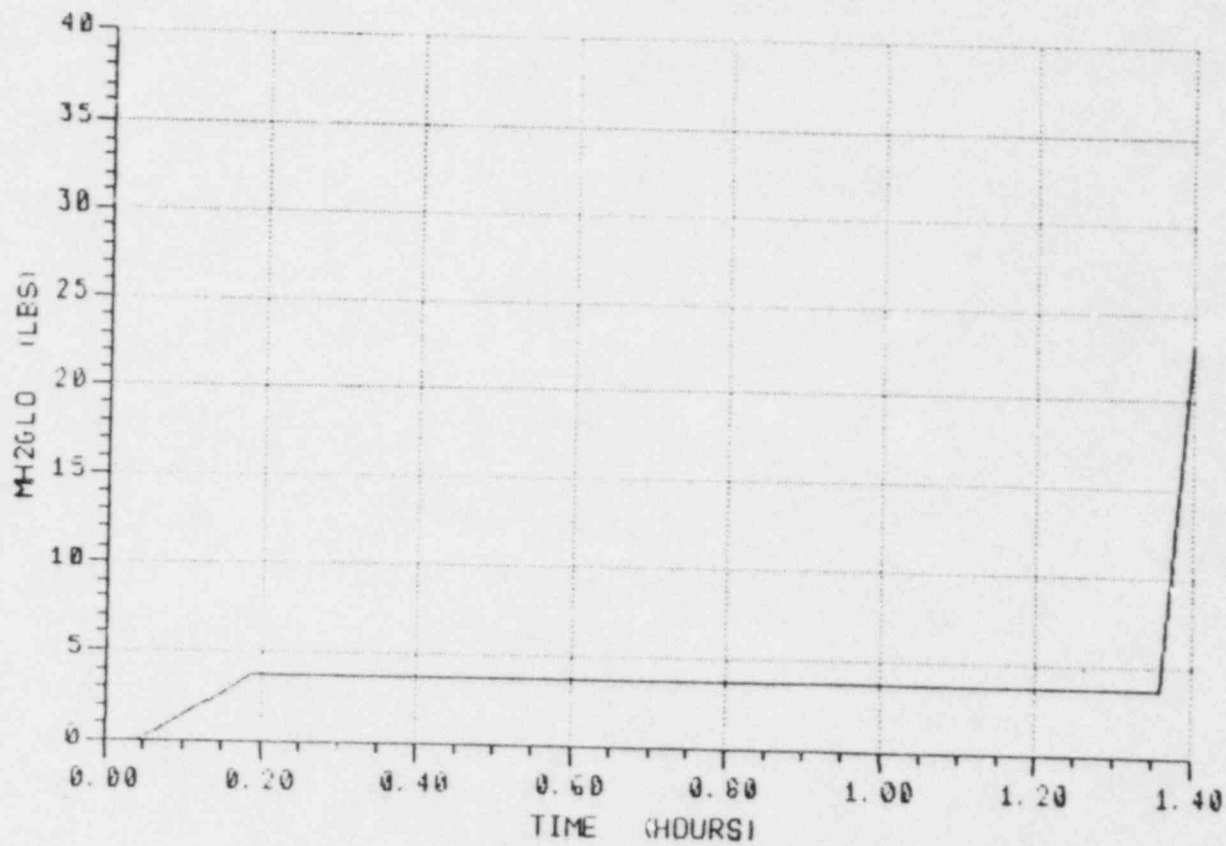


Fig. B.14 Total H₂ generated.

DRAFT

AE - GRAND GULF



Fig. B.15 Total H₂ generated.

AE - GRAND GULF

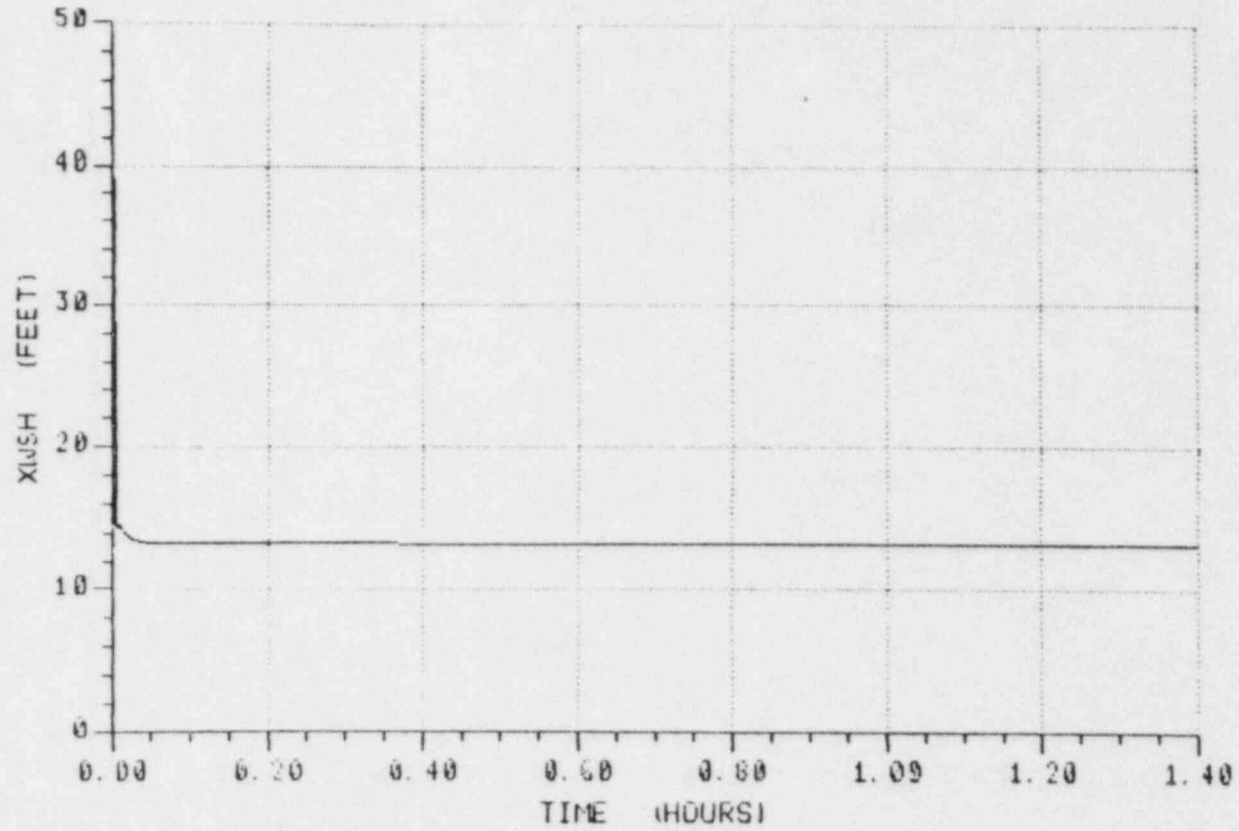


Fig. B.16 Reactor vessel water level.

AE - GRAND GULF

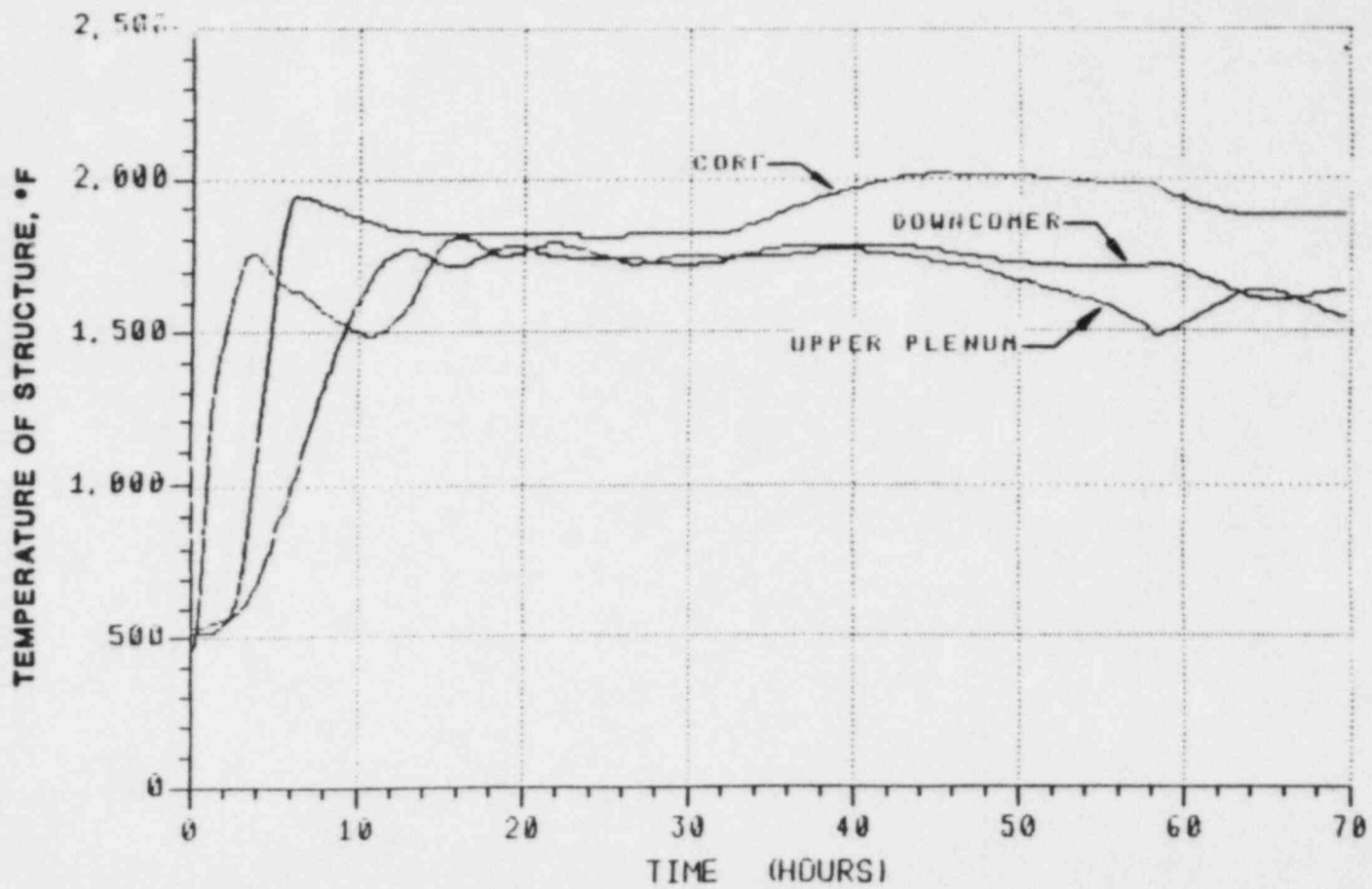


Fig. B.17 Temperature of structure, °F.

B-21

DRAFT

AE - GRAND GULF

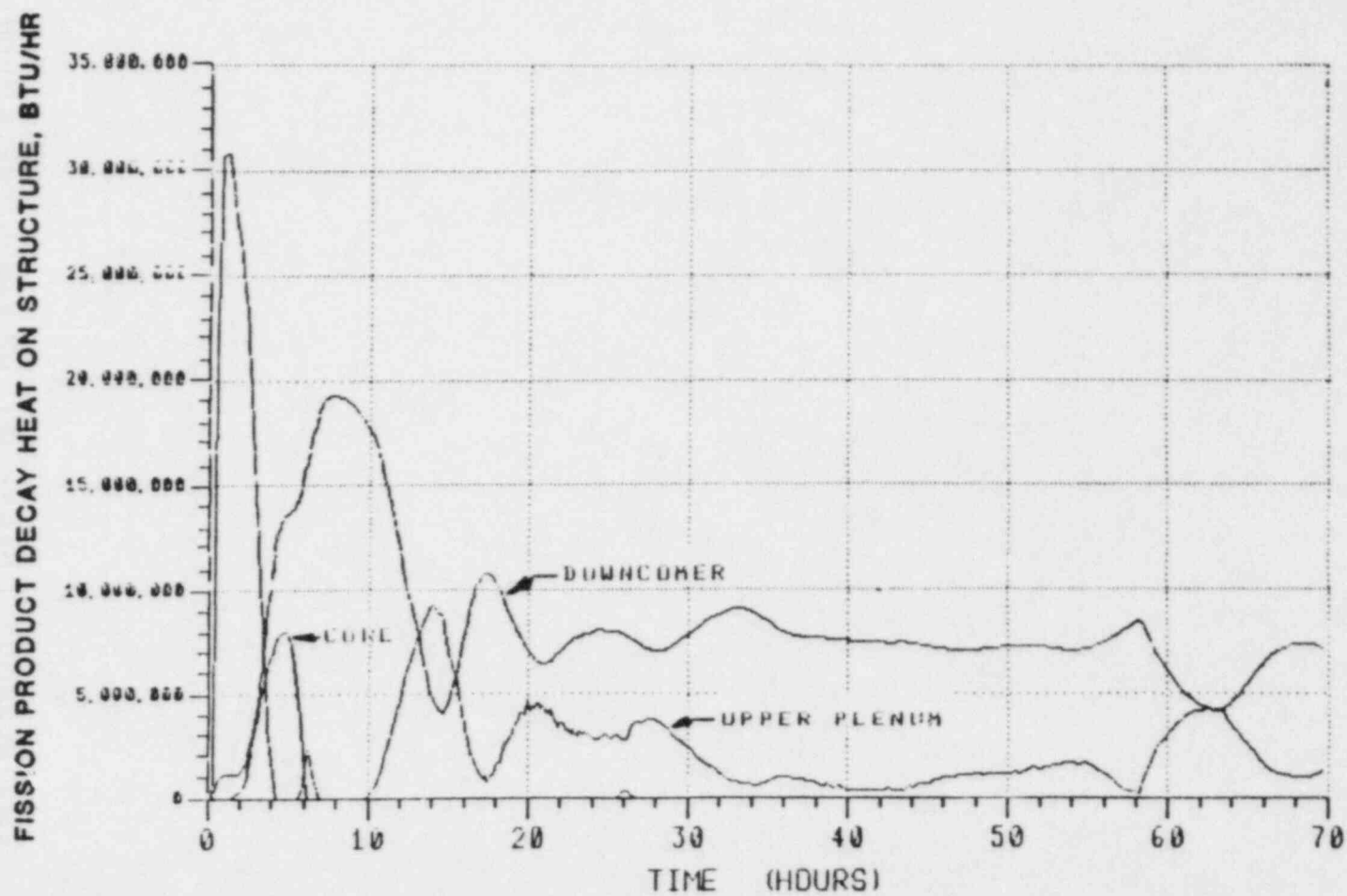


Fig. B.18 Fission product decay heat on structure, Btu/hr.

DRAFT

AE - GRAND GULF

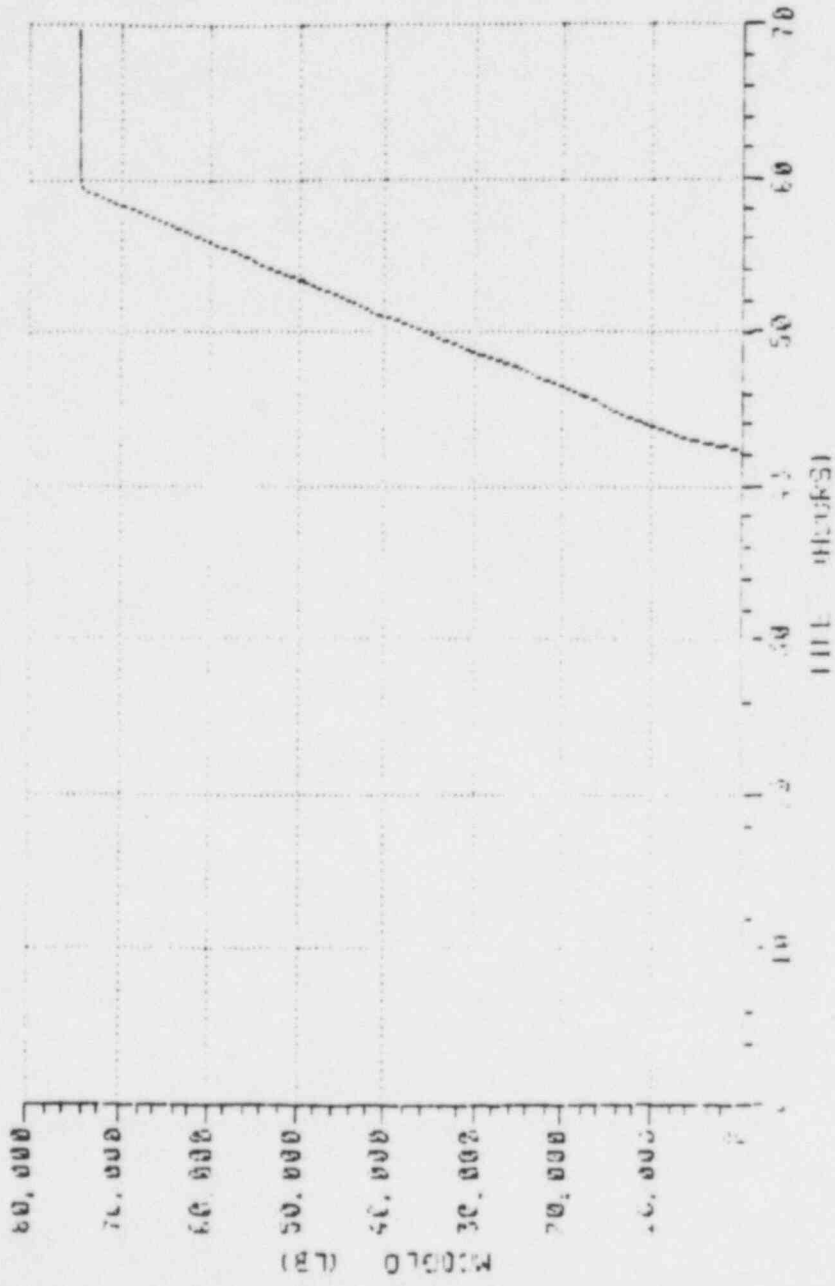


Fig. B.19 Total CO generated.

DRAFT

B-24

AE GRAND GULF

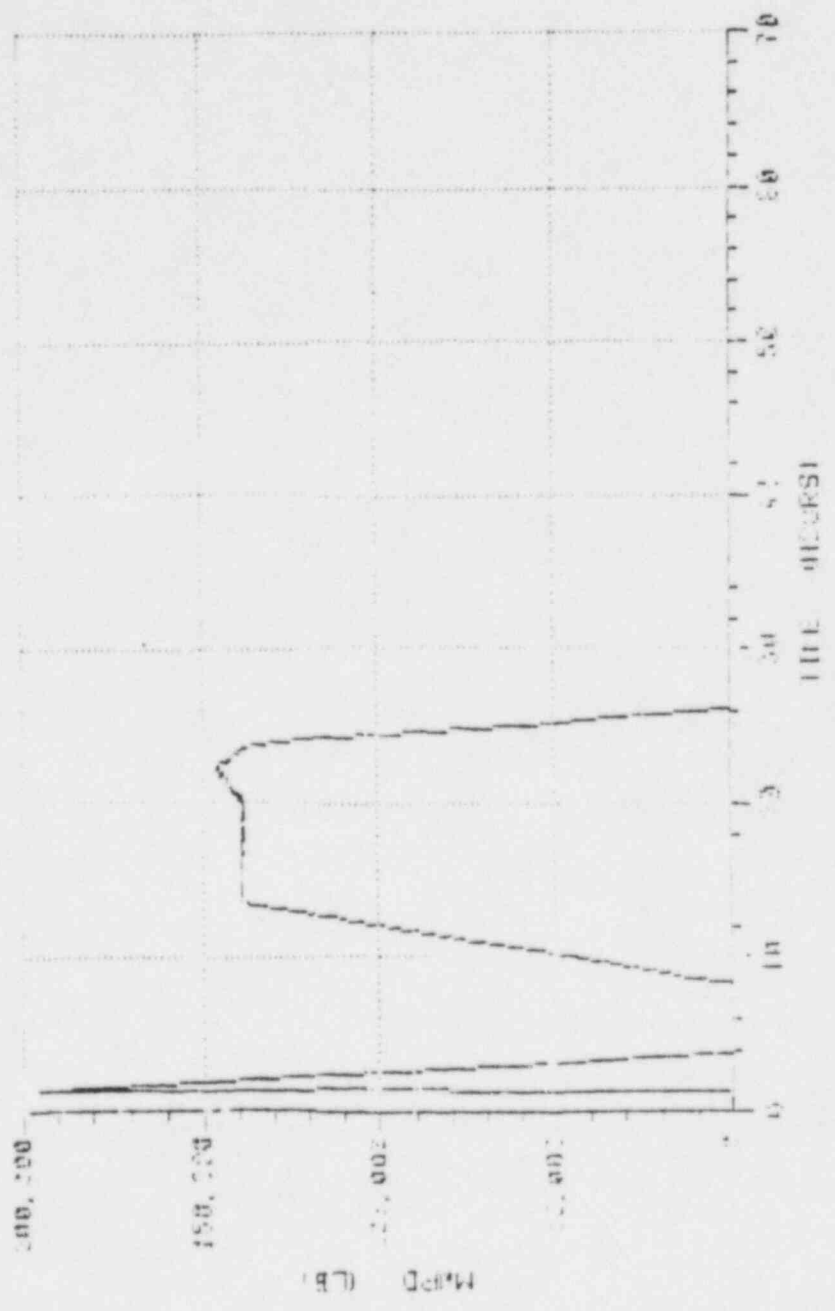


Fig. B.20 Mass of water in the pedestal.

DRAFT

AE GRAND GULF

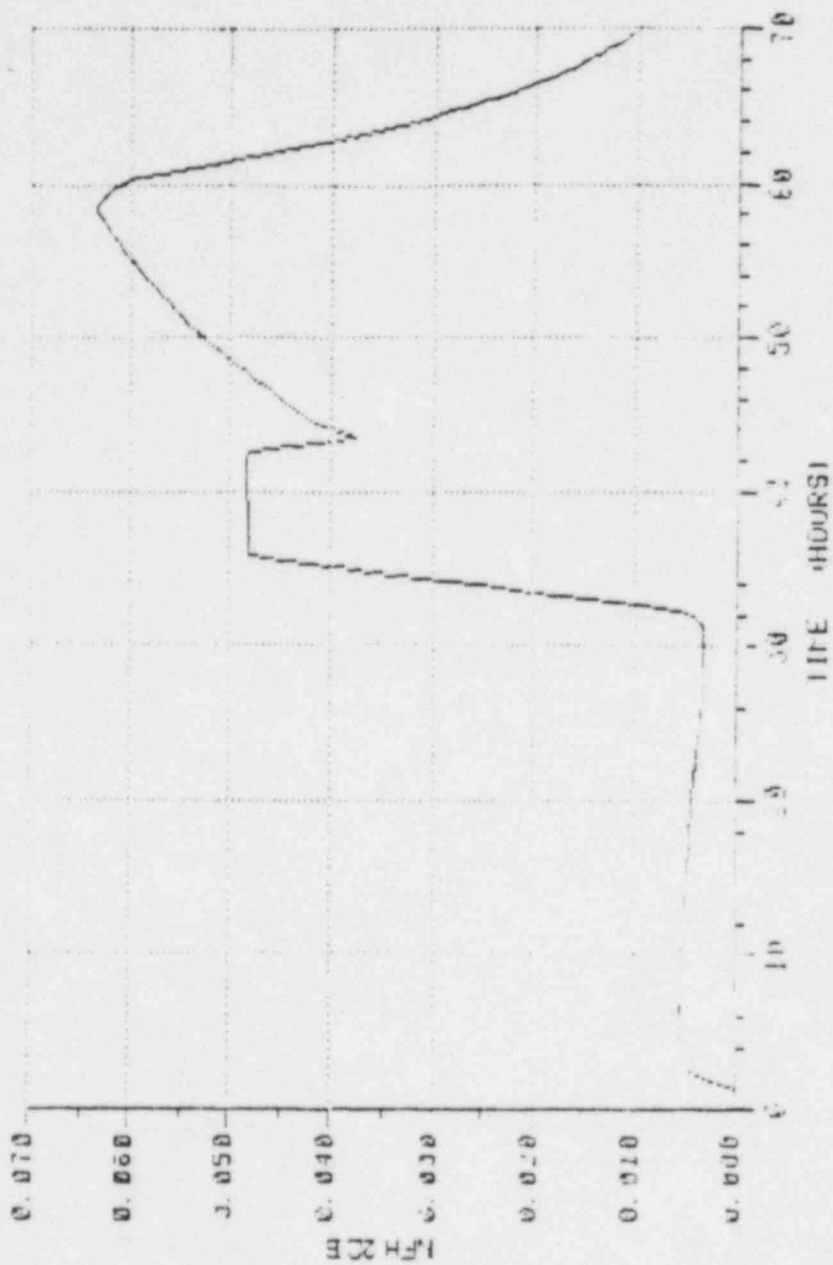


Fig. B.21 Mole fraction of H₂ in Compartment B.

DRAFT

B-26

AC - LIQUID GULF

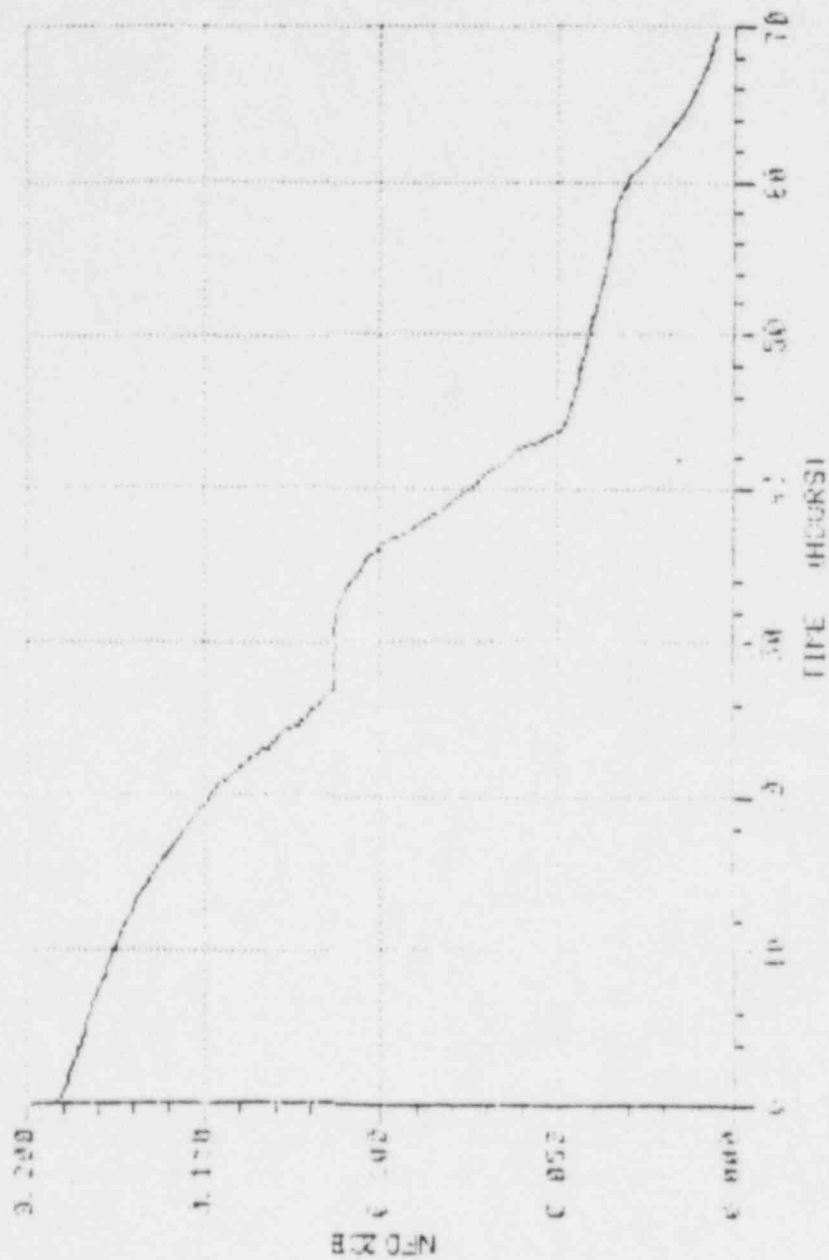


Fig. B. 22 Mole fraction of O₂ in Compartment B.

AE LEAND GULF

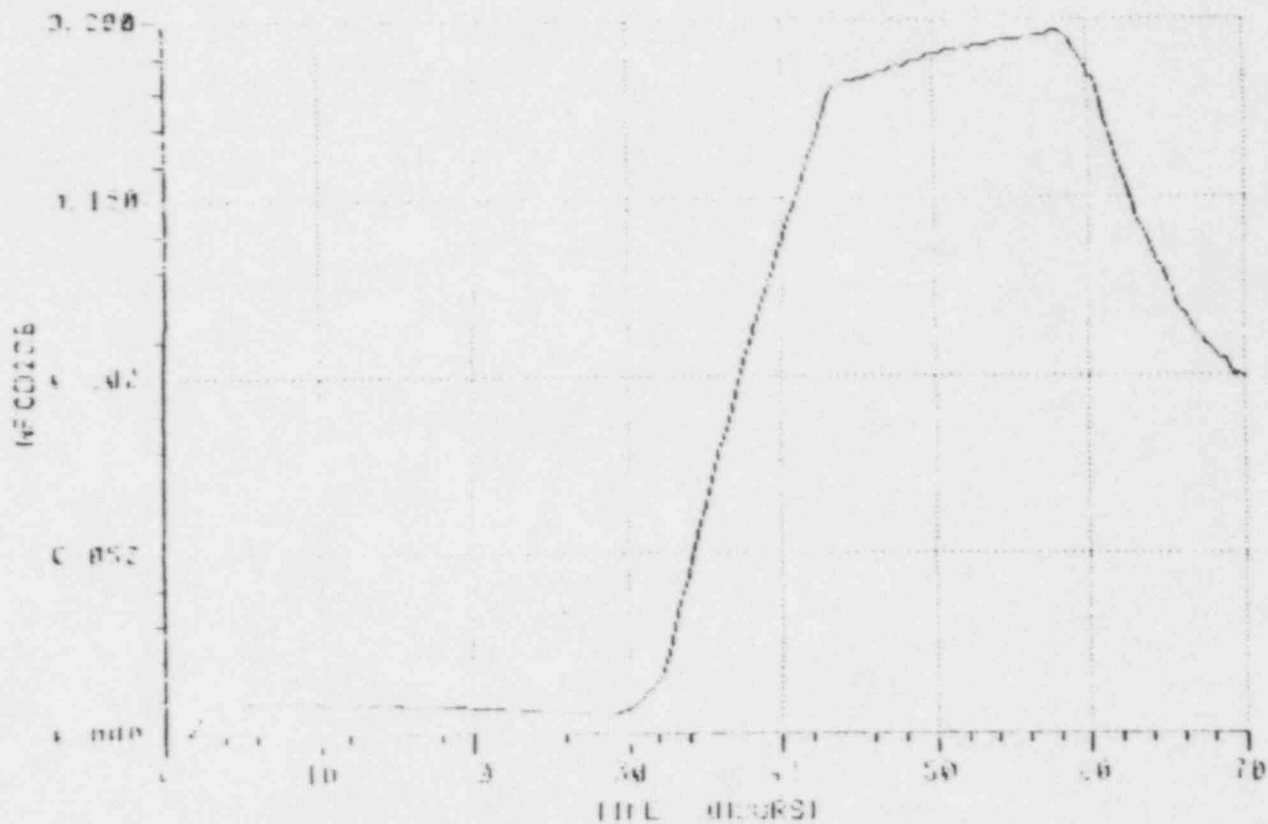


Fig. B.23 Mole fraction of CO₂ in Compartment B.

AE GRAND GULF

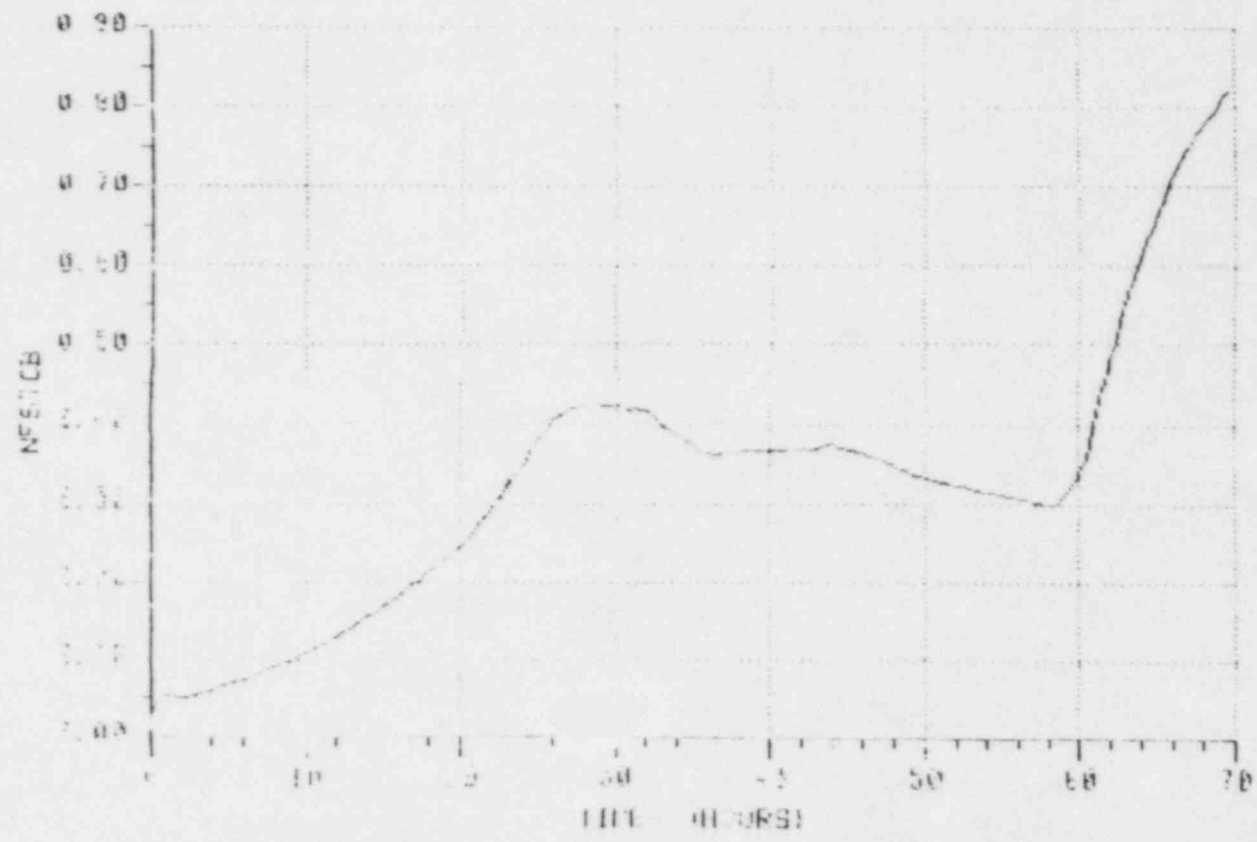


Fig. B.24 Mole fraction of steam in Compartment B.

AT GRAND GULF

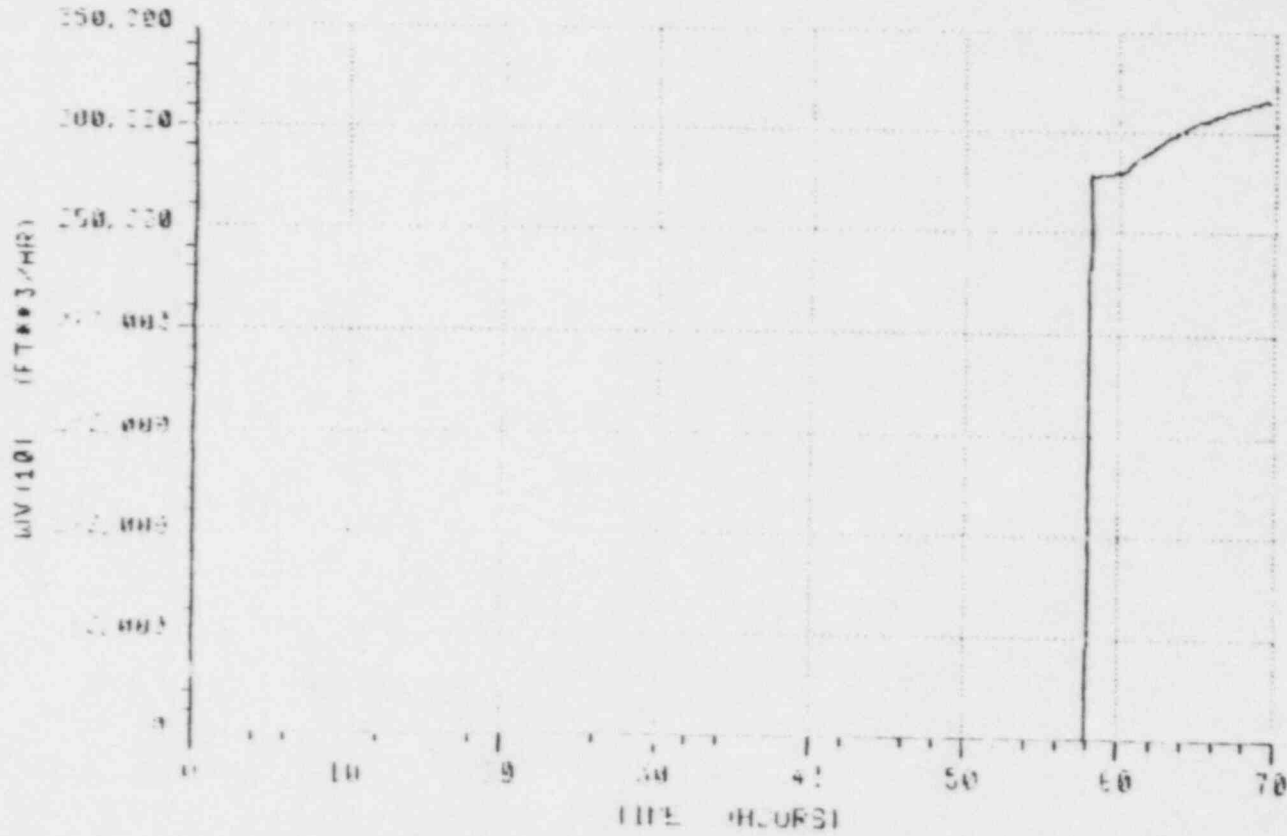


Fig. B.25 Volumetric flow out of containment.

DRAFT

AE GRAND GULF

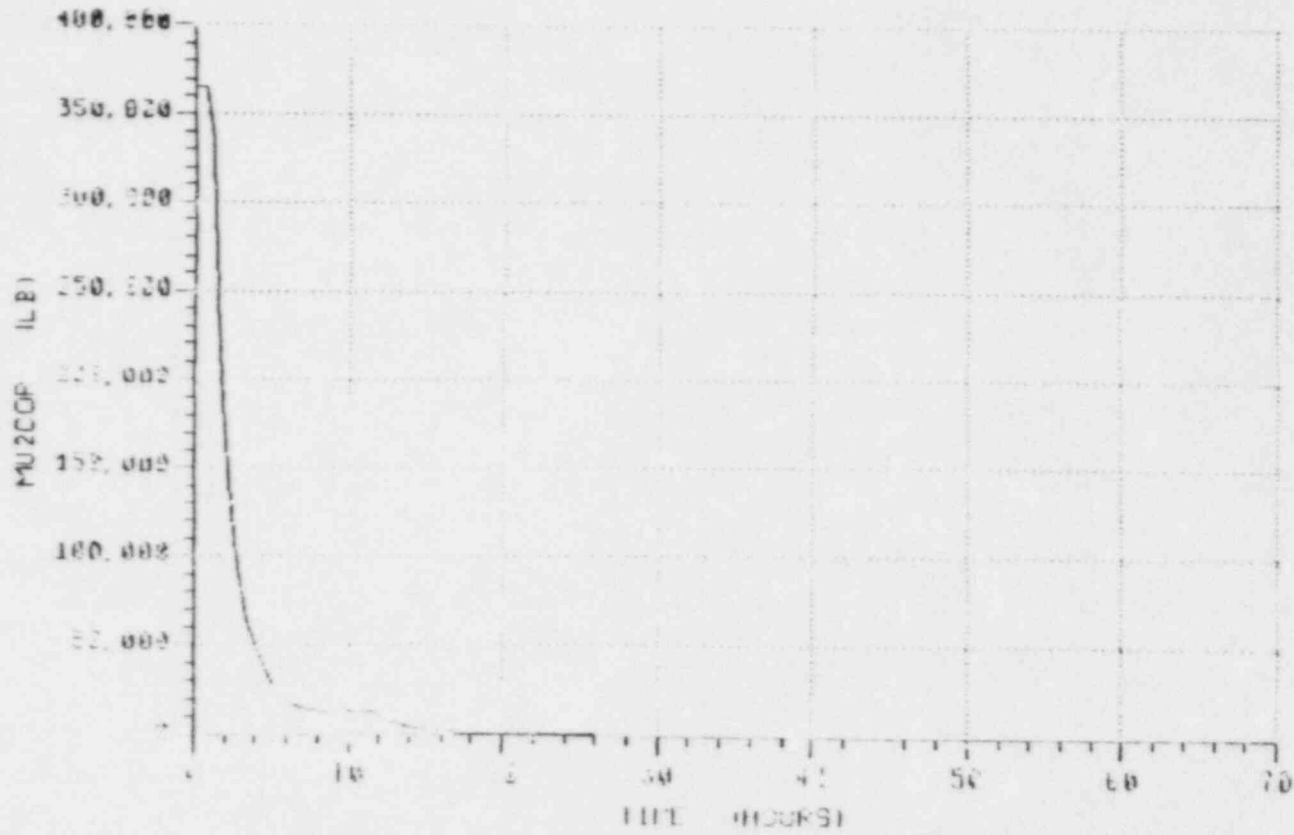


Fig. B.26 Mass of UO₂ in core region.

DRAFT

SUPPLEMENTAL PLOTS FOR SEQUENCE T_{23}^{QW}

DRAFT

B-32

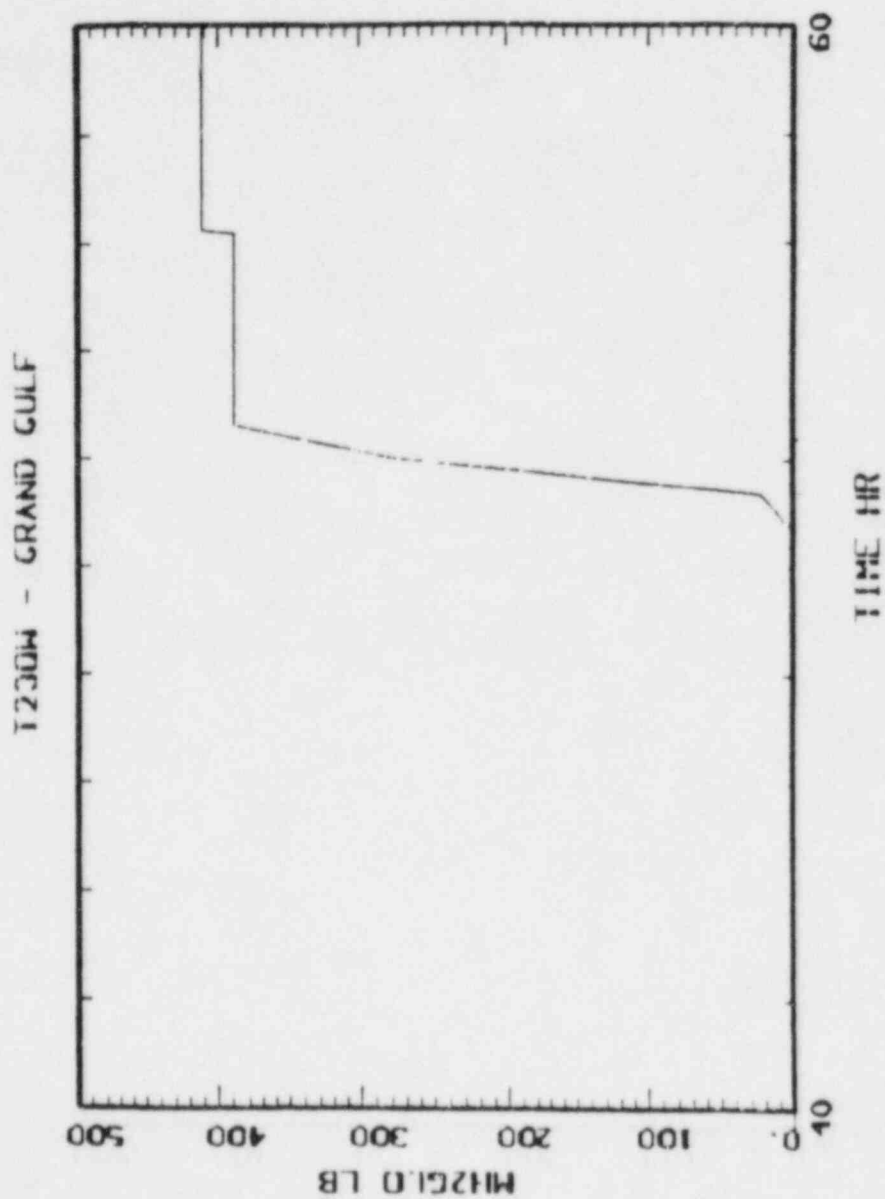


Fig. B.27 Total H₂ generated.

T230W - GRAND GULF

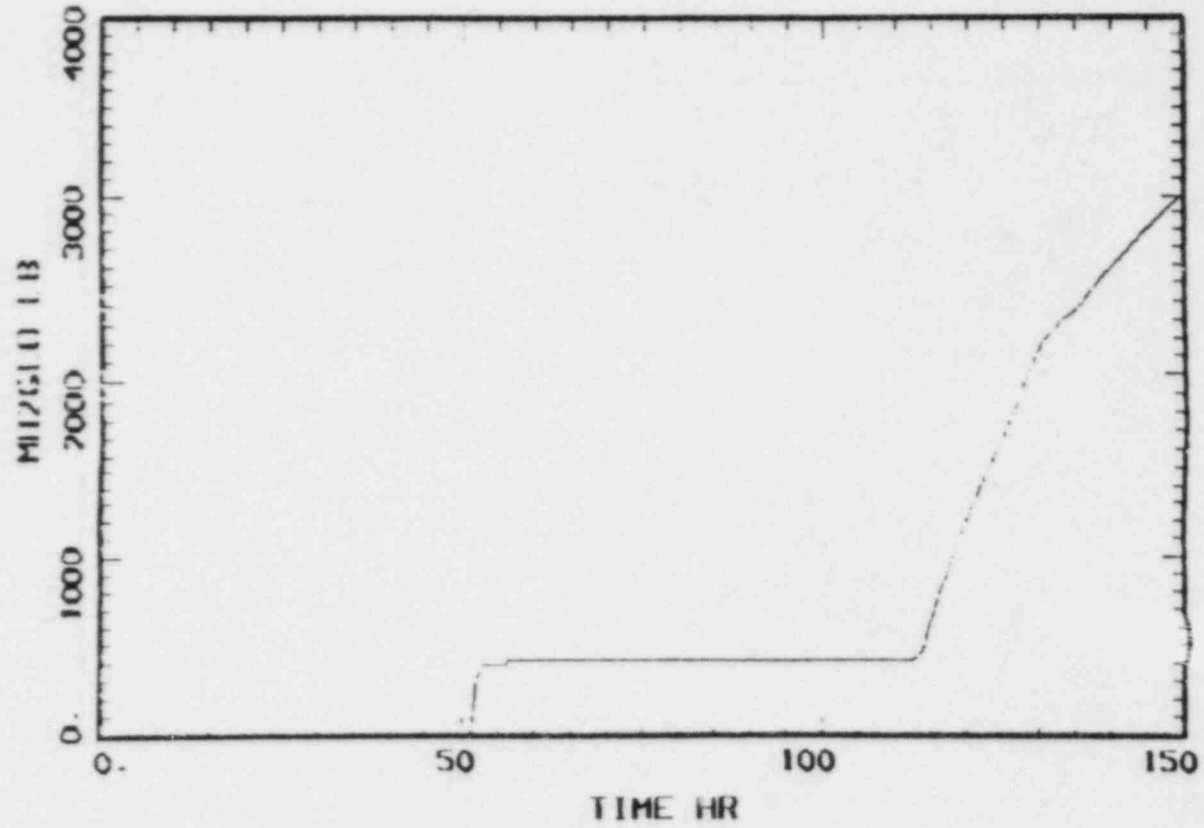


Fig. B.28 Total H₂ generated.

DRAFT

B-34

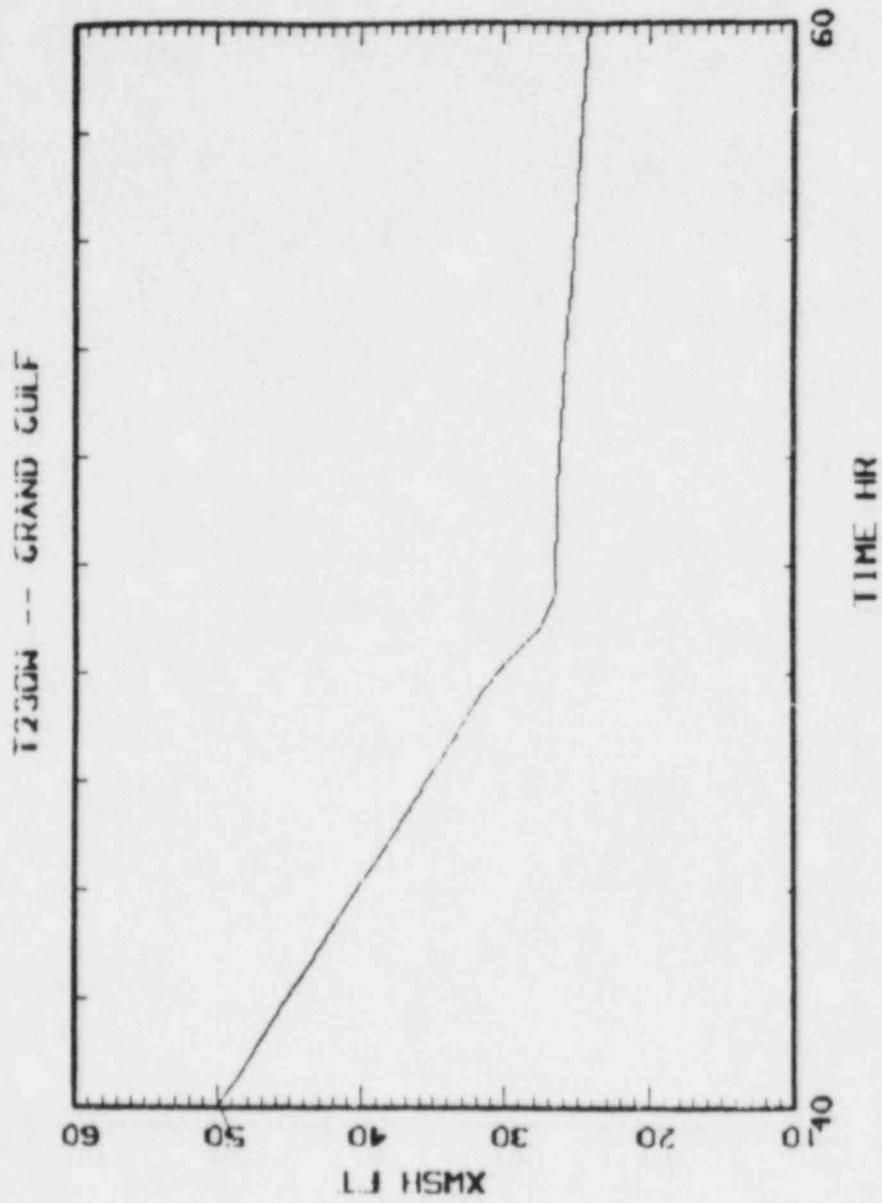


Fig. B.29 Reactor vessel water level.

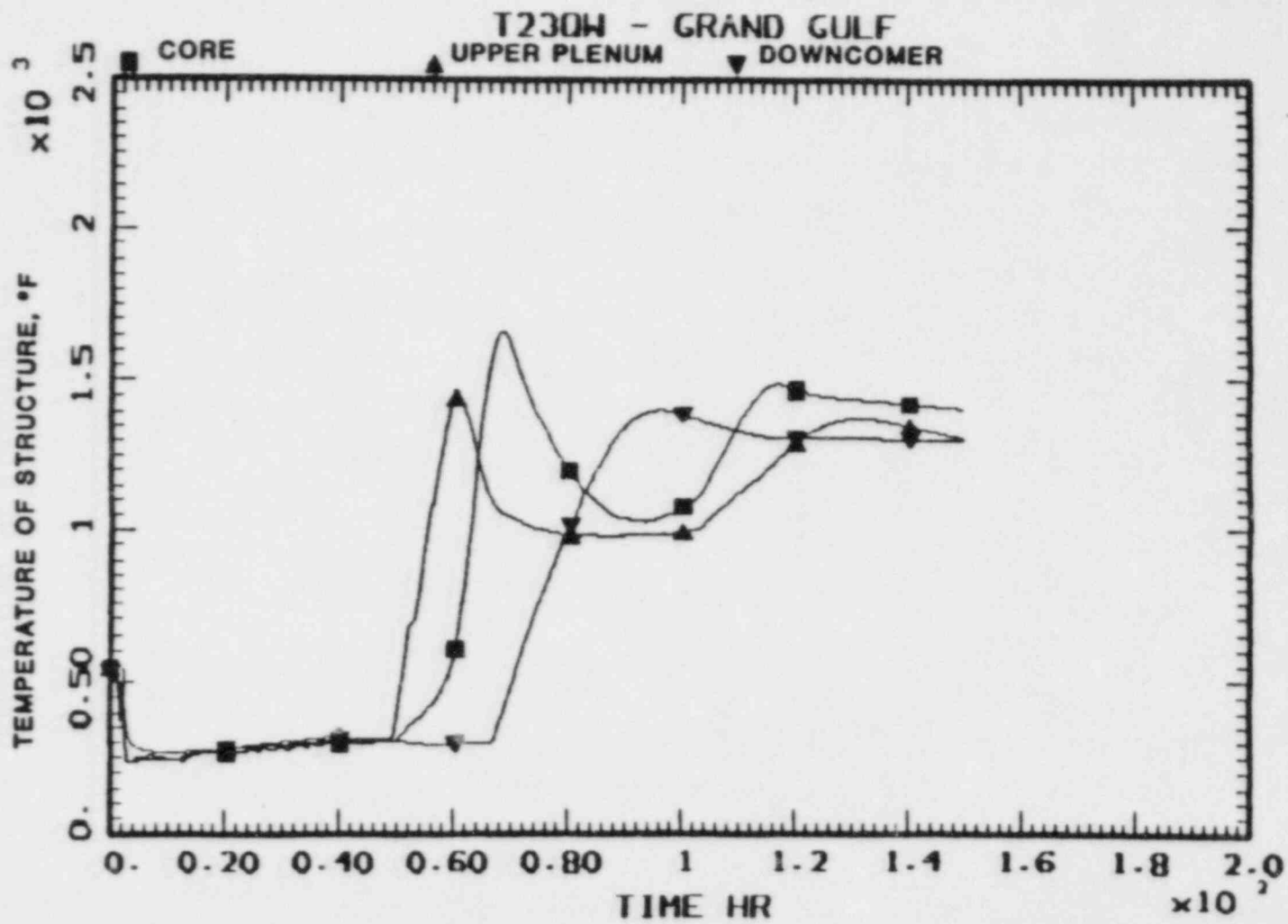


Fig. B.30 Temperature of structure, °F.

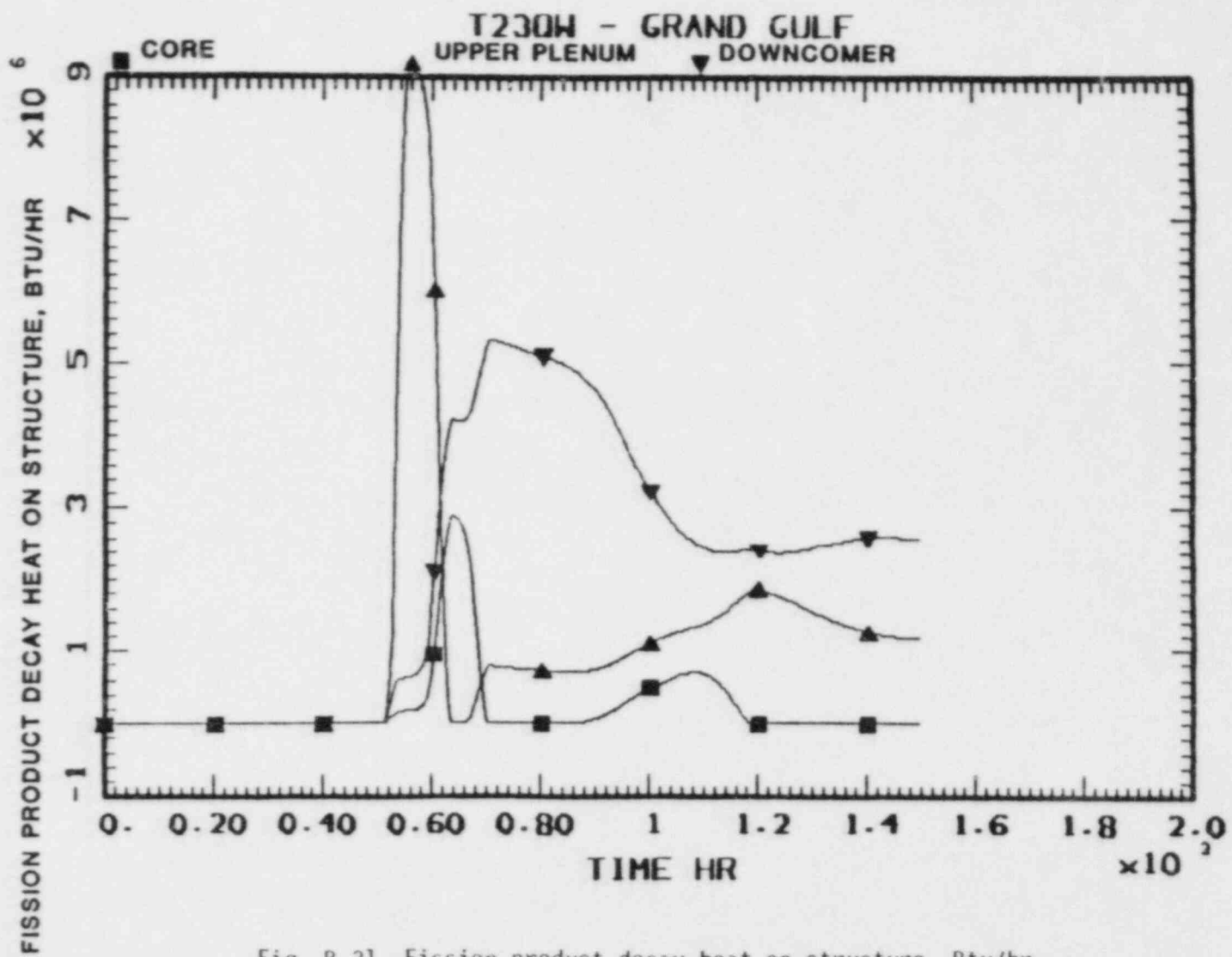


Fig. B.31 Fission product decay heat on structure, Btu/hr.

T230W - GRAND GULF

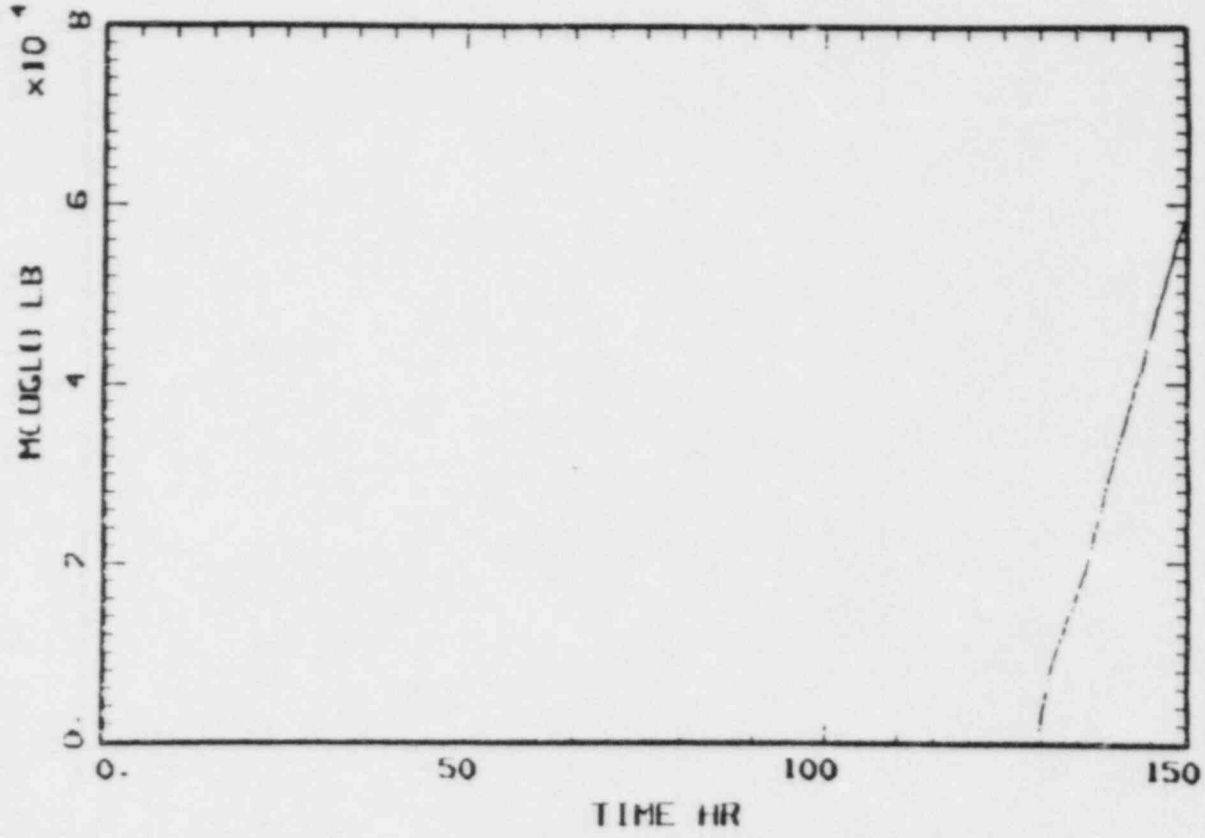


Fig. B.32 Total CO generated.

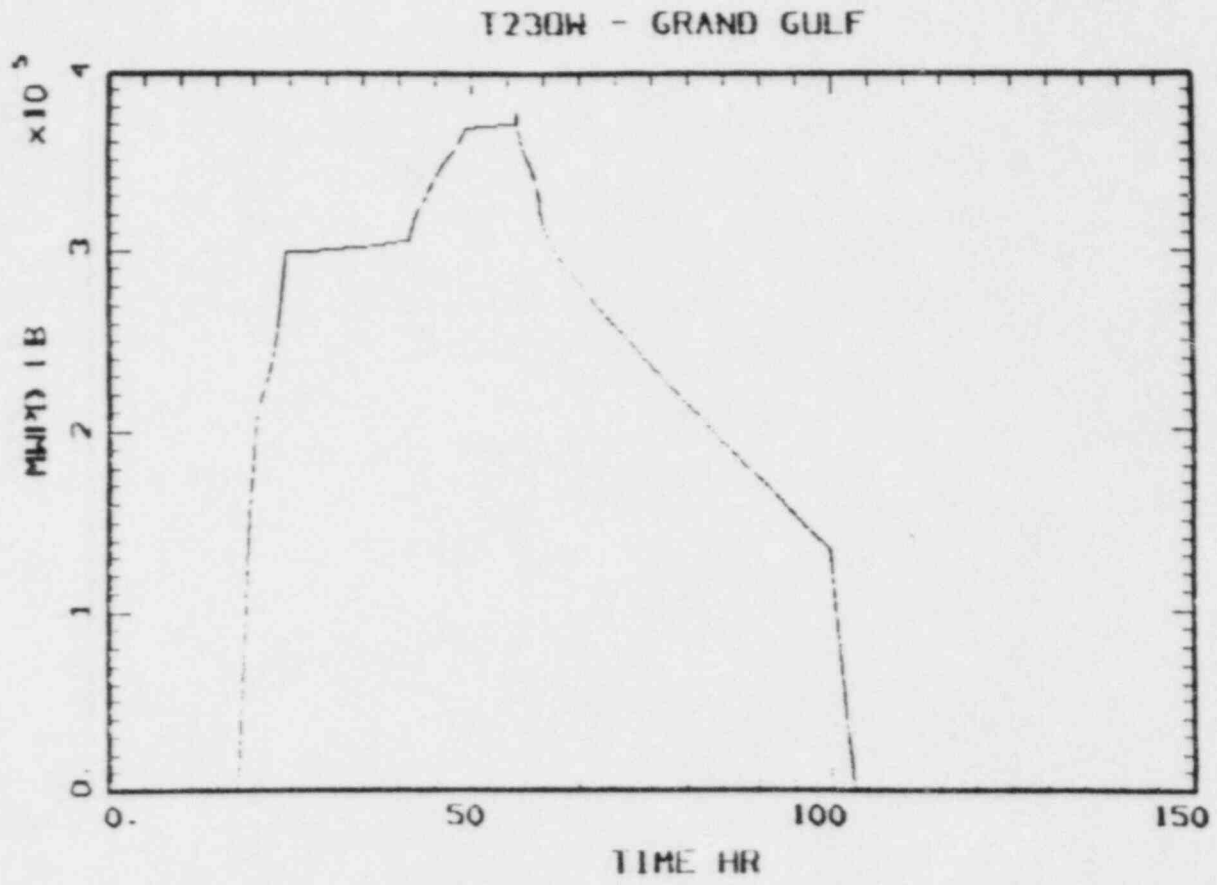


Fig. B.33 Mass of water in the pedestal.

T230W - GRAND GULF

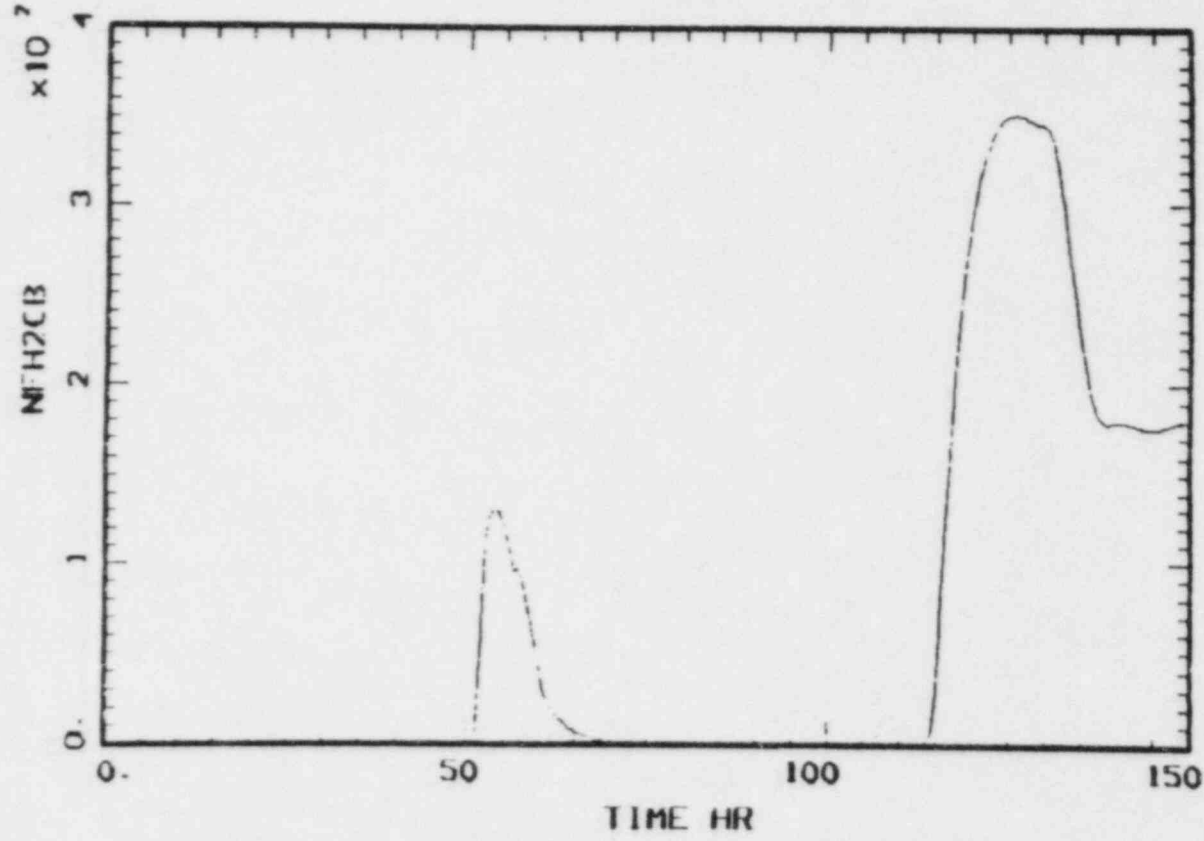


Fig. B.34 Mole fraction of H₂ in Compartment B.

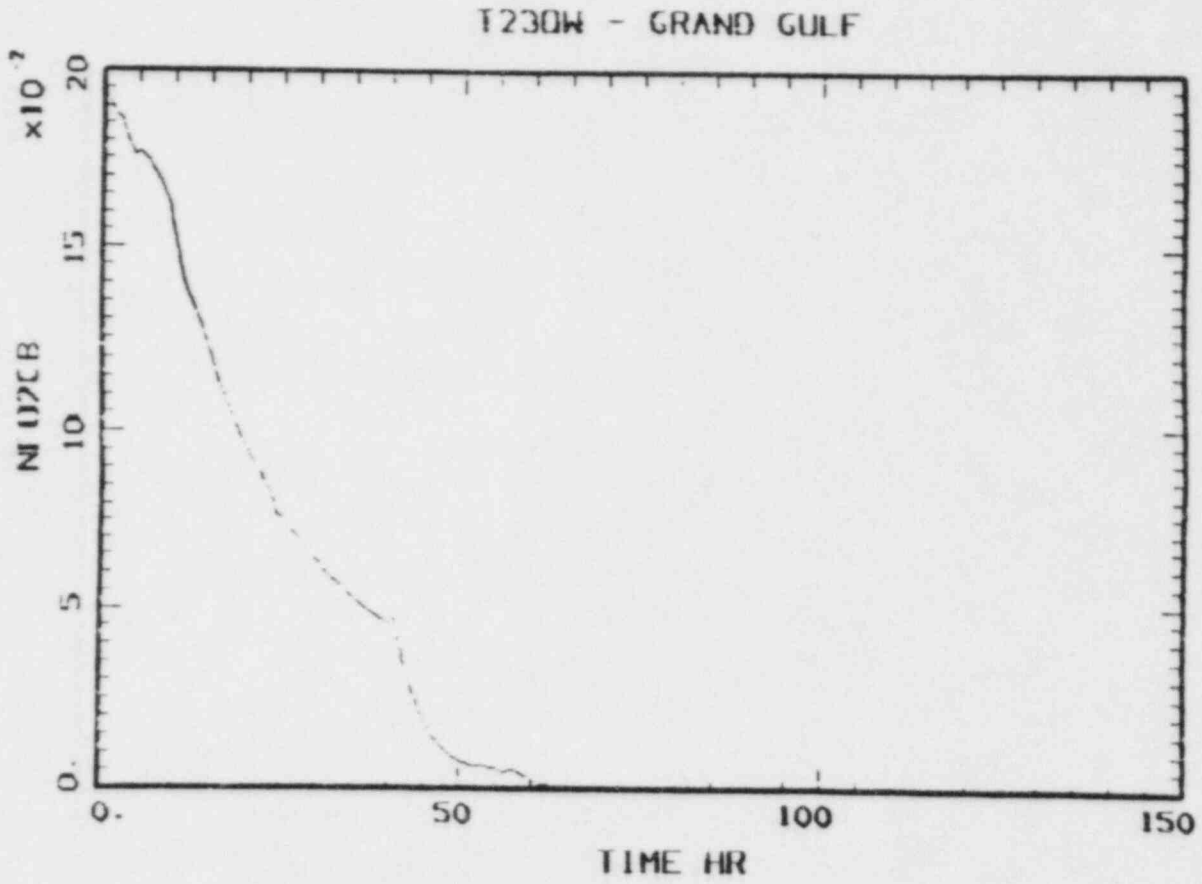


Fig. B.35 Mole fraction of O_2 in Compartment B.

DRAFT

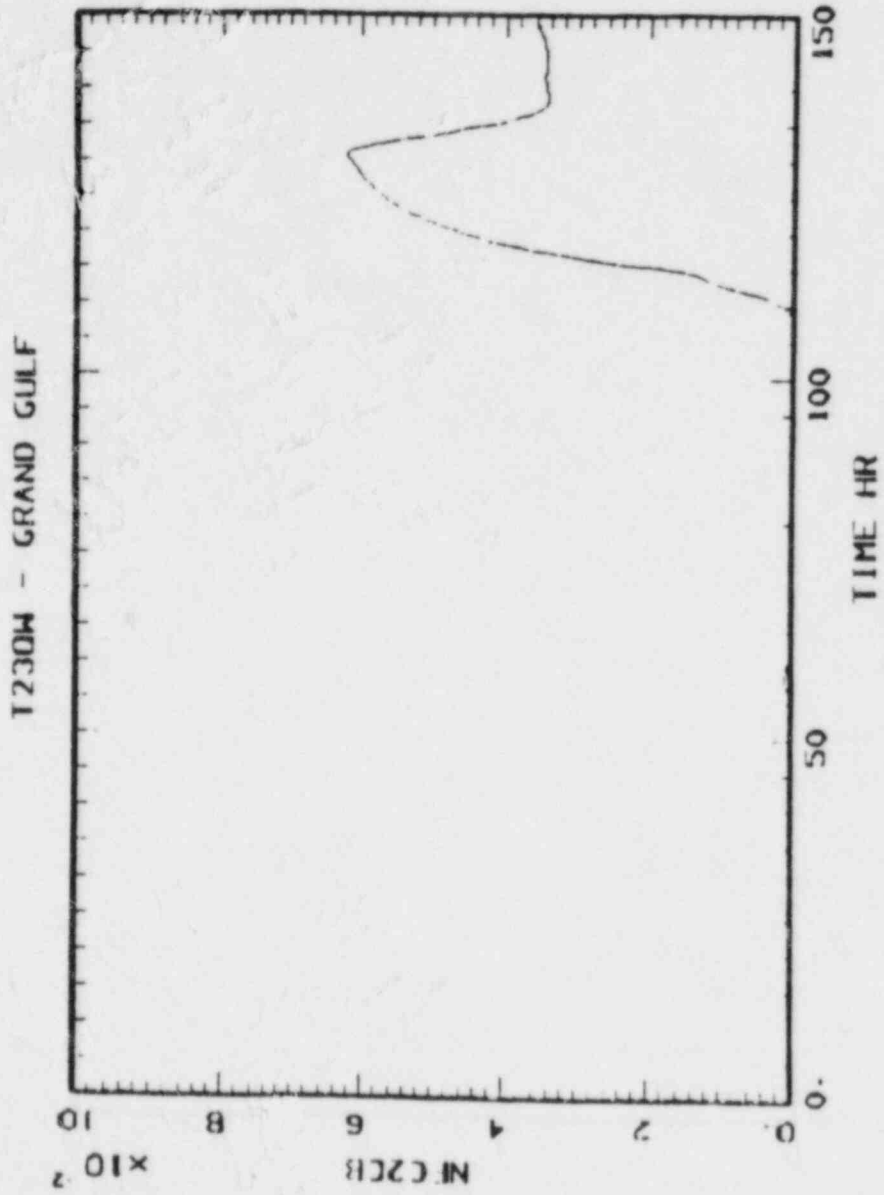


Fig. B.36 Mole fraction of CO₂ in Compartment B.

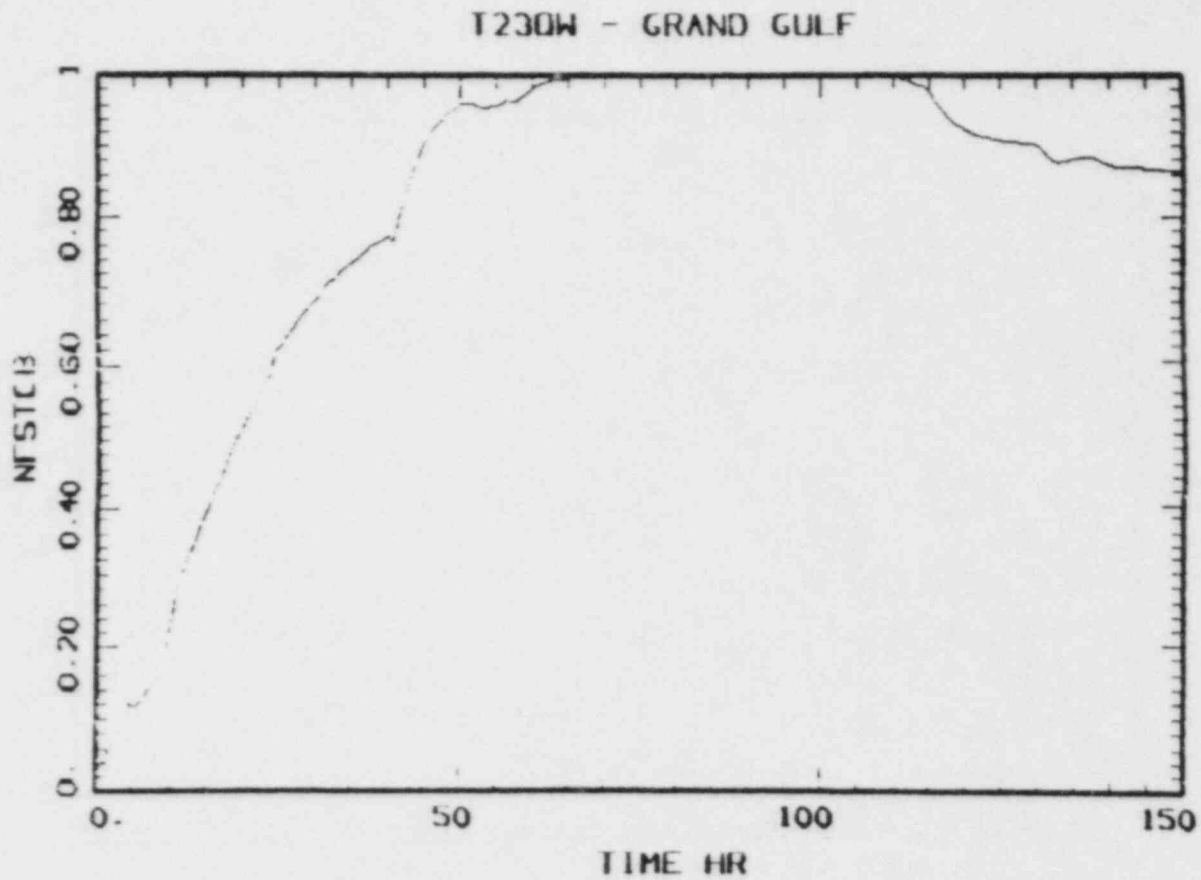
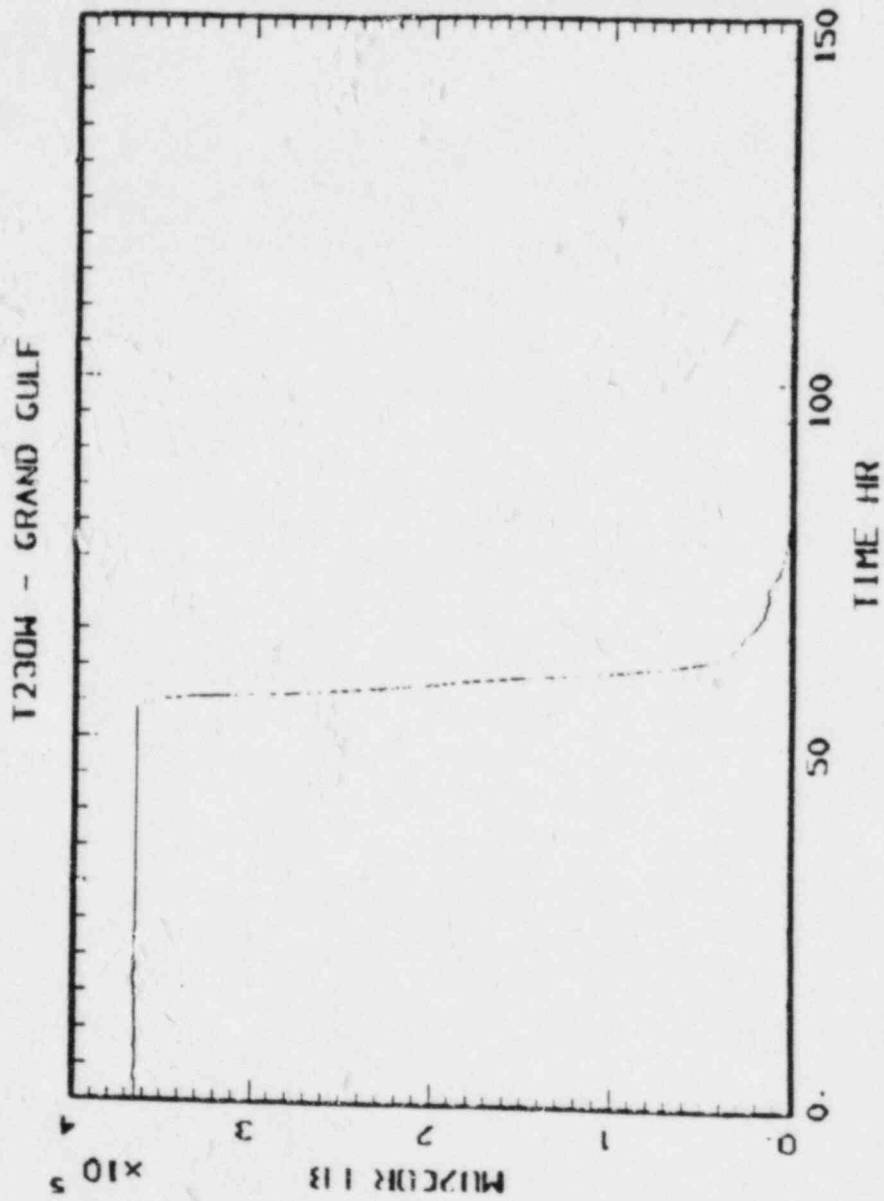


Fig. B.37 Mole fraction of steam in Compartment B.

DRAFTFig. B.38 Mass of UO_2 in core region.

DRAFT

B-44

B-45

DRAFT

SUPPLEMENTAL PLOTS FOR SEQUENCE T₂₃C

DRAFT

T23C - GRAND GULF

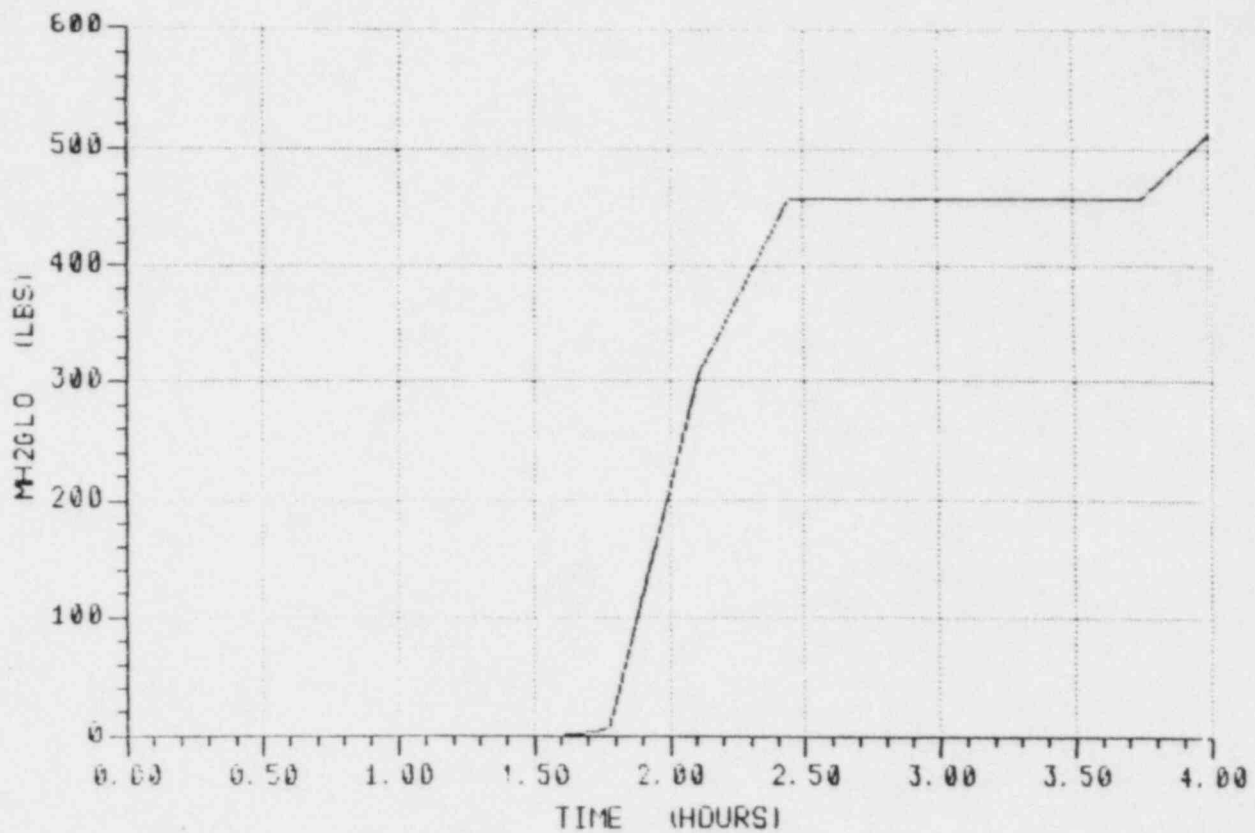


Fig. B.39 Total H₂ generated.

T23C - GRAND GULF

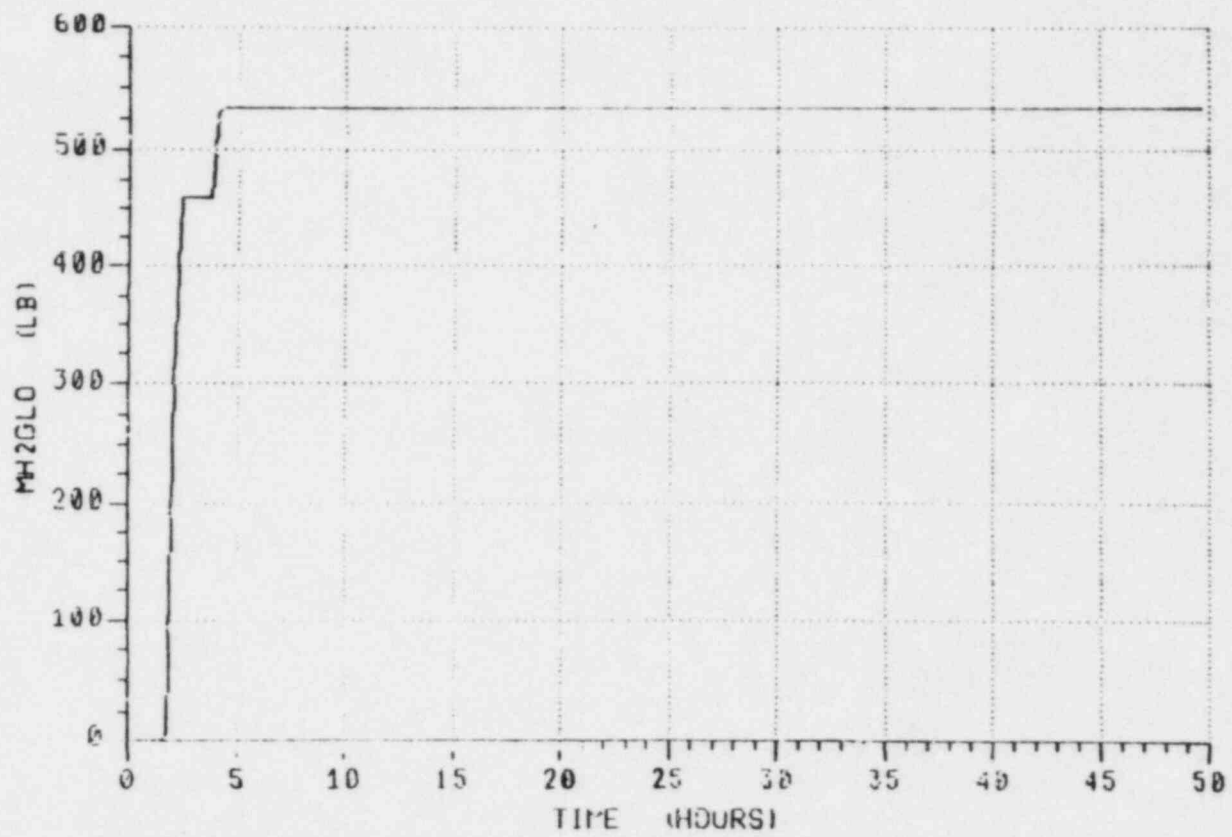


Fig. B.40 Total H₂ generated.

B-47

DRAFT

T23C - GRAND GULF

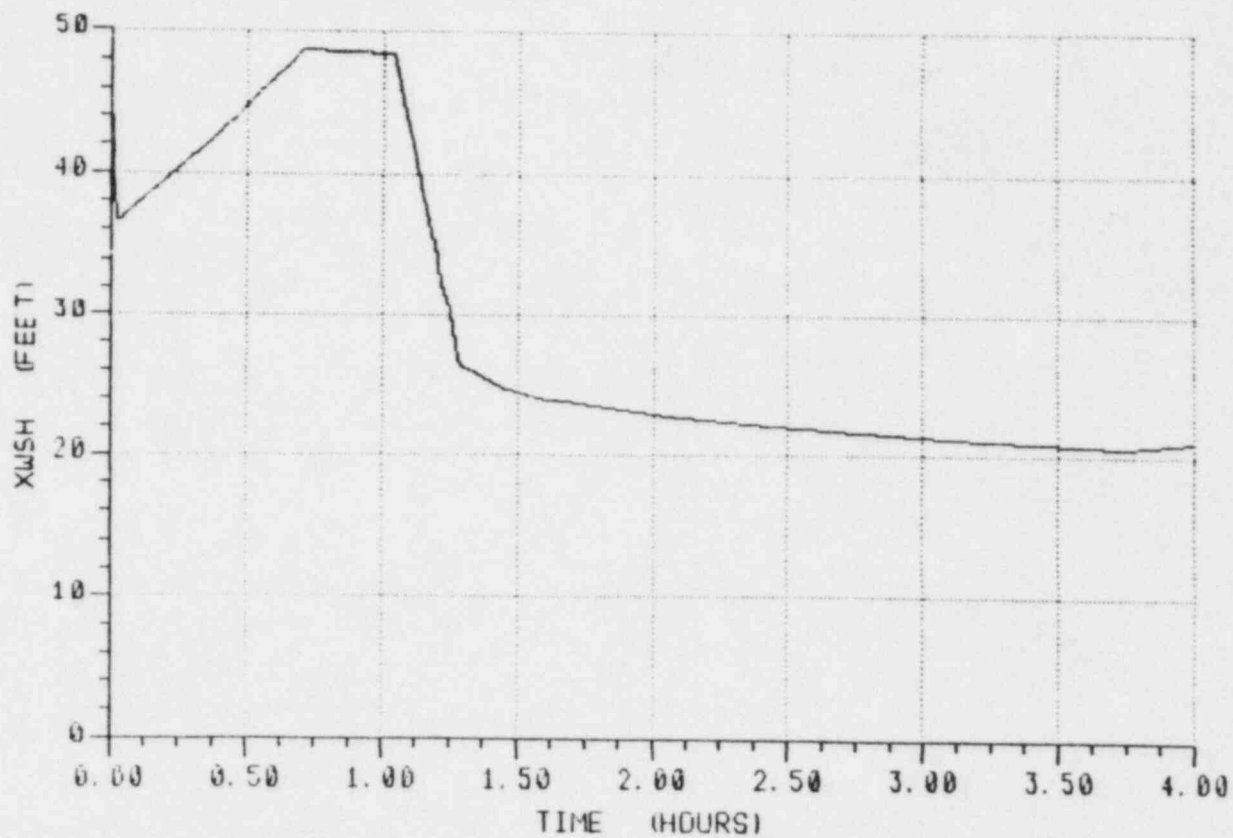


Fig. B.41 Reactor vessel water level.

DRAFT

T23C - GRAND GULF

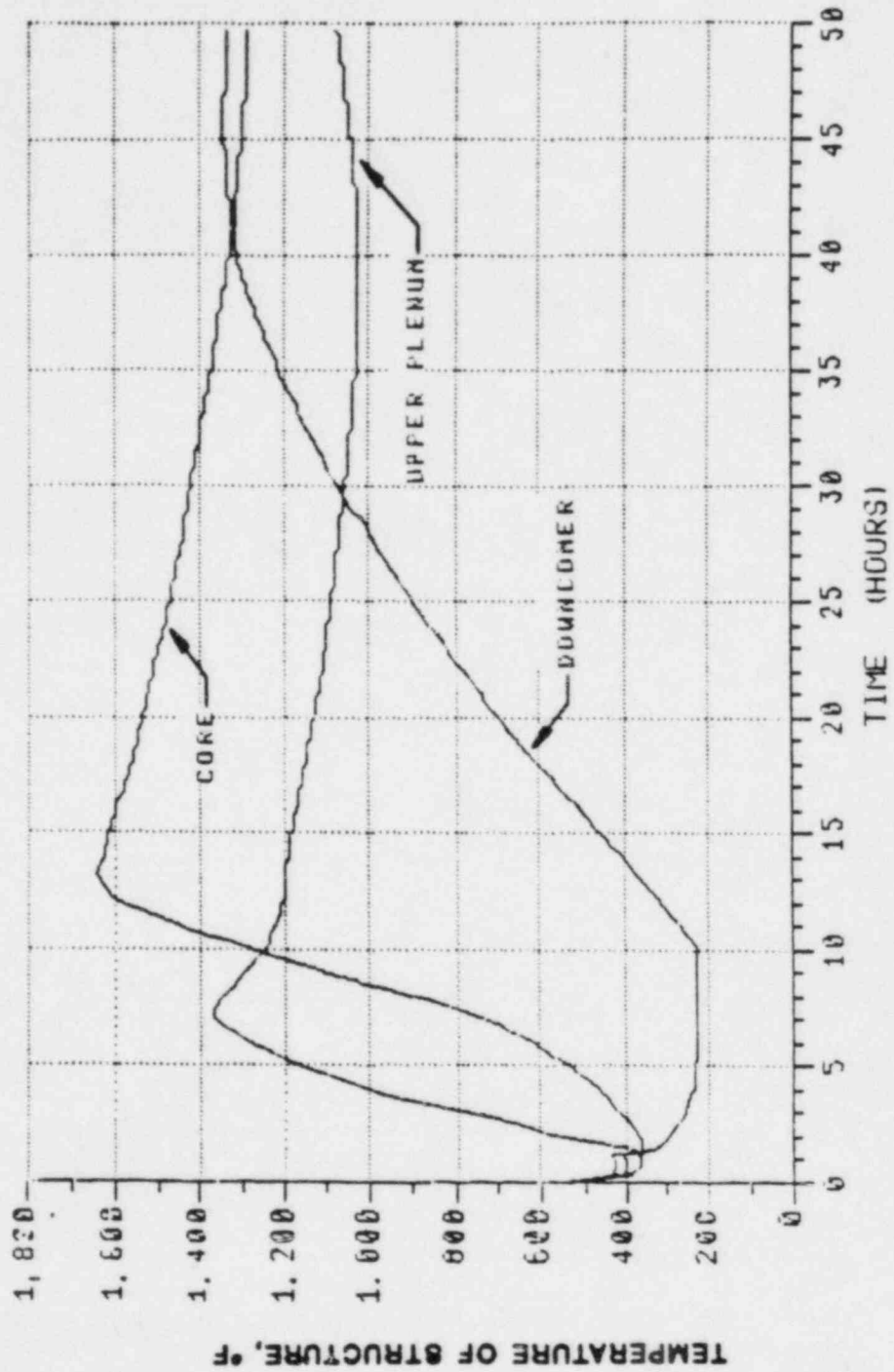


Fig. B.42 Temperature of structure, °F.

DRAFT

B-50

T23C - GRAND GULF

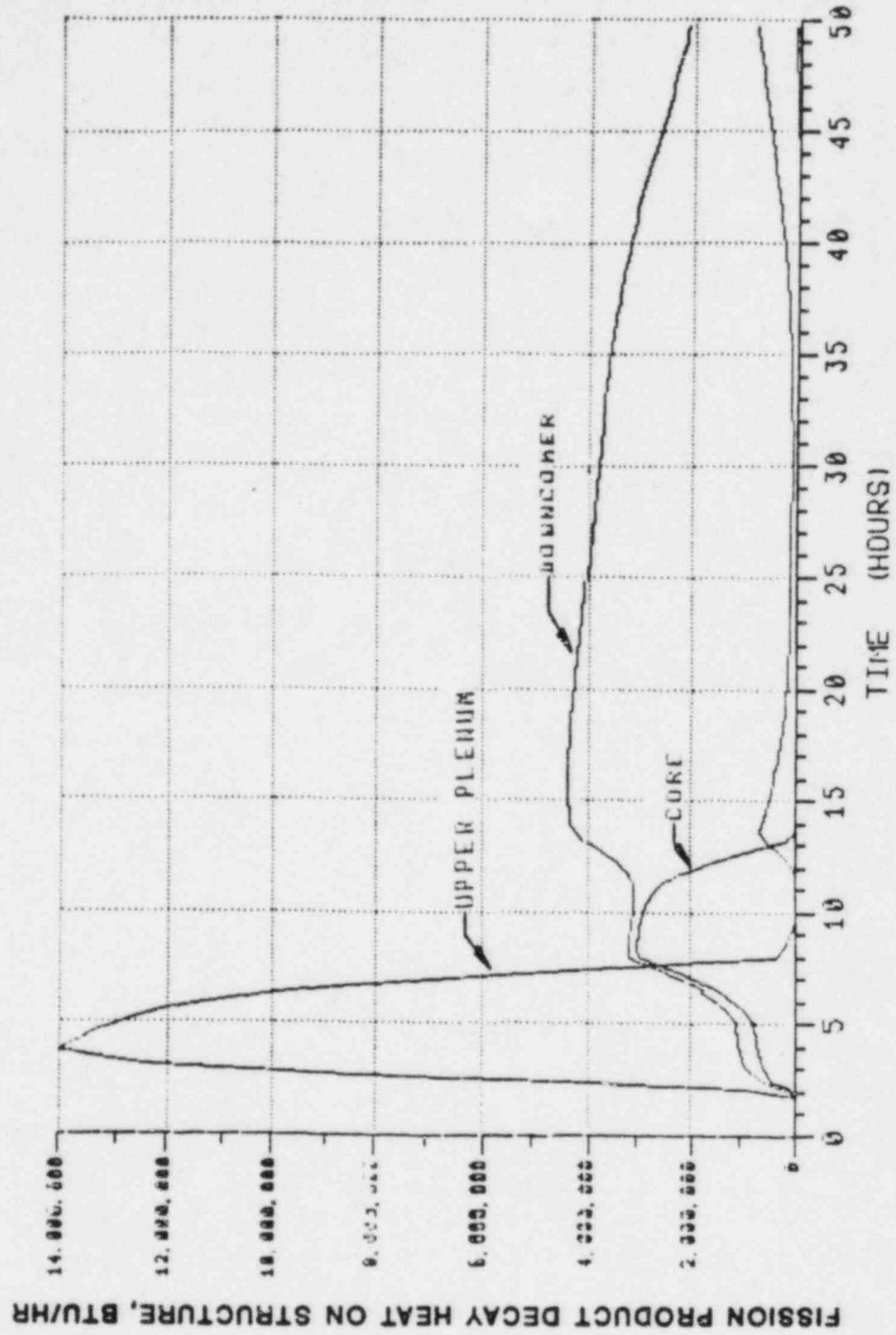


Fig. B.43 Fission product decay heat on structure, Btu/hr.

T23C - GRAND GULF

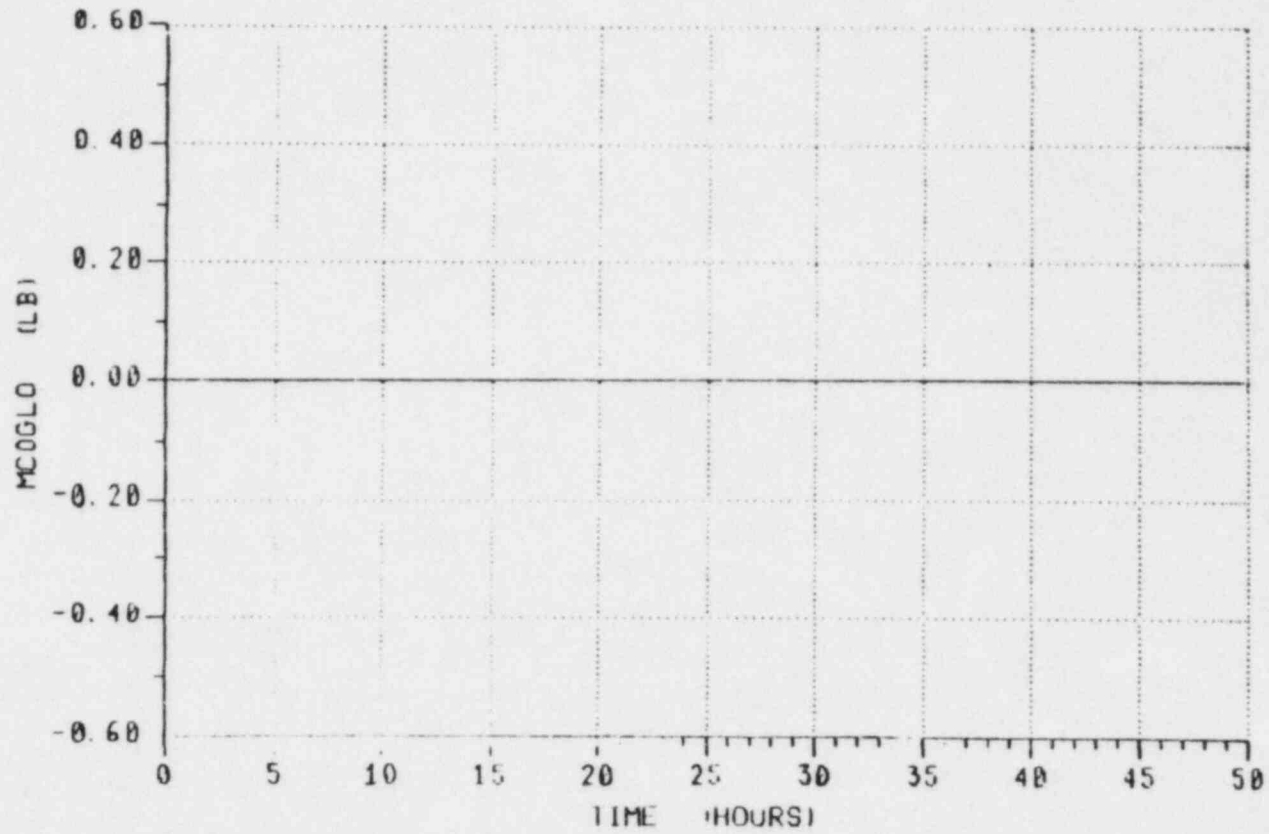


Fig. B.44 Total CO generated.

B-51

DRAFT

T23C -- GRAND GULF

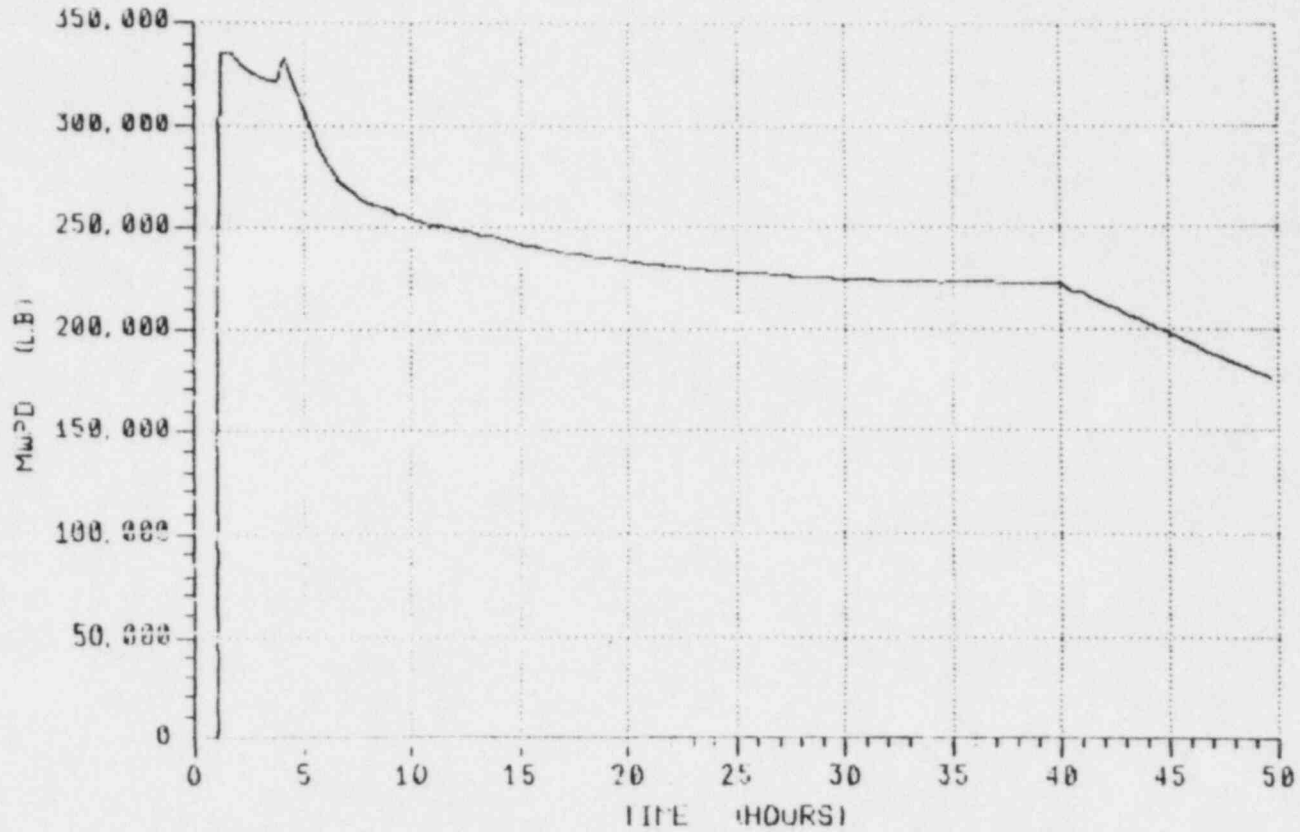


Fig. B.45 Mass of water in the pedestal.

T23C - GRAND GULF

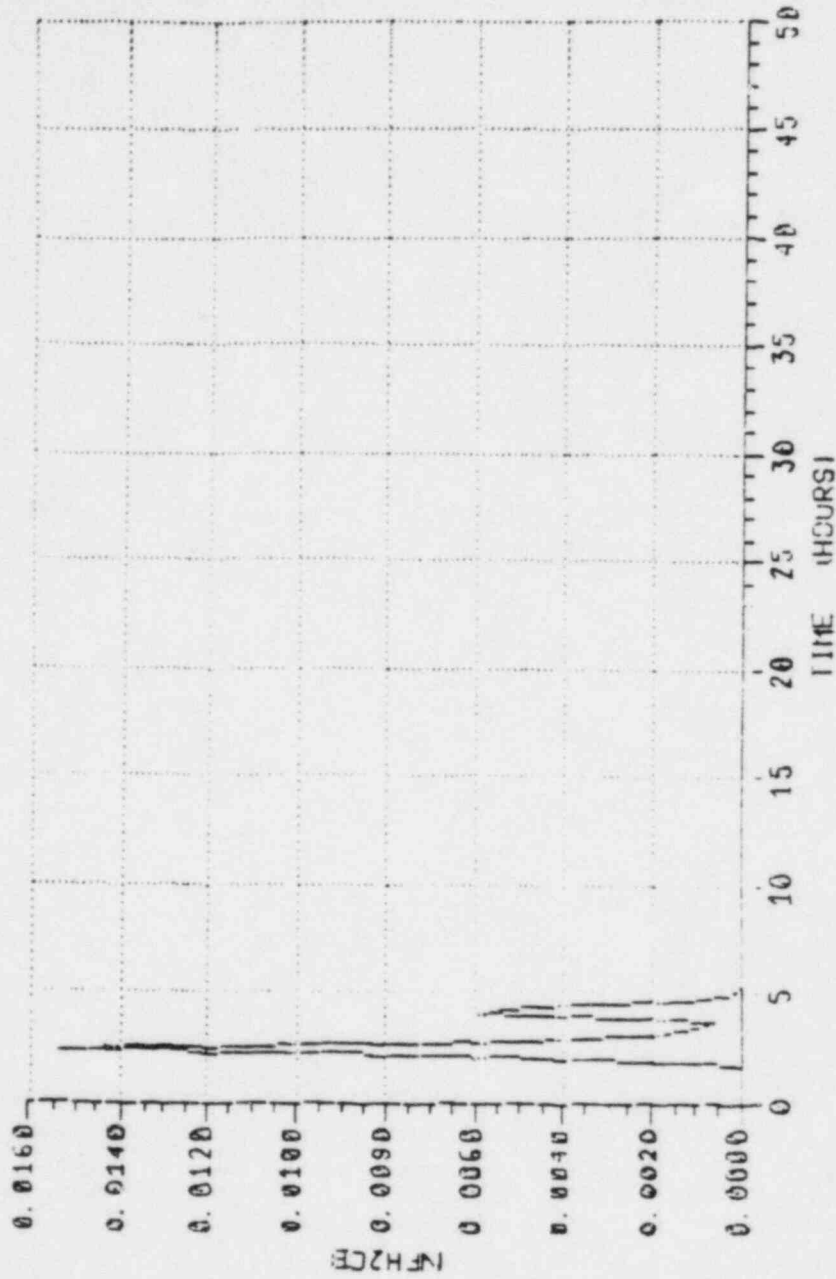


Fig. B.46 Mole fraction of H₂ in Compartment B.

DRAFT

T23C - GRAND GULF

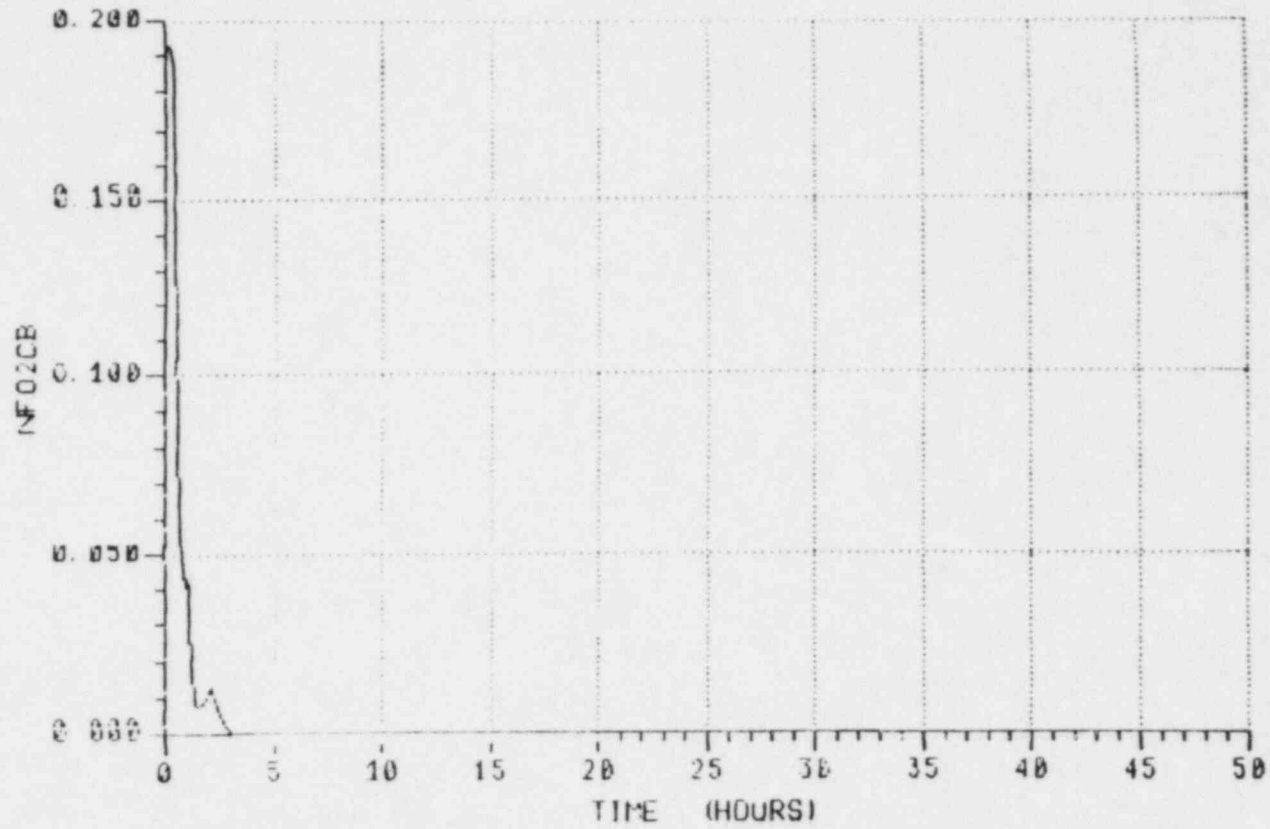


Fig. B.47 Mole fraction of O₂ in Compartment B.

T23C - GRAND GULF

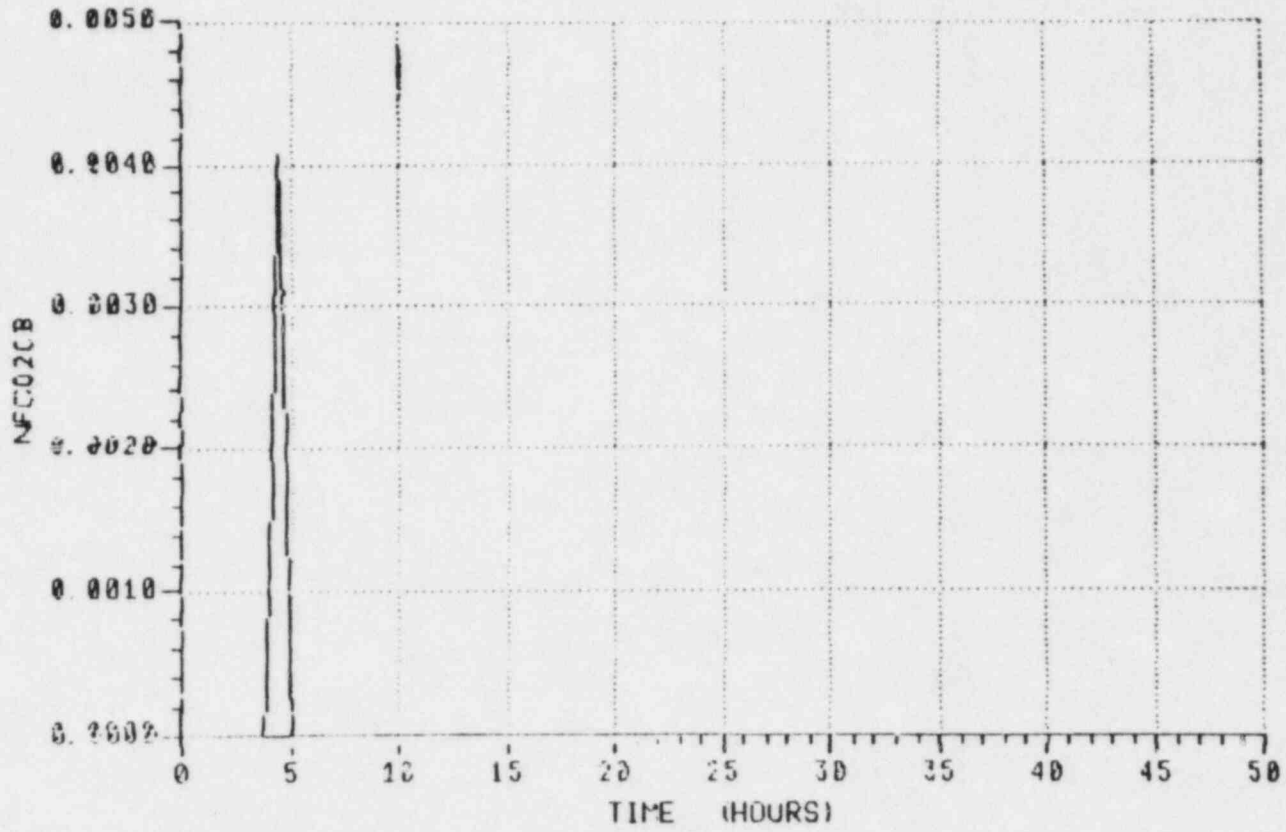


Fig. B.48 Mole fraction of CO₂ in Compartment B.

B-55

DRAFT

T23C - GRAND GULF

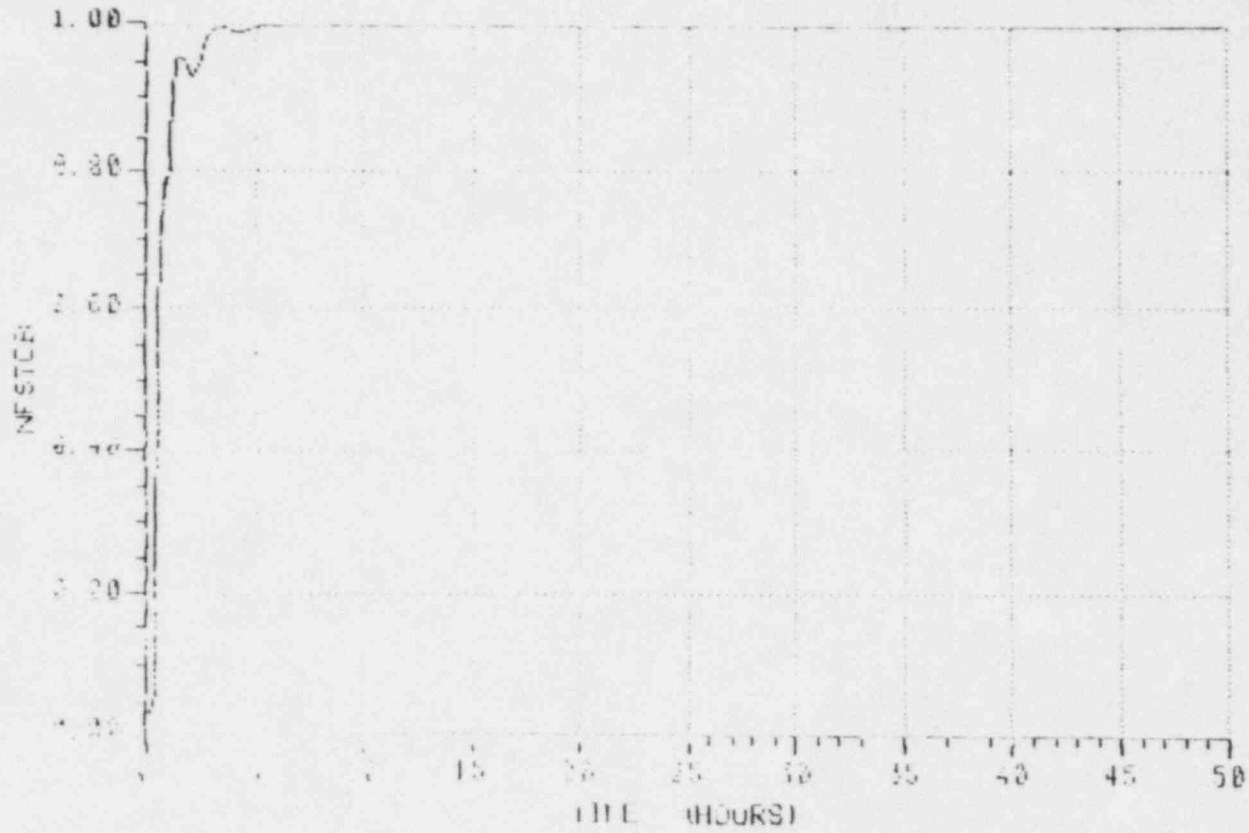


Fig. B.49 Mole fraction of steam in Compartment B.

T23C - GRAND GULF

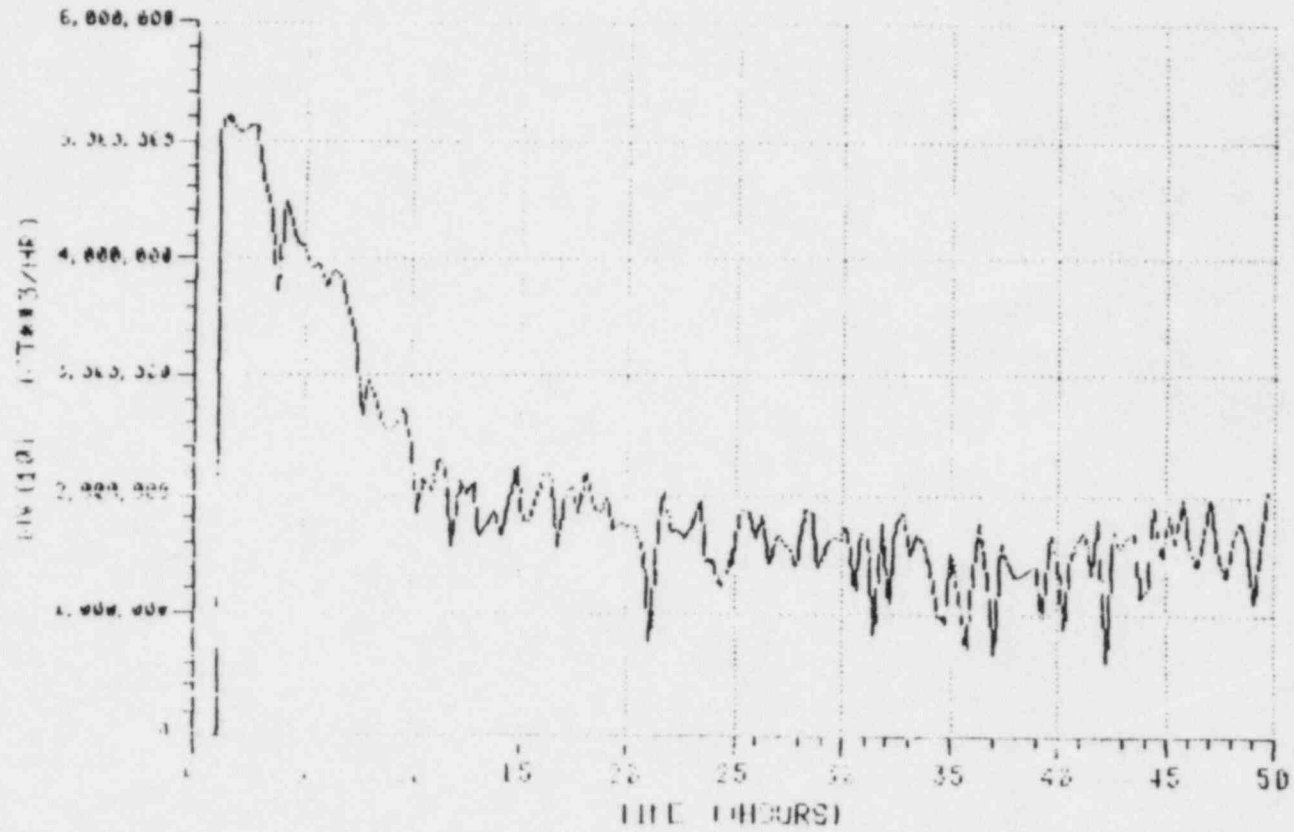


Fig. B.50 Volumetric flow out of containment.

B-57

DRAFT

T23C - GRAND GULF

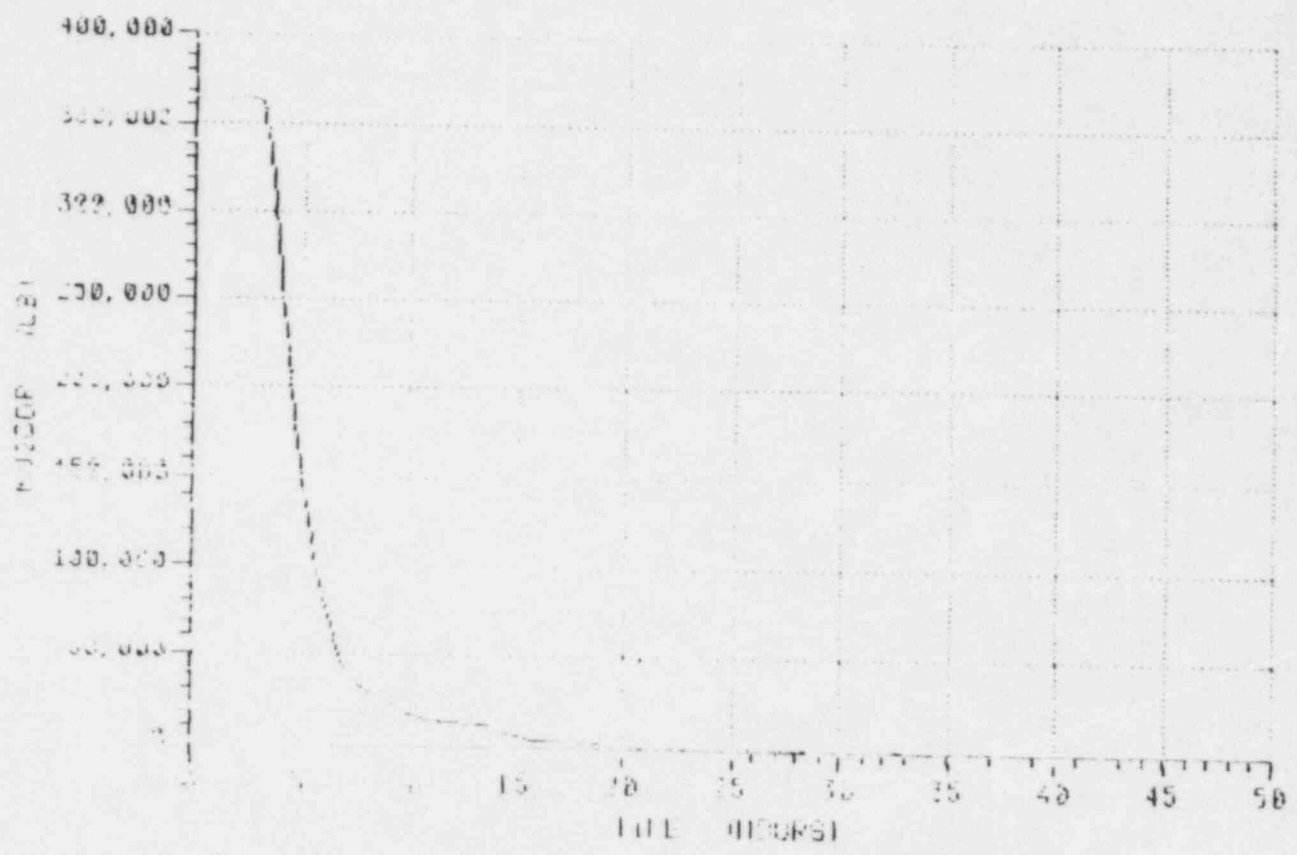


Fig. B.51 Mass of UO₂ in core region.